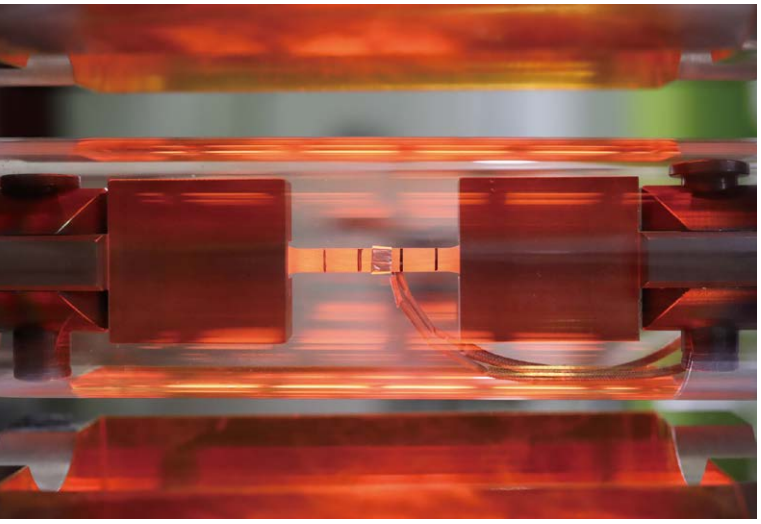

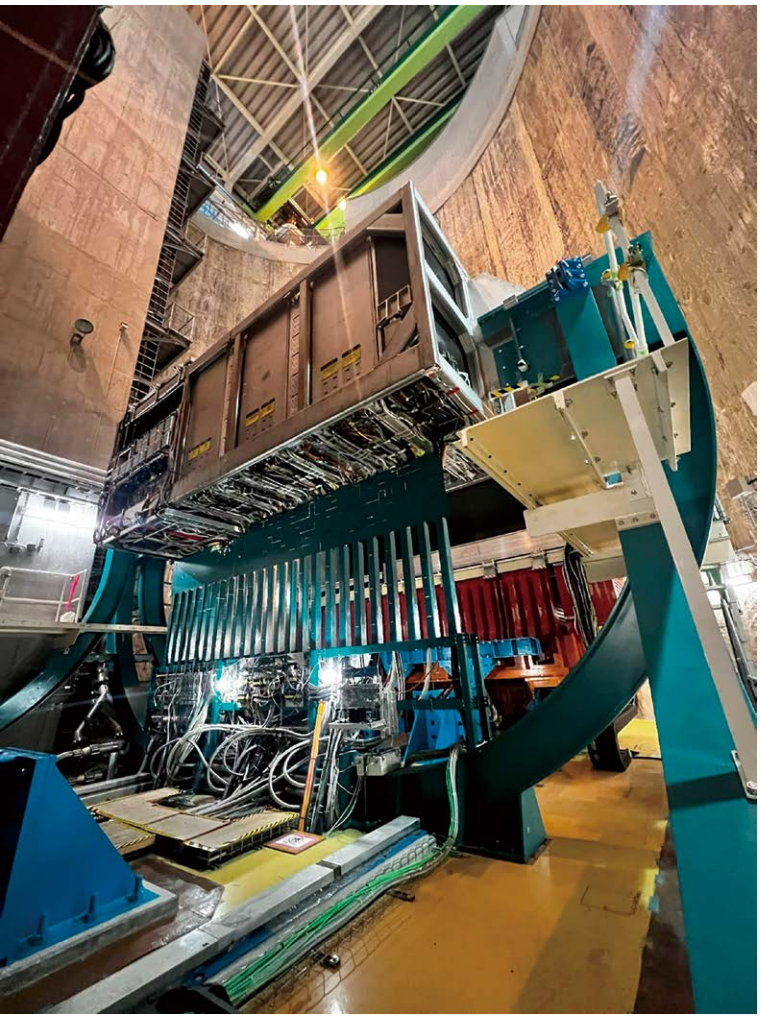

J-PARC

ANNUAL REPORT 2024

Vol. 1: Highlight

Editorial Board (April 2025 – March 2026)


Yong LIU *(Accelerator Division)*


Kaoru SAKASAI *(Materials and Life Science Division)*


Tetsuro SEKIGUTI *(Particle and Nuclear Physics Division)*


Masami IIO *(Cryogenics Section)*


Jiro SUZUKI *(Information System Section)*


Bruce YEE-RENDON *(Transmutation Division)*


Hajime NAKAMURA *(Safety Division)*


Yusuke AIZAWA *(Users Office Team)*


Narumi SUGIYAMA *(Public Relations Section)*

Cover photographs

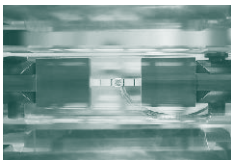
Photograph ① : Magnesium alloy undergoing high temperature deformation
Image credit: Gong WU


Photograph ② : Thinking about the future we have yet to see
Image credit: Soshi TAKESHITA

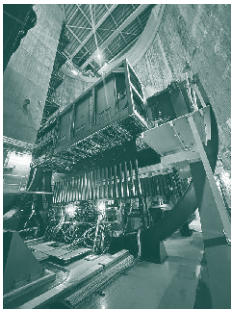
Photograph ③ : ND280 Detector
Image credit: Noriko SAITO

J-PARC Annual Report 2024

Contents

Preface

In fiscal year (FY) 2024, J-PARC advanced its accelerator performance while facing several operational challenges.

At the start of the year, the RCS successfully delivered a 1 MW-equivalent beam to the MLF, and the MR continued its beam-power ramp-up, achieving 830 kW for fast extraction to the Neutrino Experimental Facility, including a first 900 kW single-shot acceleration after RF upgrades and 83 kW for slow extraction to the Hadron Experimental Facility.

However, serious issues at the MLF neutron target system, the detection of humidity in the helium vessel in June, and a mercury-circulation system leak in December forced the suspension of all user operations in the latter half of the year. In March, a helium gas leak was found in the graphite target cooling system of the neutrino facility and neutrino user operations had to be suspended. We sincerely apologize for the inconvenience to the user community.

Scientific programs made steady progress at all facilities. At SENJU (BL18) in the MLF, a newly developed large-area neutron detector increased the sensitive area six-fold, dramatically enhancing single-crystal Bragg-peak measurements. On the muon-science front, J-PARC achieved a landmark in FY2024 by cooling and accelerating positive muons up to ~4% of the speed of light, which was recognized as the world's first successful demonstration of muon acceleration.

T2K continued precision oscillation studies with its upgraded near detector, KOTO resumed data collection following the MR upgrade shutdown, and COMET made progress in major construction milestones. The muon g-2/EDM project achieved key successes in muon cooling and acceleration.

Throughout the year, J-PARC actively engaged with the scientific community through symposia and workshops and continued discussions on future projects such as the MLF-double roadmap and long-term planning toward TS2. In October, we held the 4th J-PARC symposium with the sub-title "Futures of J-PARC, Futures by J-PARC" and welcomed more than 400 participants from around the world. We discussed past achievements and future programs of the J-PARC.

This Annual Report summarizes the progress and challenges of FY2024. I would like to express my deep appreciation to all users, collaborators, and staff for their continued dedication. J-PARC remains committed to improving operational reliability and advancing the scientific potential of our facility.

Takashi Kobayashi
Director, J-PARC Center

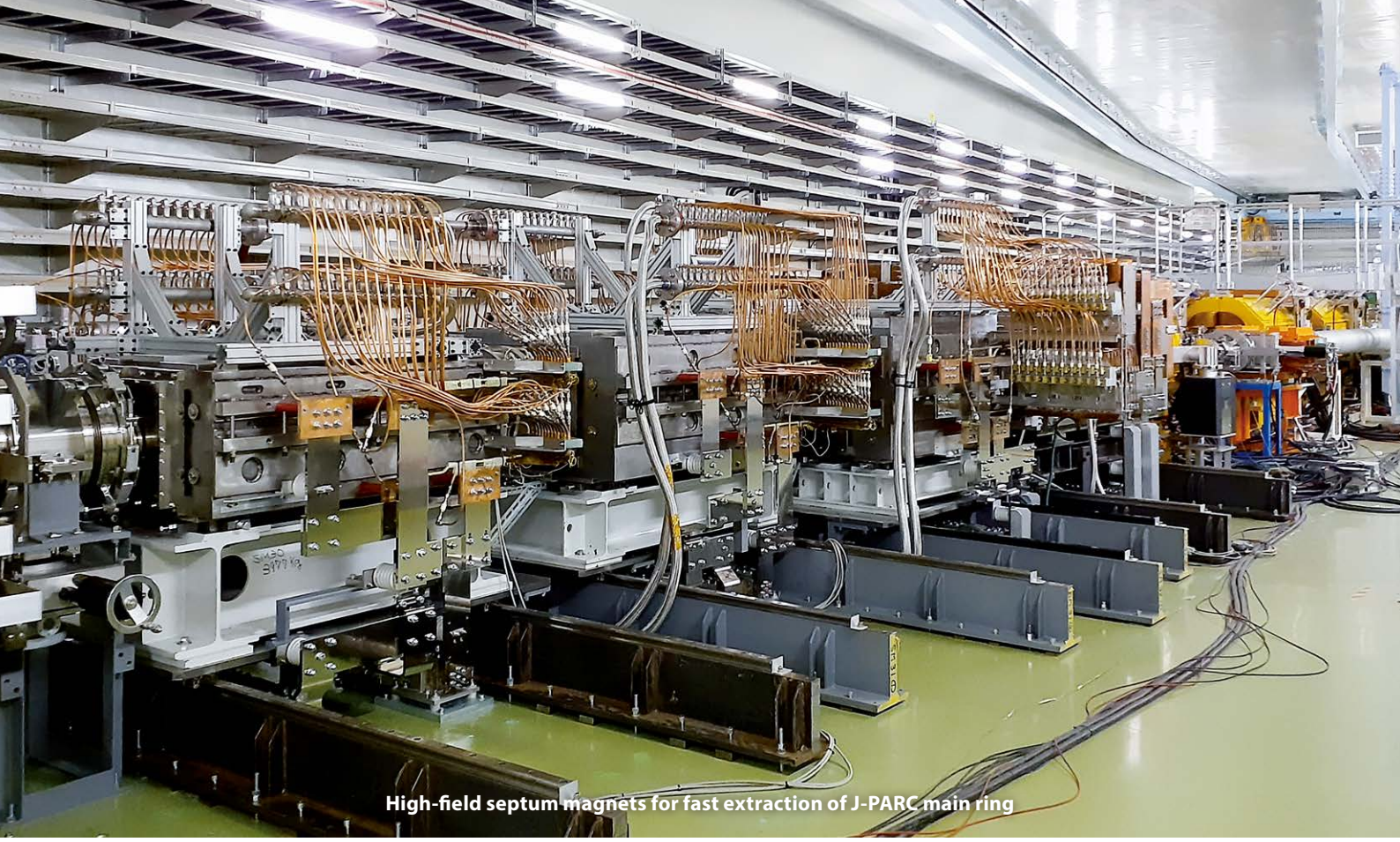

High-field septum magnets for fast extraction of J-PARC main ring

Accelerators

Overview of the Accelerator

The J-PARC facility consists of three accelerator facilities: Linac, RCS (Rapid Cycling Synchrotron) and MR (Main Ring synchrotron). The proton beams extracted from the RCS are delivered to the Materials and Life Science Experimental Facility (MLF) for neutron and muon experiments, and are also injected to the MR. The MR has two beam extraction modes, the fast extraction (FX) mode to the Neutrino Experimental Facility (NU) and the slow extraction (SX) mode to the Hadron Experimental Facility (HD).

The beam power history for the MLF and the MR (NU and HD) in fiscal year (FY) 2024 is shown in Fig. 1. The MLF began long-term continuous operation of 950 kW (1 MW output in RCS) in April. The beam powers of the NU and HD were increased to 830 kW and 83 kW in FY2024, respectively.

At the linac facility, a scorch mark was observed in a chiller (terminal block) for the cooling-water system, and on July 5th the public fire department judged that it was a fire incident, immediately after the start of 2024 summer maintenance. Since the cause investigations and safety measures were completed before the end of maintenance, the incident did not affect the operating schedule.

(1) Operation for the MLF

At the RCS, one of the 12 RF systems malfunctioned in June 2022, and the beam operation had been conducted with 11 systems since then. As the acceleration voltage was insufficient and caused a slight beam loss during 1 MW operation with 11 systems, the beam power had been reduced. Therefore a transformer rectifier was delivered, and the RF system was restored to 12 units

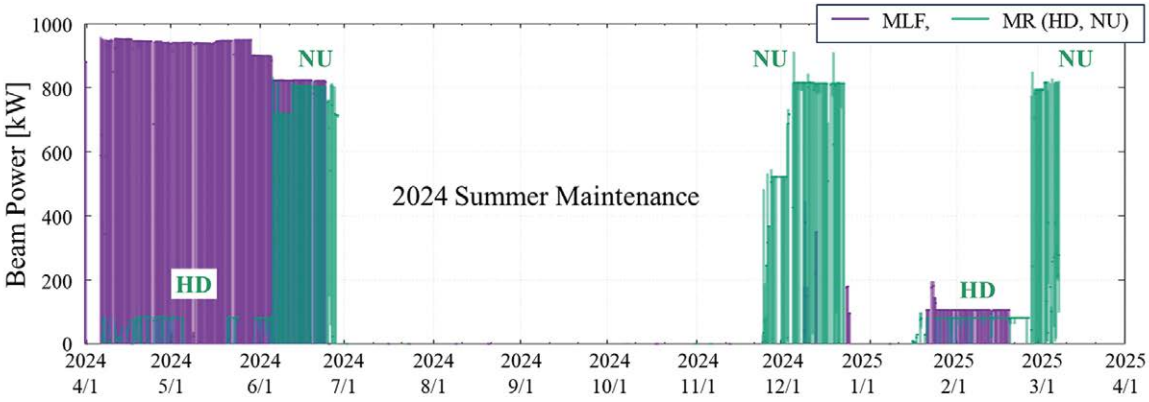

Fig. 1. Beam power history for the MLF and MR (NU, HD) in FY2024

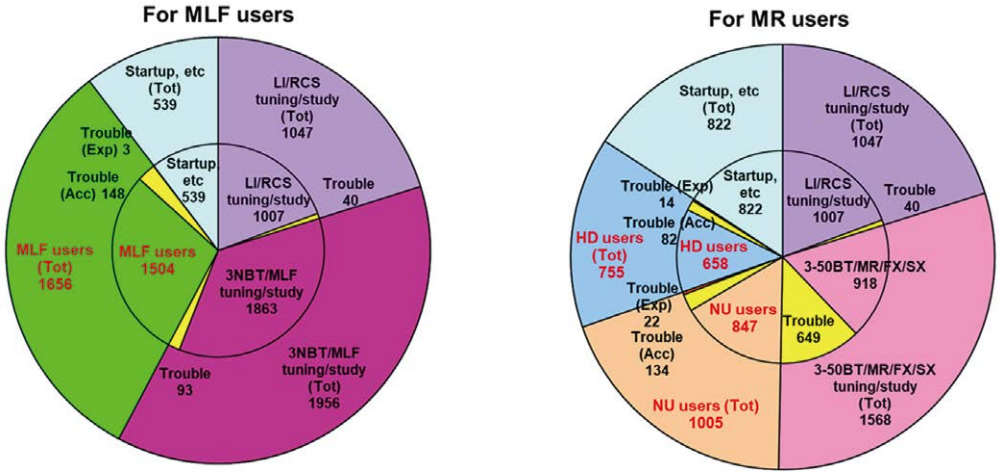

Fig. 2. Operation statistics for MLF (left) and MR (NU, HD) (right) in FY2024

in March 2024, and continuous 1 MW operation was started at the RCS in April. The MLF operated at 950 kW for about two months, but in order to reduce electricity costs, one RF system was stopped in late May, and the beam power was reduced to 900 kW. On June 24, the amount of moisture in the helium vessel of the MLF neutron source exceeded normal levels, requiring a detailed investigation of the cause and consideration of countermeasures. As a result, the MLF operation, which had been planned until July 1 before the 2024 summer maintenance, was immediately suspended.

During the maintenance, the replacement of the mercury recirculation pump was conducted, but a defect occurred that prevented the mercury recirculation system from achieving its prescribed performance. As a result, all MLF user operation was canceled until March 2025 (Fig. 1 shows a record of 100 kW operation around February, but displays beam study operation, not user operation.). The net user operation hours and the beam availability rate for the MLF in FY2024 were 1,504 hours and 91 % (Fig. 2).

(2) Operation for the NU and HD

The MR operation in FY2024 began with beam supply to the HD. By updating the power supply and other equipment, the repetition cycle was shortened from 5.20 to 4.24 secs during continuous operation with a beam power of 83 kW, and was started in April 2024. At the NU, after achieving 760 kW in 2023, further detailed beam tuning was carried out. As a result, continuous operation with 800 kW was started in June 2024 (Fig. 3).

On June 24, since one cooling tower in the MR No. 2 machine building malfunctioned and reduced the cooling capacity of the cooling water, the beam power was reduced to 700- 750 kW. In late June, as the outside temperature and humidity rose, it became difficult to sufficiently lower the water temperature in the RF cavity. Therefore, the MR operation, which had been planned until July 8 before the 2024 summer maintenance, was

Fig. 3. Group photo taken to celebrate the achievement of 800 kW and 80 kW at MR

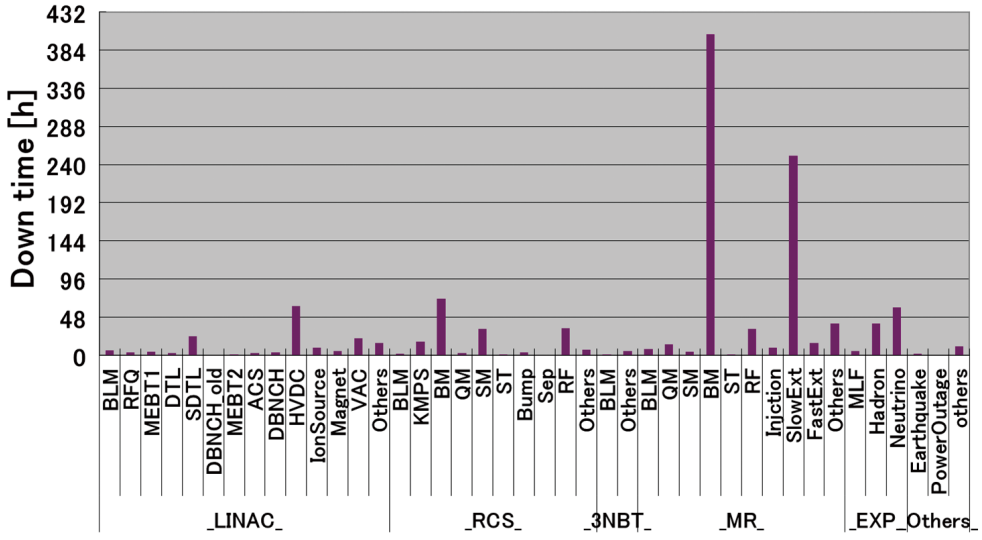

Fig. 4. Downtime for each accelerator components in FY2024

suspended on June 28 due to concern that the nanocrystalline soft magnetic alloy used in the RF cavity could be damaged.

The MR operation after summer maintenance began at the NU facility. Continuous operation was conducted at a beam power of 830 kW, but on March 4, 2025, the beam supply from the MR to the NU was suspended due to a decrease in the flow rate of helium gas used to cool the neutrino production target. In order to determine the exact cause, further inspection inside the helium vessel of the target station was required. As this process was expected to take more than three months, beam operation at the NU was suspended in the first half of 2025. Beam operation at the HD began as planned in January and continued until the end of February. During this period, the accelerator was able to operate with a high stability. The net user operation hours and the beam availability rate in FY2024 were 847 hours and 84 % for the NU, and 658 hours and 87 % for HD, respectively (Fig. 2).

(3) Downtime for each accelerator component.

The downtime for each accelerator component in FY2024 is shown in Fig. 4.

The longest downtime was caused by a malfunction in bending magnet No.116 (BM116) in the MR ("_MR_ BM" in Fig. 4). On May 5th, 2024, during beam operation, total beam loss occurred just downstream of BM116. The beam operation was stopped, and an investigation of BM116 was

conducted inside the accelerator tunnel. As a result, it was found that a layer short had occurred in the upper coil of the magnet. It took approximately two weeks to replace the magnet with a spare, and beam operation was resumed on May 20.

The next long downtime was caused by a failure of the power supply for the MR SX bump electromagnet 2 ("_MR_ SlowExt" in Fig. 4). This power supply failure occurred twice, in May 2024 and January 2025, causing the MR operation to be suspended for approximately six

days and three days, respectively. The cause of both failures was a malfunction of the IGBT unit. Due to the need to identify and replace the components, as well as verify the integrity of other units, the restoration process required this prolonged period.

From April to May 2024, frequent shutdowns occurred in the power supply system of the bending magnet in the RCS ("_RCS_ BM" in Fig. 4). The total downtime was approximately 70 hours, but there were 26 shutdowns. Upon investigation, it was determined that there was an abnormality in the control system of the DC power supply unit, and the issue was resolved by replacing the control board components.

The prolonged shutdown of the linac was caused by a problem with the klystron high-voltage power supply ("_LINAC_ HVDC" in Fig. 4). There were several shutdowns, but the most time-consuming recovery was due to insulation deterioration in the high-voltage cable used in the No. 5 klystron high-voltage power supply on November 30th. It took time to identify the fault location and replace the cable, and about 20 hours to recover and resume operation.

Linac

Overview

The J-PARC linac has been operating with a nominal peak beam current of 50 mA. High availability of more than 90% (to the MLF) was also maintained during FY2024. Beam studies have been conducted to resolve some issues such as beam loss mitigation, and confirmation of feasibility for further high intensity operation due to the demand of downstream facilities.

Accelerator components status: ion source

The operation history of the ion source in FY2024 is shown in Fig. 5. Presently the ion source is being operated with an H^- beam current of 60 mA at the exit of the ion source for user operation (corresponding to 50 mA peak current to RCS). In December 2024 and March 2025, the ion source extracted more than 72 mA beams for high-intensity beam study. Figure 6 shows the continuous operation time record and the beam current increase of the RF ion source (from 2014). The replacement cycle has gradually extended with increased operational experience. In RUN#91 (Nov. 2023 – July 2024), the continuous operation time of the ion source was extended to 4,962 hours. (6.9 months) without replacing the ion source during the run.

The RF internal antenna coil had previously been procured from a single supplier. To ensure inventory security and improve procurement reliability, a J-PARC-made antenna coil was developed. We have confirmed that no significant impurities were emitted from the antenna, and the horizontal and vertical emittance of the H^- beam were comparable to those observed with the currently used antenna coil. An endurance test of the RF input energy to the antenna coil was also carried out. This offline bench test simulated more than around 5,500 hours of the ion source operation. To speed up this test, the RF input and duty cycle were increased. The test has conducted with an average RF power of 3 kW, which is five times higher than nominal

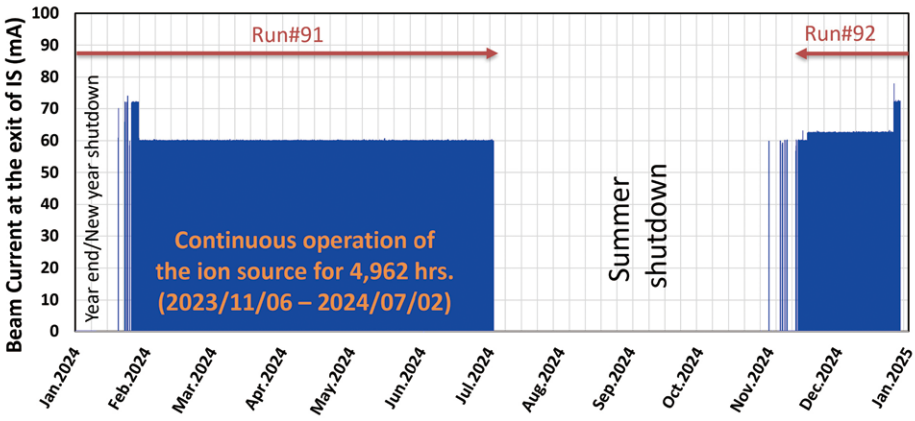

Fig. 5. Operation history of the ion source in FY2024

operation. Durability was verified by testing three antennas, all of which remained intact throughout the tests.

RF cavities

The RFQ trip rate is approximately 12/day at 25 Hz beam operation to the MLF in FY2024, the same as before. An auto-restart system for the RFQ trip has been running since March 2020. The system resumes beam operation at the next macro-pulse after the RFQ trip. Also, the beam stop associated with RFQ trips (e.g., MPS by the beam loss detection) occur approximately once a day during the user operation.

RF trip by detecting the arcing (fast interlock system cut off the RF input when light emission is detected via an optical fiber) at the RF window occurred frequently in SDTLs 14A and 15A. To investigate, a movie camera was attached to the cavity view port on the opposite side of the tank, and the light emission was observed at both cavities as shown in Fig. 7. Discoloration was observed near the edge of the ceramic windows of the removed RF couplers, so they were replaced with new ones during the winter maintenance period. After the replacement of these couplers, the cavity operation became stable during user operation.

The average trip rates per cavity of DTLs and SDTLs in FY2024 were approximately 0.2 trips per day. The operation of the ACS cavities was more stable than the other accelerator sections. The number of trips of all the ACS cavities was less than once per day.

RF system

We use 20 klystrons for the 324-MHz system, and 25 klystrons for the 972-MHz system. The operation time of the oldest five klystrons reached more than 98,000 hours for the 324MHz system, which corresponds to the entire period since the linac operation was started. In 2024, two 324-MHz klystrons were replaced with new ones due to the decrease in breakdown voltage. Operating times of the failed klystrons were 47,700 h and 93,000 h for DTL1 and SDTL05, respectively. No 972 MHz klystron was replaced in FY2024. The operation time of most klystrons for the 972MHz system reached more than 67,000 hours. The operation time of the klystrons as of the end of March 2025 are shown in Fig. 8.

In the klystron high-voltage power supply system, a degradation of breakdown voltage was observed near the connector of the 110 kV coaxial cable connecting the high-voltage DC power supply to the capacitor bank. The affected cable was replaced with a spare, and beam operation resumed about 20 hours after the initial shutdown.

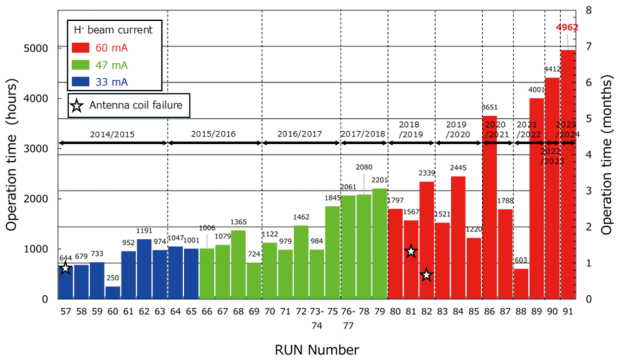

Fig. 6. History of continuous operation time of the RF ion source

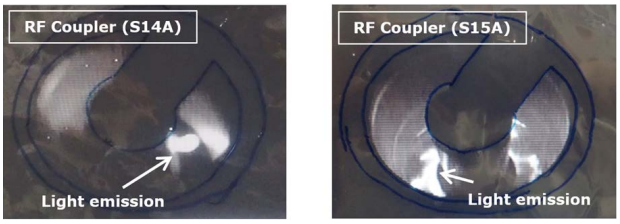

Fig. 7. Camera images revealed light emission near the ceramic window

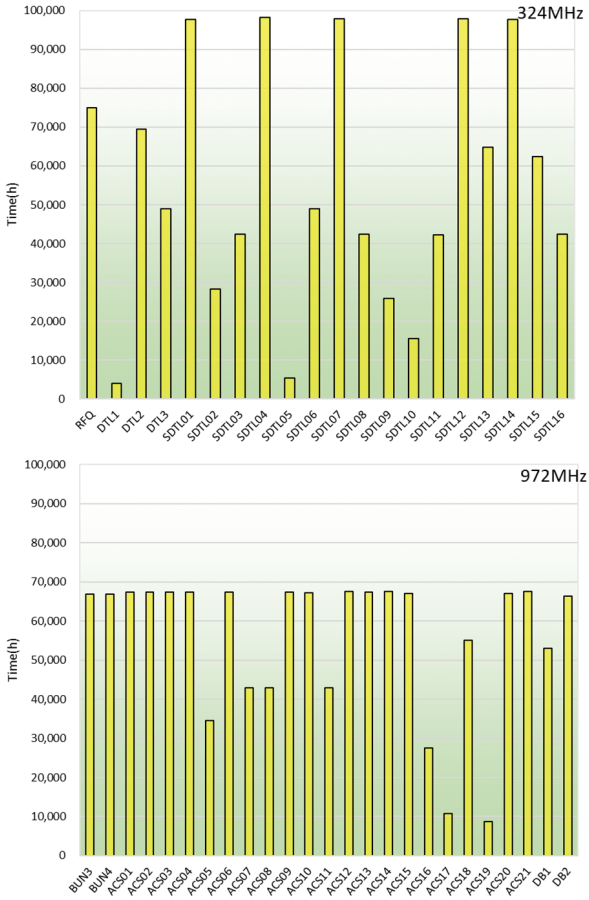

Fig. 8. The operation time of the 324-MHz klystron (top) and 972-MHz klystron (bottom) as of the end of March 2025

Beam study

At 50 mA, chop leakage remained within acceptable limits, consistent with results reported last year. At 60 mA, however, it became a significant challenge, not only due to the larger beam envelope associated with higher current but also as a consequence of earlier tuning strategies. Initial measurements at 60 mA revealed leakage levels exceeding the RCS requirements, as shown in Fig. 9, where the red trace (60 mA) clearly surpasses the allowable limit, thereby necessitating a revision of the 60 mA tuning strategy.

Subsequent beam studies identified improved settings that balanced transmission efficiency and leakage suppression, leading to a markedly reduced chop leakage level at 60 mA, as shown in Fig. 10, now well below the required level. Therefore, systematic studies of chop leakage dependencies on the LEBT, RFQ tank level, and scraper settings were conducted, and the optimized parameters for leakage suppression will be retained as a baseline for future high-current studies and operations, while further refinements will continue.

During routine 50 mA operation, beam transmission has been stable and reproducible, remaining suitable for long-term user operation with no significant losses observed downstream of MEBT1. However, in the early stage of 50 mA operation, a rapid increase in residual radiation was detected in DTL1, which was attributed to an enlarged beam envelope, suboptimal lattice settings, and alignment deformations induced by the 2011 Great East Japan Earthquake; this issue was successfully mitigated by locally increasing the quadrupole strengths.

Looking ahead to 60 mA operation, a central challenge will be preventing similar radiation build-up in the DTL while controlling emittance growth. Indeed, emittance growth was already evident in the MEBT1–DTL region at 50 mA and became more pronounced at 60 mA. To address this, simulations showed that stronger transverse focusing enhances transmission and suppresses emittance growth in the DTLs. Guided by these results, the DTL lattice was re-optimized with transverse focusing strengthened by 10–16%. Subsequent beam studies in December 2024 and March 2025 confirmed the effectiveness of this approach, demonstrating a 26% reduction in transverse emittance (Fig. 11) to a level comparable with 50 mA operation. These improvements were reproducible, underscoring the robustness of the method, and further investigations are planned to refine this scheme and assess its applicability to even higher-intensity operation.

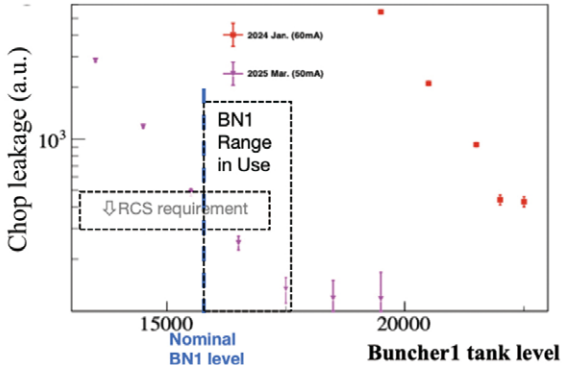

Fig. 9. First measured chop leakage for 60mA, January 2024

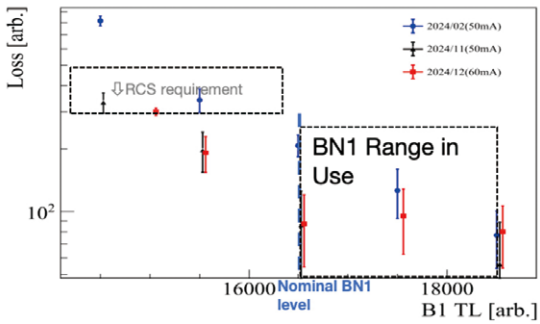

Fig. 10. Markedly improved chop leakage measurement for 60mA, December 2024

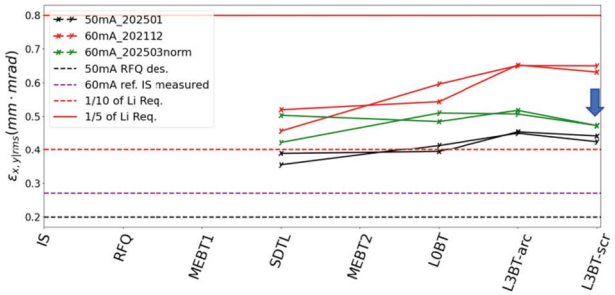

Fig. 11. Emittance improvement of 60mA, March 2025

RCS

Operation status

The RCS output beam power was limited to 950 kW-equivalent until FY2023 because one transformer-rectifier in the RF system was out of operation due to damage in

FY2022. A new transformer-rectifier was manufactured and installed at the end of FY2023, as shown in Fig. 12. Thereafter, the entire RF system could be operated and the full acceleration voltage restored, enabling the RCS to accelerate a 1 MW-equivalent beam again in FY2024.

The 1 MW-equivalent user operation for MLF started from April in FY2024 and the RCS could stably deliver a high intensity beam stably during that operation. This is an important milestone for J-PARC as it means that a design beam power for the user operation has been achieved. Figure 13 shows the number of particles per day delivered from the RCS to the MLF. The user operation for MLF started in FY2009 and the RCS has steadily increased the output beam power. A single-shot acceleration of 1 MW-equivalent beam at the RCS succeeded in FY2014, after which the comprehensive beam commissioning for the beam loss reduction and some improvements at the MLF target enabled us to achieve the desired design value in the 15th year.

After the success of 1 MW-equivalent user operation, the beam power has been reduced to 950 kW-equivalent again by intentionally keeping off part of the RF system to suppress electric power consumption and save costs. Just before the summer shutdown, there was a problem with the MLF target in which moisture was detected and user operation was stopped before the scheduled day. The RCS delivered the beam only to the MR during that period.

After the summer shutdown, regrettably the user operation for the MLF could not be restarted because a leakage happened at the mercury pump in the target. The RCS did not deliver the beam to the MLF in the latter half of FY2024 and delivered it only for the MR until February 2025. After that, there were unfortunately problems with both the neutrino target and the MR. Consequently, the RCS conducted the beam commissioning during Mar. in 2025. In these beam tests, the beam loss at 1 MW has been further reduced from that of 1 MW operation so far.

The availability of the RCS was not very high in the first half of FY2024 because the power supply of the bending magnet stopped so many times: 21 times in April and 11 times in May. The interlock information suggested that an over current happened at one of the choke transformers of the resonant network in the bending magnet system, and that an over voltage had also happened at the rectifiers in the DC power supply for the bending magnet. We checked the high power main circuit of the power supply and also checked the resonant network consisting of the choke transformers and capacitor banks according to the interlock information. However, we could not find any problem in these parts. In fact, each time the power supply stopped, it was possible to restart it.

After many stoppages, we noticed that the sudden stopping of the power supply triggered the interlock of the over current and over voltage. This meant the over current and over voltage were not the cause but the result of the interlock. Furthermore, we noticed that the DC power supply sometimes stopped alone before the AC power supply turned on. After that, we suspected problems with the control system of the DC power supply, and measured the control signals at the DC power supply. Finally, we found that the operation command signal was suddenly going down at the DC power supply, due to the malfunction of the DAC board for the reference signal generation. After replacing the DAC board with a spare one, the power supply no longer stopped. The total

Fig. 12. Installation of the new transformer-rectifier

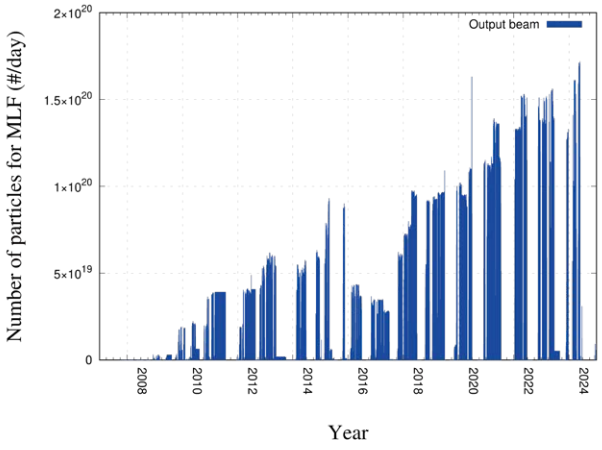

Fig. 13. History of the number of particles per day for the MLF from the RCS

amount of time that operations were suspended before the cause was identified was 72 hours.

Consequently, the availability of the RCS for MLF user operation in FY2024 was 95.1 %, while it was 98.3 % in FY2023.

Hardware improvement

We have been replacing RF cavities since 2021. The new single-ended cavity consumes 40% less power at 1 MW beam acceleration than the conventional push-pull type, as shown in Fig. 14. Furthermore, it can accelerate the beam up to 2 MW using existing power supplies and amplifiers. Three cavities were replaced during the summer shutdown in FY2024, bringing the total to 6 of 12. The replacement work will be completed in FY2028.

We also have been installing a transverse instability damper for the kicker magnet since 2022. The instability damper consists of the diodes and resisters as shown in Fig. 15. Two instability dampers have been installed additionally during the summer shutdown in FY2024. Consequently, four of the eight kicker magnets have been fixed by the instability dampers. The beam commissioning and simulation results suggest that this situation is adequate to restore the transverse tunability up to 2 MW beam acceleration.

For the charge exchange foil, a pure carbon foil made at J-PARC has been used since FY 2023 instead of the Hybrid type thick Boron-doped Carbon (HBC) foil, which was used before. The advantage of the pure carbon foil is that the deformation is smaller than the conventional HBC foil. Five pure carbon foils have been used from FY2023 to FY2024, and 1 MW user operation for MLF and 800 kW user operation for neutrino have been successfully conducted by using the pure carbon foil. As a result, we are confident about using the pure carbon foil and decided to install only pure carbon foils into the stack of the charge exchange equipment after the summer shutdown in FY2024.

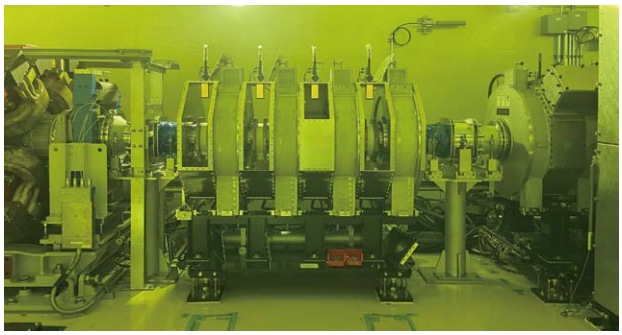

Fig. 14. Installation of the new cavity

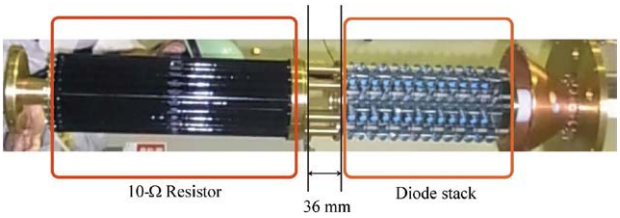

Fig. 15. Impedance damper

Summary

In FY2024, the RCS could accelerate the 1 MW beam again because one of the transformer-rectifiers in the RF system recovered. The stable user operation of the 1 MW beam for the MLF has been achieved and this was an important milestone for J-PARC.

On the other hand, the RCS experienced problems and availability was worse than in previous years. In particular, it took a long time to resolve the problem of the bending magnet power supply.

Three new RF cavities with lower than conventional power consumption were installed successfully, and 6 of the 12 cavities have now been replaced so far. Furthermore, two transverse instability dampers for the kicker magnets were installed and four of the eight kicker magnets have been fixed so far. This situation was enough to restore the transverse tunability up to 2 MW beam acceleration.

MR

Overview

The J-PARC Main Ring (MR), which provides 30-GeV proton beams to the neutrino experimental facility (NU) by fast extraction (FX) and to the hadron experimental facility (HD) by slow extraction (SX), is now in the middle of the beam power ramp-up.

In the FX mode operation, a project to increase the beam power to more than 1 MW is in progress. We are now increasing the beam power while reducing the operation cycle and increasing the beam intensity step by step in line with hardware upgrades, finally aiming to achieve 1.3 MW with a repetition cycle of 1.16 s and a

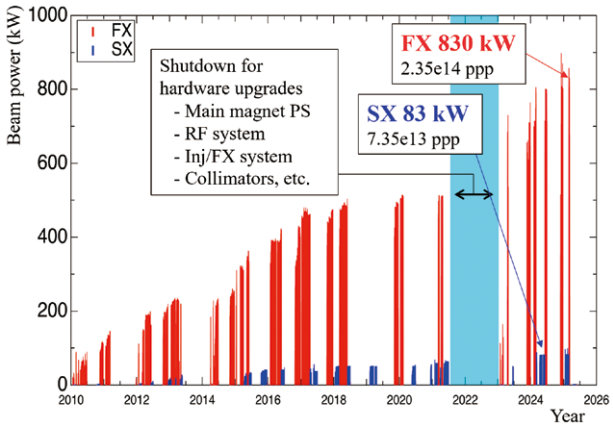

Fig. 16. MR beam power achieved to date

Fig. 17. Replacement work of the main bending magnet

beam intensity of 3.3×10^{14} ppp. To realize faster repetition rates and accommodate higher beam intensities, the MR upgraded the main magnet power supplies, RF system, injection and fast extraction devices and collimators with a shutdown period of around one year from July 2021. Via the hardware upgrades, the FX operation cycle has been shortened from 2.48 s to 1.36 s to date, and beam commissioning at this operation cycle is being vigorously promoted in parallel to user operation. In FY2024, the FX beam power continued to increase steadily in line with the progress in beam dynamics tuning and hardware improvements, achieving a stable beam operation at a beam power of 830 kW. This broke the 760 kW recorded in FY2023 (Fig. 16).

Beam power upgrade in the SX mode operation is also underway. In FY2024, with a repetition cycle reduced from 5.20 s to 4.24 s, we realized a stable beam operation at a beam power of 83 kW (Fig. 5), exceeding the previous record of 64 kW, which was achieved before the high-repetition rate upgrade.

The MR beam operation before the summer shutdown was interrupted several times due to mechanical problems such as a layer short of the main bending magnet coil, a failure of the IGBT unit in the SX bump magnet power supply, and a rise in the cooling water temperature due to a cooling tower failure. However, all these problems were addressed, and the MR steadily improved its beam performance and continued to operate stably thereafter. The operational availability of the MR in FY2024 was 84% (NU) and 87% (HD).

Layer short of the main bending magnet coil

On May 5, 2024, during SX beam operation, a layer short of the upper coil in the main bending magnet occurred. At that time, the beam was unable to complete even one revolution and was lost immediately after the failed main bending magnet. Since there was no abnormality in the output current of the power supply, the main bending magnet was inspected in the tunnel. Although no abnormalities were found in visual and odor inspections, a significant decrease in the impedance was observed for the upper coil, confirming that there was a short in the upper coil layer.

Fortunately, a spare main bending magnet was available so we were able to replace the failed main bending magnet (Fig. 17) and resume the beam operation within two weeks. In addition, in preparation for the recurrence of such a failure, the failed main bending magnet was repaired. Since there was a spare upper coil, the failed coil was replaced with the spare during the winter beam shutdown period, and the magnet is now available as a spare.

This is the second failure due to a layer short of the main bending magnet coil. The first occurred in 2016. The previous failure was caused by a decrease in insulation performance due to water leakage from the coil joint. As there is a possibility that a similar cause led to the current failure, we plan to investigate the cause of the layer short in cooperation with the manufacturer and use the findings in the manufacture of the next spare coil.

Regarding hardware improvements implemented during the summer shutdown period, the MR is continuing hardware improvements in stages for further beam power ramp-up.

The collimator system had been upgraded in stages since 2021, and the last collimator unit was installed during the summer shutdown period in 2024 (Fig. 18). The number of collimators was originally four, but it has increased to seven. The current configuration of the collimators adequately covers all the directions in the

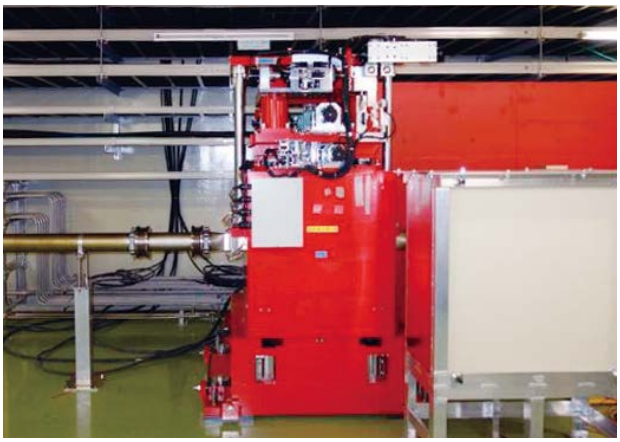

Fig. 18. Newly installed collimator

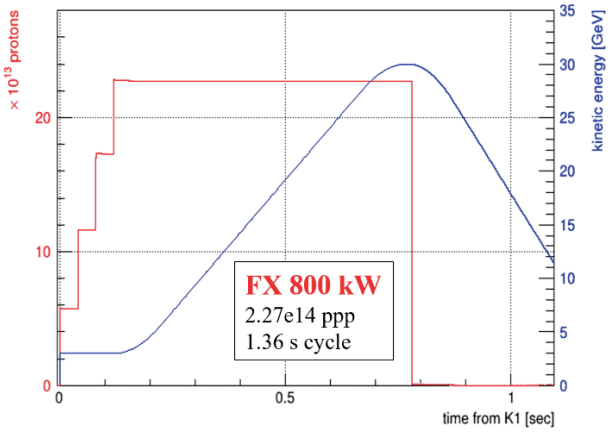

Fig. 19. Circulating beam intensity during the 800-kW FX operation, where "K1" indicates the timing of injection start

transverse phase space, achieving better beam loss localization efficiency as is shown later.

The power supply of the pulsed bending magnet, which is used to switch the beam destination to the MR and MLF, was also updated to address shorter FX operation cycles. Since its startup after the summer shutdown, it has been operating very stably.

The RF anode power supplies were also upgraded to accommodate higher beam loading. The number of output inverter units in each anode power supply was increased from (16, 12, 13) to (18, 14, 16) for the 4-gap cavities, 3-gap cavities and 4-gap second harmonic cavities, respectively. With this upgrade, the MR is now capable of beam operation of >900 kW.

In addition, main magnet power supply tunings were vigorously conducted. One is the current pattern tunings for a new beam optics to be introduced for further beam loss reduction, completed in the summer shutdown period as planned. Another is to further shorten the FX operation cycle from 1.36 s to 1.28 s. This is also progressing as planned and is to be completed by the next summer shutdown period in 2025, with the aim of introducing the shorter operation cycle after the fall of 2025.

FX beam tuning and operation

In FY2024, the FX mode operation was conducted in June 2024, November to December 2024 and February to March 2025.

As described in the last annual report, in December 2023, the MR reached a major milestone achieving a beam power of 760 kW, and exceeding the original design performance of 750 kW. Detailed beam dynamics tuning continued thereafter for further beam power ramp-up, including precise beam optics tuning to establish the 3-fold symmetry of the MR lattice; tune manipulation at the early stage of acceleration to minimize the effect of resonance crossing; intra-bunch feedback to mitigate beam instabilities; collimator gap adjustments; optics manipulation at the flattop to secure a sufficient aperture for the off-axis extracted beam trajectory; linac and RCS tuning to reduce the injection beam emittance, and more.

In addition, to improve the output current ripples of the main magnet power supplies, great efforts were made to reduce noises in their current feedback circuits. These continuous efforts in both beam dynamics tuning and hardware tuning steadily reduced beam loss and we achieved an 800-kW stable beam operation in June 2024 within the permissible beam loss level (Fig. 19); the beam loss was estimated to be 0.8% (0.6 kW) in the injection energy region and most of it was well localized at the collimator section (Fig. 20). Since then, the routine beam power has further increased along with the progress in beam dynamics tuning, reaching 830 kW as of March 2025.

In addition, in December 2024, after upgrading the RF anode power supplies, a 900-kW beam acceleration was successfully demonstrated for the first time, albeit with a single shot (Fig. 21). The beam loss was estimated to be 1.9% (1.7 kW). Although this is still well below the collimator limit of 3.5 kW, it needs to be reduced to less than 1% to maintain a sufficient hands-on maintenance environment. To this end, we plan to introduce new beam optics. In the new optics, the vertical phase advance in the arc section is adjusted to minimize the driving terms of the systematic resonances near the operating point, so further beam loss reduction is expected. As described above, the hardware preparation

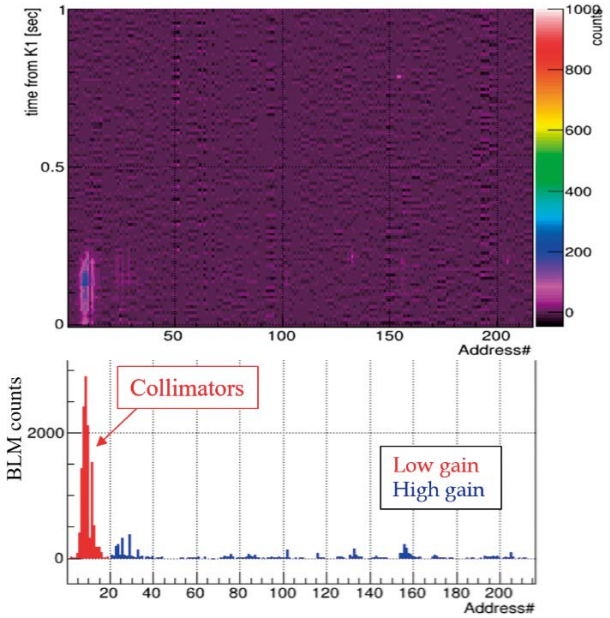

Fig. 20. Beam loss monitor counts along the ring during the 800-kW FX operation, where "address" indicates the sequential number of the main quadrupole magnets

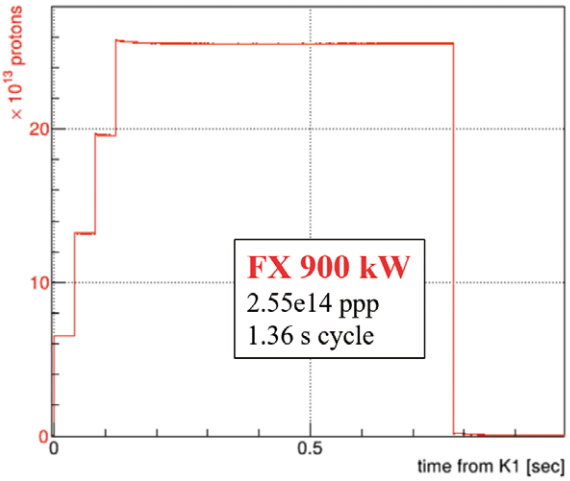

Fig. 21. Circulating beam intensity during the 900-kW FX beam study

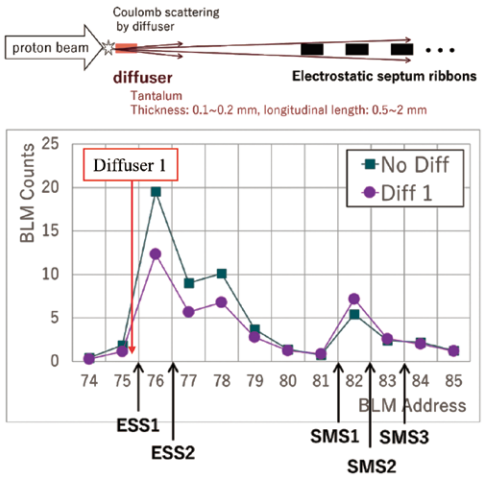

Fig. 22. Beam loss monitor counts in the SX section during the 80-kW SX operation with and without the diffuser

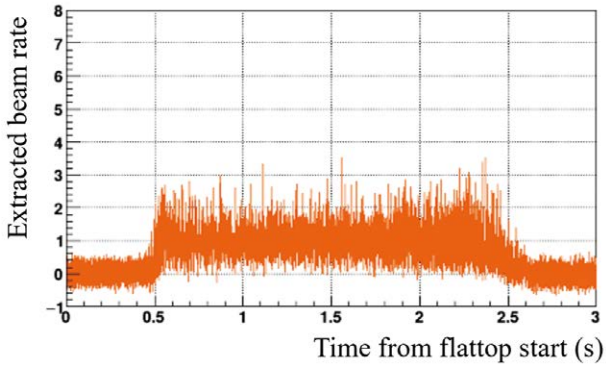

Fig. 23. Beam spill structure during the 80-kW SX operation

for the new optics is complete. We aim to achieve a stable beam operation at >900 kW with further efforts for beam loss reduction.

SX beam tuning and operation

The SX mode operation was conducted in April to June 2024 and January to February 2025.

In April 2024, the MR launched its first SX operation with a repetition cycle reduced from 5.20 s to 4.24 s. A two-step de-bunching technique mitigated beam instability excellently during SX. Furthermore, a diffuser installed upstream of the first electrostatic septum (ESS) successfully reduced the number of beam particles hitting the ESS ribbons, leading to significant beam loss reduction (Fig. 22). Via these efforts, in June 2024, we achieved a beam power of 83 kW with extremely high extraction efficiency of 99.65%, which broke the previous records (65 kW and 99.5%). The spill duty factor was also significantly improved from 61% to 83% through the optimization of the transverse RF knockout parameters and the spill feedback control based on the real-time beam rate measurements (Fig. 23). The current ripple reduction of the main magnet power supplies also contributed to the improvement of the spill duty factor.

The next goal in the SX mode operation is to achieve 90-kW beam power in early FY2025 and proceed with further beam tuning with a view to 100-kW beam operation.

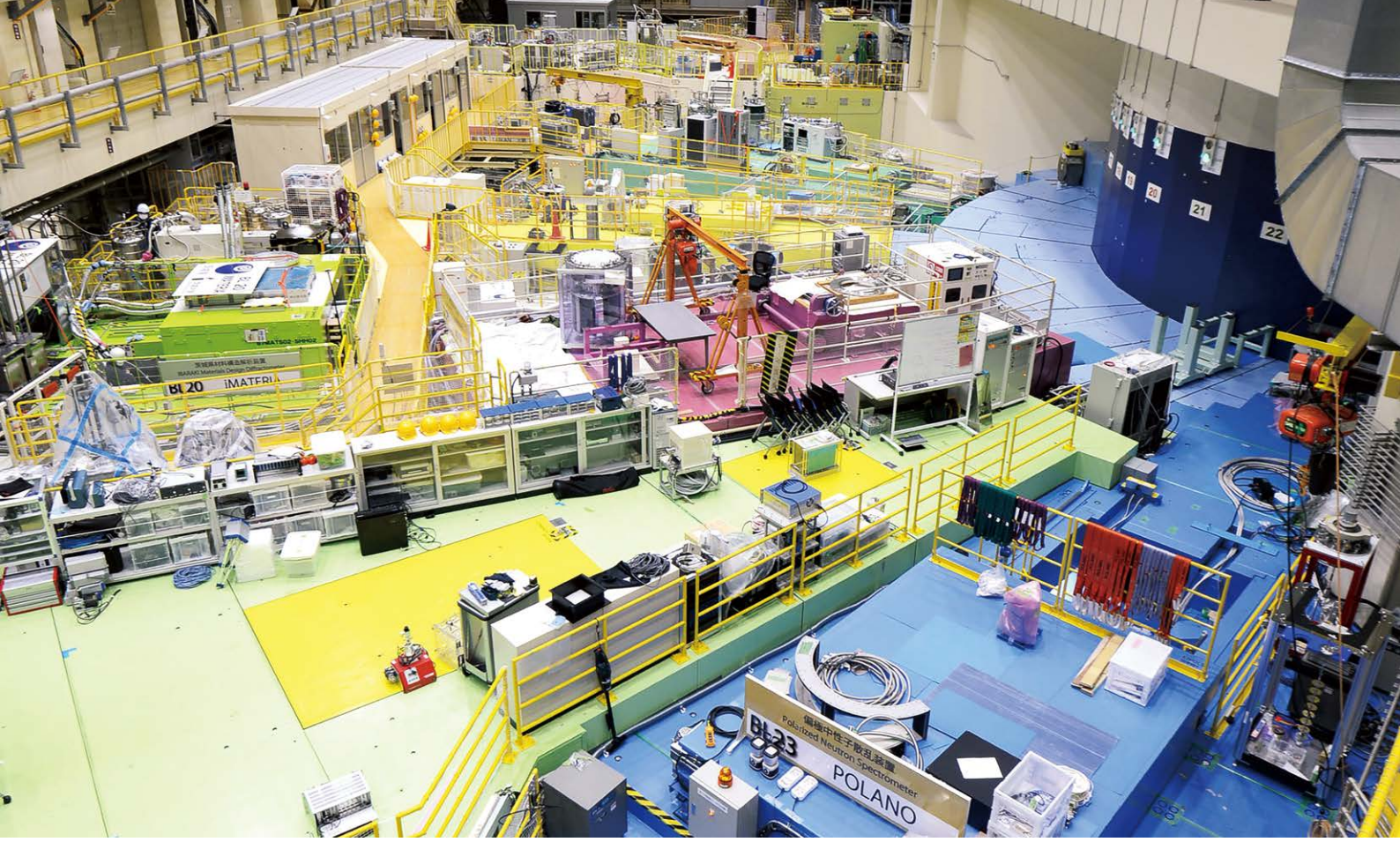

Materials and Life Science Experimental Facility

Overview

The neutron target system has undergone continuous improvements to achieve stable operation at 1MW proton power and a 2-year lifetime for the target vessel. In 2024, MLF operated stably with a beam power equivalent to 1 MW (the highest recorded) from April 8 to May 29. This marks a significant milestone for MLF. However, the neutron target system subsequently encountered difficulties, resulting in the outage of user programs. In June, there were issues with water detection in the Helium Vessel. In December, there was a gas leak from the mercury circulation system pipe. The former problem led to the termination of the 2024A operation, a week earlier than initially planned. The latter terminated all user programs in FY 2024. This is a serious situation for MLF, and we sincerely apologize for the inconveniences caused by the outage.

In addition to the risk reduction of the neutron target system maintenance, the "MLF-double" project is underway to enhance the effectiveness of MLF. Its goals are not only scientific outcomes, but also strengthening the robustness of the facility operation, gaining neutron and muon flux at the sample position, constructing beamlines at vacant beam ports, forming sustainable development teams of devices and software, and so on. Some of these have already been completed. It is crucial to engage in discussions with the community regarding the MLF roadmap from short-term to long-term. MLF-double is the middle-term roadmap until 2030, and the target station two (TS2) aiming at starting user programs with TS2 until 2040 is the long-term roadmap. These are continuous roadmaps to pursue higher potentialities of neutron and muon science. Opportunities to discuss with the community of MLF have been provided

since 2024. At the MLF symposium (domestic) in March 2024, MLF-double was presented. In the J-PARC symposium in October 2024, the future plans of J-PARC, ISIS, SNS, ESS, and PSI were presented. Additionally, five satellite meetings of the J-PARC symposium were held: the 19th Korea-Japan Meeting on Neutron Science, Deuterium Science Entering an Advanced Phase, Future on Muon Elemental Analysis (FUME), the 9th International Symposium of Quantum Beam Science at Ibaraki University (ISQBS2024), and a Workshop on Polarized Neutron Sciences and Technology.

Advancements in neutron and muon science have led to the exploration of new fields. The application of muons to interdisciplinary studies with heritage science and quantum beams (muon, neutron, and synchrotron radiation) has emerged as a global trend. Two international conferences in this field were held, the KEK "Cyprus Meets Japan" symposium in Cyprus, and the International Conference on Neutron in Heritage Science (NHS2024) in China. Additionally, the 9th Symposium on "Integration of Arts and Sciences" in Akihabara, Tokyo, attracted over 200 attendees, including online participants.

Two annual meetings were convened to identify new applications and fields for MLF activities. The Annual Meeting on Industrial Application for Neutron was held on July 21-22 as a hybrid meeting to effectively promote the utilization by enterprises and industry of MLF and the reactor neutron source JRR-3 of JAEA.Approximately 247 participants attended in person, while 135 participated online. MLF consistently engages with these parties and organizations to foster mutual benefits through the utilization of quantum beams. The Neutron & Muon School was held from December 9-13 as a KEK-IINAS School (Inter-Institution Network for Accelerator Science) at J-PARC and JRR-3 campuses. 72 participants attended online lectures, while 31 attended face-to-face lectures and theses-on-training sessions.

We will continue to maximize the utilization of MLF, one of the most advanced neutron and muon facilities. We cordially request your collaboration in helping to shape the profound impact of MLF activities.

Neutron Source Section

1. Operational overview

The beam operation for the user program in FY2024 started on April 8 with beam power of 990kW, equivalent to 1MW (the highest recorded), at the outlet of the 3GeV rapid cycling synchrotron (RCS) (950kW at the MLF) and continued until May 29. A press release was issued (https://www.j-parc.jp/c/en/press-release/2024/05/31001348.html). From May 29, the beam power decreased to 900 kW due to a budget shortfall caused by soaring electricity costs. Moreover, from June 5, the beam power was further decreased to 830kW due to a change of the accelerator mode of MR. The beam operation of MLF ended on June 24 due to the detection of water problems in the Helium Vessel, and maintenance works during the long outage started.

When the MLF beam operation started on December 9 after the long outage, the monitoring value of the radioactivity at the MLF exhaust tower showed a tendency to be higher than normal, and the beam operation was suspended. It was suspected that the sealing performance of the mercury pipe flanges, which were fastened during the replacement of the mercury pump, was insufficient. Therefore, we improved the remote handling method and work procedures, and successfully replaced the metal O-rings on the mercury pipe flanges. After resuming beam operation on April 7, normal monitoring results from the MLF exhaust tower were observed, allowing the 900kW proton beam user program to start on April 15.

The availability of the beam operation for the user program before the long outage in FY2024 was 82.1% but MLF was out of the operation in the latter half of FY2024.

2. Maintenance work overview

As previously mentioned, the long outage at MLF started on June 24. On July 18, the mercury target vessel used, which was in operation from 2018 to 2019, was transported from the MLF to the storage building (the so-called RAM building), where a total of seven used target vessels were stored at that time. The problem with the water detection in the Helium vessel was investigated and the cause was presumed to be the slightly humid air inflow. Therefore, countermeasures were taken to avoid this occurrence.

On September 9, specimens were cut out success-

fully from the fore front wall of the used target vessel which was operated for the long-term user program with the highest beam intensity recorded of 950 kW. The maximum damage depth on the specimens was measured and the full beam power (1MW) for the next two-year operation of the target vessel was decided.

In September, a problem at the power manipulator which remotely loosens and tightens bolts of the target vessel occurred. After investigation, it was found that the cause of the problem was the failure of an electrical device. The power manipulator could be operated normally by replacing the electrical device, resulting in a three-week delay. After that, the mercury target vessel used was successfully replaced with a new one on October 21. The new one has an improved mercury flow channel structure with the split bubbler generator, similar to the previous target vessel used during 2023 and 2024.

For the first time since the MLF operation started, the mercury circulation pump (Fig. 1) was also replaced successfully from November 5 to November 8. In parallel, periodic voluntary inspections of the cryogenic circulation system were conducted in accordance with the High Pressure Gas Safety Law, and it was confirmed that there were no major problems.

After the maintenance works ended and the MLF beam operation started, it was found that there were signs of unusual radioactive material during the proton beam tuning from December 9. It was suspected that the sealing performance of the mercury pipe flanges, which were fastened during the replacement of the mercury pump, was insufficient. Therefore, we repeatedly practiced remote-handling works to fasten the pipe flanges properly using mockups, and improved the remote control method and work procedures (Fig. 2). Finally, the metal O-rings on the mercury pipe flanges were success-

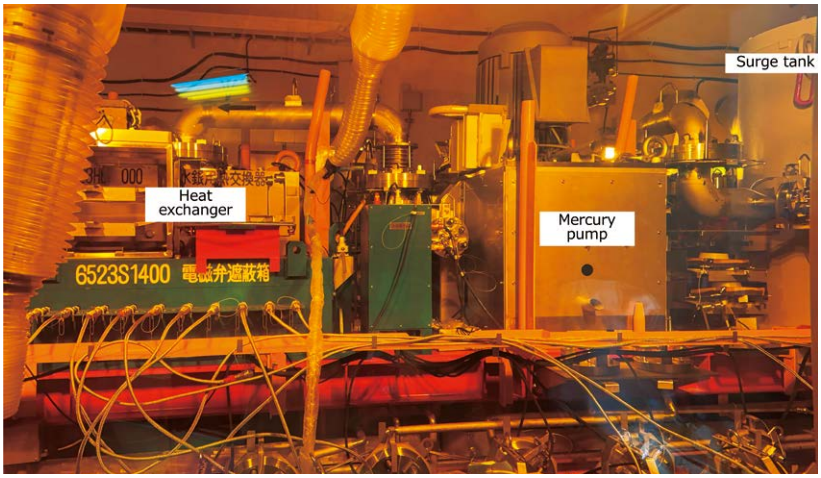

Fig. 1. The mercury circulation pump on target trolley in hot cell room

Fig. 2. The remote handling practices at HENDEL building (uncontrolled area)

fully replaced.

The remote handling test of the moderator and reflector assembly was conducted using a spare assembly, as in the previous year. An assembly consists of three moderators, a reflector and a shielding plug, and only the used moderators and reflector are replaced, while the shielding plug is reused, similar to the proton beam window. Because the operating lifetime of a moderator and reflector assembly is relatively long, 30,000 MWh, equivalent to 8 years at 1MW, the previous remote handling operation was conducted during the commissioning period before the MLF beam operation began more than 10 years ago. Unfortunately, as a problem occurred during the test, the test was not completed and it will be retried later.

Neutron Science Section

1. User program

In the period of the year 2024, 147 (out of 301 applicants) and 113 (321) proposals have been approved as general neutron experiments for the proposal rounds 2024A and 2024B, respectively. The Promotion for Industrial Use and the Priority Use for National Projects were also admitted for new proposals. For the long-term proposals 2024L, Neutron Science Section (NSS) had six applications of which three were successful together with four ongoing proposals for the next term, and two completed assignments were reviewed.

In 2024, the MLF encountered several problems costing many experimental days. As a result, a large number of experiments had to be postponed, causing a lot of confusion not only among visiting users but also at the MLF site. Most of the experiments can be carried over the next round 2025A.

2. Instruments update

A new scintillation detector system has been accommodated at the backward detector bank of Super-HRPD (BL08) attempting single crystal measurement. The two-dimensional ^{6}Li glass scintillator can provide spatial high-resolution with a single pixel size of 6 x 6mm^2 sufficient for detecting sharp Bragg peaks from single crystals. Also, in a newly developed area detectors for sharp peaks from single crystals were mounted at the SENJU (BL18) diffractometer. The set of new detectors has a size of 128 x 192 pixels, far surpassing the previously used standard size of 64 x 64 pixels (see Fig. 3). Two detectors have been installed in 2024, and it is planned that there will be nine of the same types of detectors, not only expanding the detecting area but also making the measurements appropriately without detector bank gaps.

We have made many efforts to realize neutron polarization analysis based on pulsed-neutron source for several years. POLANO (BL23) is one of those instruments utilizing polarized neutrons for inelastic measurements in MLF. After taking a long time to develop and manufacture the polarization and magnetic devices, all those device components were placed on the POLANO beamline by 2023. In 2024, on-beam polarization commissioning had been commenced. In Fig. 4, the first data on liquid sample deuterated methyl acetate $C_3D_6O_2$ is shown. The data set of non-spin flip (NSF) process and spin-flip (SF) process shows a large difference in scattering processes originating different scattering cross-sections.

3. Other activities

The Neutron Science Section (NSS) was arranged and contributed to several meetings below. Through these activities many of the ideas, discussions, and cooperations are fostered.

1) Joint J-PARC-ESS & SAKURA Workshop (June 10-12, 2024 at J-PARC Research Building)
2) The Annual Meeting on Industrial Application for Neutron (July 11th-12th, 2024 at Akihabara Convention Hall)
3) The 4th J-PARC Symposium 2024 (October 15th-17th, 2024 at Mito City Civic Center)
4) The 8th Neutron and Muon School (December 9th-13th, 2024 at J-PARC)
5) Quantum Beam Science Festa 2024 (March 12th-14th, 2025 at TSUKUBA International Congress Center)

Regarding other outcomes from neutron beamlines at MLF, 207 scientific articles have been published in the year of 2024, and 19 press releases also issued.

4. Awards

Sixteen MLF-related awards were given this year, and the following three represent the main contributions

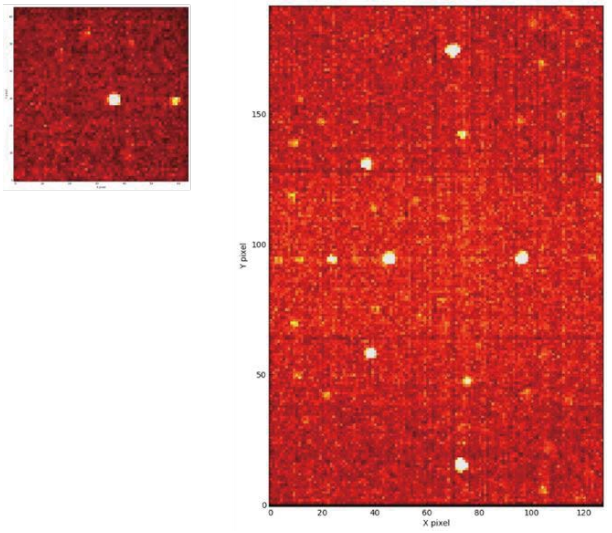

Fig. 3. Diffraction pattern of the standard sample ($12CaO \cdot 7Al_2O_3$) observed with the new detector (right). The detector area has increased significantly compared to the conventional detector (left).

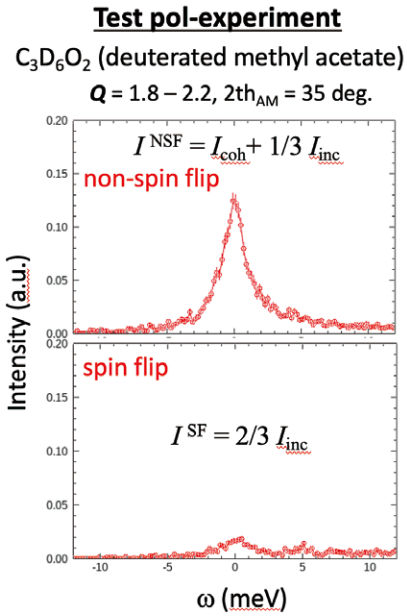

Fig. 4. Polarized neutron-diffraction measurements for deuterated methyl acetate $C_3D_6O_2$. The separation of coherent and incoherent scattering can be achieved by independently conducting spin-flip and non-spin-flip measurements.

of the NSS.

1) The 22th Young Researcher Award, The Japanese Society for Neutron Science
   "Research on Novel Physical Properties in Ce Compounds", UETA Daichi (BL12)
2) The 22th Young Researcher Award, The Japanese Society for Neutron Science
   "*In Situ* Pulsed Neutron Diffraction Study on the Mechanism of Mechanical Properties of Advanced Structural Materials", YAMASHITA Takayuki (Former Post Doc. BL19)
3) International Magnesium Science &Technology Award Excellent Paper of the Year
   "*Strengthening of aMg and long-period stacking ordered phases in a Mg-Zn-Y alloy by hot-extrusion with low extrusion ratio*", HARJO Stefanus, GONG Wu, AIZAWA Kazuya, KAWASAKI Takuro, YAMASAKI Michiaki (BL19)

Neutron Instrumentation Section

A large, rectangular scintillation neutron detector has been developed for the major upgrade of SENJU, a time-of-flight Laue neutron diffractometer constructed in the MLF in 2012 [1]. Thirty-seven detectors have been implemented in the instrument, where each detector module has a moderate detection area of 256 × 256 mm^2 [2]. By replacing the original detectors with the larger ones the physical gaps between the original detector modules can be decreased. Hence, it improves the data collection efficiency of SENJU significantly.

Figure 5 shows a photograph of the developed prototype large area detector [3]. The prototype detector is made based on ^{6}Li:ZnS scintillator and wavelength-shifting fiber technology. The detector has a neutron-sensitive area of 512 × 768 mm^2. A pixel size is maintained to 4 × 4 mm^2 similar to that of the original detector. The neutron-sensitive area is six-fold of the original detector. The filling factor, which is defined as the ratio of the neutron-sensitive area to the detector surface, improves from 0.73 to 0.85 compared to the original detectors. The prototype detector exhibited a detection efficiency of 43±3 % for a neutron with a wavelength of 2.1 Å, and a ^{60}Co gamma-ray sensitivity less than 10^{-7}. These detector performances are acceptable for use in the beamline. The large-area detectors offer advantages beyond the simple benefit of replacing

Fig. 5. Photograph of the prototype large area detector for SENJU

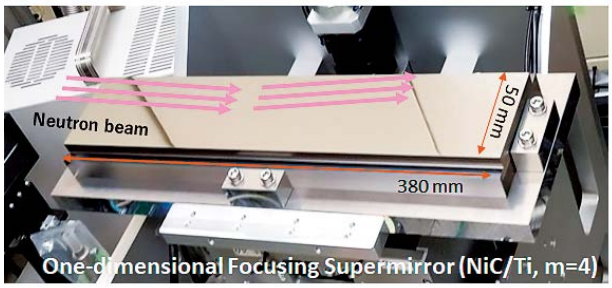

Fig. 6. Photograph of the one dimensional elliptical focusing supermirror

multiple detectors with a single unit. The reduced area of the detector edges relative to the detection surface increases the effective area available for data analysis. It also facilitates sample alignment and contributes to the efficient use of the allocated beam time. Currently, two large area detectors are installed in the instrument, and their effectiveness has been demonstrated. Plans are underway to add seven more detectors in future.

Neutron focusing devices are extremely important to enhance the neutron intensity at a sample. A large-size neutron focusing supermirror has been developed by using an ion beam sputtering apparatus. Figure 6 shows a photograph of a one-dimensional elliptical neutron focusing supermirror designed specifically for one of the neutron reflectometers, SHARAKU. The NiC/Ti multilayer films are sputter-deposited onto a quartz substrate that is figured into an elliptical shape. This supermirror focuses a neutron beam to a small spot at more than 3 m downstream of the mirror, achieving high neutron brilliance equivalent to tens of times the values achievable with conventional slit collimation. Feasibility tests are being conducted to realize Grazing-Incidence Small- Angle Neutron Scattering measurements in SHARAKU.

References

[1] K. Oikawa et al., JPS Conf. Proc. 1, 014013 (2014)

[2] T. Kawasaki, et al., Nucl. Instr. & Meth. A 735, 444 (2014)

[3] T. Nakamura, et al., presented at Position-Sensitive Neutron Detectors 2024 (PSND 2024), Oxford, Apr. 2024.

Muon Section

1. Overview

While the MLF achieved stable high-power operation at 1 MW at the beginning of this fiscal year, beamtime before summer maintenance and after February was cancelled due to problems at the neutron source. Though it is regrettable that the muon facility also lost the opportunity to produce results at 1 MW, each muon beamline has been upgraded for the future and stabilized to avoid unexpected trouble. This article provides an overview of some notable topics in the Muon Section.

2. H line extension

In the H-line, the highest-intensity muon beams with a wide-tunable range of momentum are available, and a precise measurement of the hyperfine structure of muonium (MuSEUM), a search for μ-e conversion (DeeMe), etc., are at present conducted in only the H1 general-purpose experimental area. The extension plan for the new H2 area was launched, and a new branch was constructed. In the H2 area, the frontend part of the muon accelerator will be installed. It will be extended further to produce a novel low-emittance muon beam by accelerating muons up to 212MeV using linear accelerators, most of which will be installed in an extension building next to the MLF. The low-emittance muon beam enables the J-PARC muon g-2/EDM experiment and a transmission muon microscope (TμM). The laser resonant

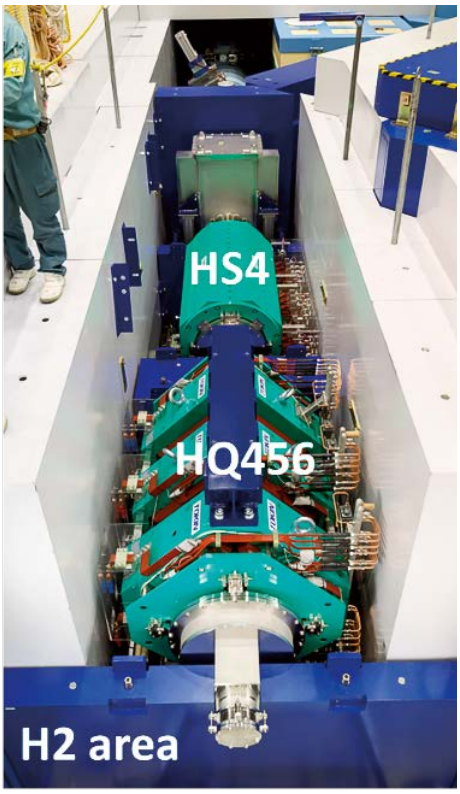

Fig. 7. New magnets installed in the extension of the H line to the H2 area

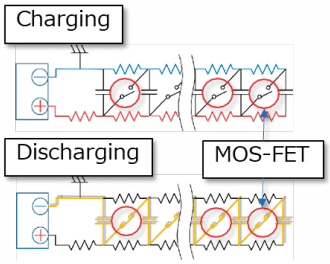

Fig. 8. A schematic figure of the MARX circuit

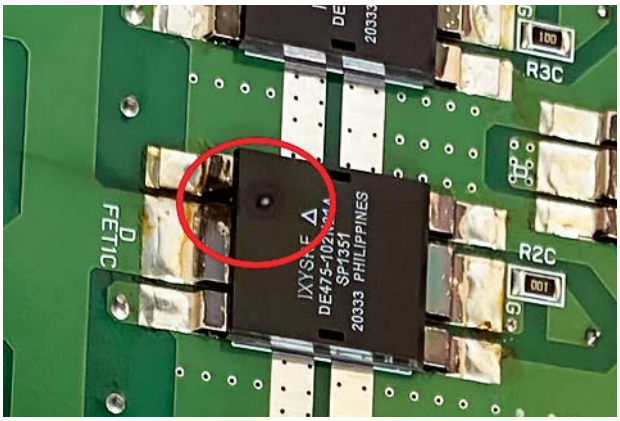

Fig. 9. The outer mold is damaged in the failed MOS-FET, suggesting heat due to conduction between the drain and the source.

ionization method developed in the U-line was adopted for muon cooling, which is key to efficient acceleration, and the preparation of an intense VUV laser system has been carried out. The beam commissioning is planned for the next fiscal year. As shown in Fig. 7, a new solenoid and a new quadrupole triplet with wide apertures of 610mm and 400mm respectively, were installed after the bending magnet that switches between the two experimental areas. As the final focusing magnets to the H2 area, they can achieve a low-loss transmission and a low-leakage field on the muon stopping target.

3. S line kicker system

The S line provides muon beams to all four experimental areas simultaneously; two areas are under operation, and the others are planned. A kicker magnet enables this operation by separating the double bunch structure of the muon beam. The kicker power supply consists of 24 MARX-type high-voltage generator units. In the original design, Si MOS-FETs were employed for fast switching (Fig. 8.). In recent years, the number of failure events in the MARX unit has increased, resulting in the stoppage of user experiments. The cause was identified as being deterioration due to the aging of the Si MOS-FET (Fig. 9.). Because Si units were discontinued and SiC units became compatible, we started replacing the Si MOS-FETs with SiC units. In the last fiscal year, a MARX unit was replaced with a SiC-based unit to demonstrate the operation mixed with the existing Si-based units. Based on the positive results, we replaced the other three units with SiC-based units and started fabricating substitutes for the remaining units in this fiscal year. In the next fiscal year, the whole system will be replaced. So far, no failures have occurred in the replaced units.

4. Progress in the U line

The U line provides the highest intensity surface muon beam among the four MUSE beamlines dedicated to generating the ultra-slow muon (USM) beam, which is essential for studying the material properties of thin films and interfaces. In the last fiscal year, improvements in USM beam transport efficiency and better compatibility with simulations were achieved. In this fiscal year, we focused on understanding the surface muon beam to enhance the USM yield and stability further. The generation efficiency of USM is critically dependent on the spatial overlap between the sur-

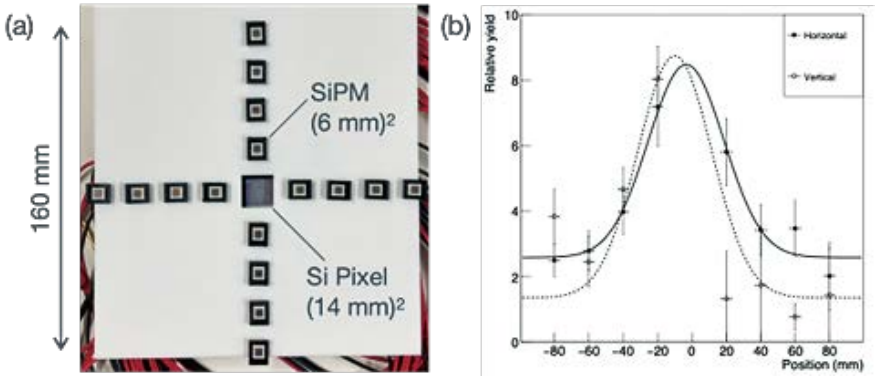

Fig. 10. Surface muon beam profile monitor: (a) Photograph of the detector. A 50 μm thick scintillation film was placed directly on top of the SiPM. (b) Profile measurement result under the transport conditions normally used for USM generation.

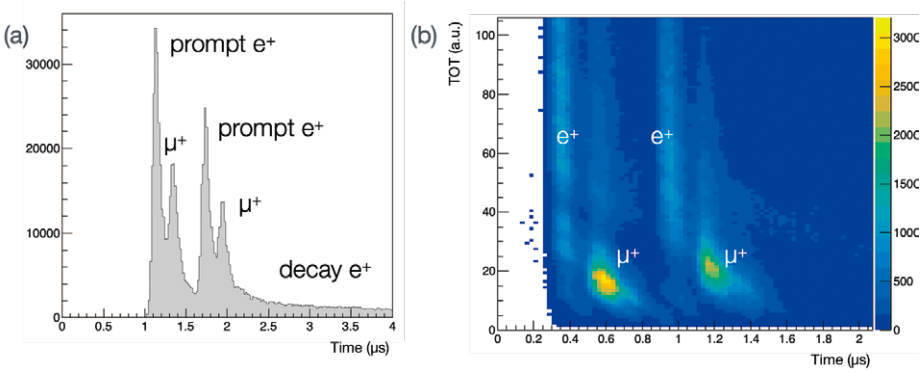

Fig. 11. Surface muon measurement with a silicon pixel detector: (a) Time spectrum, (b) Correlation between TOT and time. TOT is a quantity corresponding to the pulse height of the signal when a particle hits a pixel. TOT distinguishes Muons and positrons.

face muon beam and the ionization laser light. To measure the surface muon beam profile from the U line, which had been difficult to assess quantitatively, a new detector combining a thin-film scintillator and a silicon photomultiplier (SiPM) was developed. Using this detector, the beam profile was successfully measured as shown in Fig. 10. A detector based on the Timepix3 chip, developed by CERN, was integrated into the central part of the monitor. Figure 11 shows the measured time spectrum and the time-over-threshold (TOT)-time correlation. It was demonstrated that the beam flux can be measured while avoiding pileup effects. Using this detector, we can observe the source beam directly to identify and resolve hardware issues in the transport system. Moving forward, we will increase the USM beam intensity and stability.

Technology Development Section

Instrument control system

IROHA2 is the standard control software framework for J-PARC MLF. It integrates multiple servers, including instrument management, device control, sequence control, and integrated control, to support experimental procedures. Currently, many beamlines at MLF use IROHA2 to control experiment devices and data acquisition systems and perform the automatic experiment. Furthermore, IROHA2 has a web UI, allowing users to remotely execute experiments without requiring dedicated software installation. Fig. 12 shows a schematic diagram of the IROHA2 system.

In recent years, the MLF has been promoting open access to experimental data. To achieve this, attaching

metadata describing the measurements themselves to the neutron data is essential. In FY2024, we added a new feature to IROHA2 that retrieves sample and proposal information from the sample database and incorporates it into the measurement metadata for efficient data generation.

While IROHA2's web UI facilitates monitoring of measurement status, it lacks a mechanism for external services to check the status. Therefore, we implemented a web API that provides measurement ID and status information, enhancing cooperation with external services.

We intend to continue improving and maintaining IROHA2 over the next few years. Simultaneously, recognizing that IROHA2's technology is becoming outdated, we will also develop the next-generation control system.

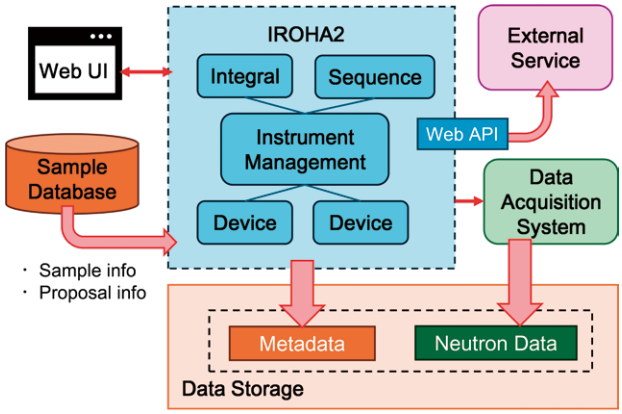

Fig. 12. The structure of IROHA2 and the relations with other systems

Software denoise and theoretical analyses

We applied deep learning based denoise to neutron 2D and 3D data [4]. Figure 13 shows a result on a Bragg edge imaging dataset. The spatial distributions of the materials properties from the denoised datasets became closer to those from the datasets of a better statistical quality. In the near future, we will verify this on phantom datasets with known materials properties. We will also consider the error bars in the denoised intensities.

We revisited the hydrogen nuclear quantum states calculations on H incorporated in metals and intermetallics within adiabatic approximation on the hydrogen nuclear potential. The potential was calculated through a series of first principles calculations. We reduced the number of calculations by using the spatial symmetry around the hydrogen atom. Our procedure can predict the H inelastic neutron scattering spectra for any atomic arrangements [5].

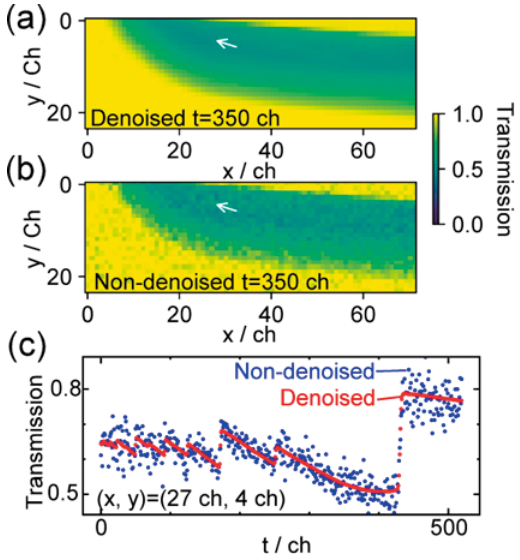

Fig. 13. Denoise example on Bragg edge imaging dataset: Cross-sections of denoised (a) and non-denoised (b). Denoised and non-denoised spectra (c), at position indicated by arrow in (a) and (b).

References

[4] K. Tatsumi et al., J-PARC symposium 2024.

[5] K. Tatsumi et al., J. Phys.: Condens. Matter 36 (2024) 375901.

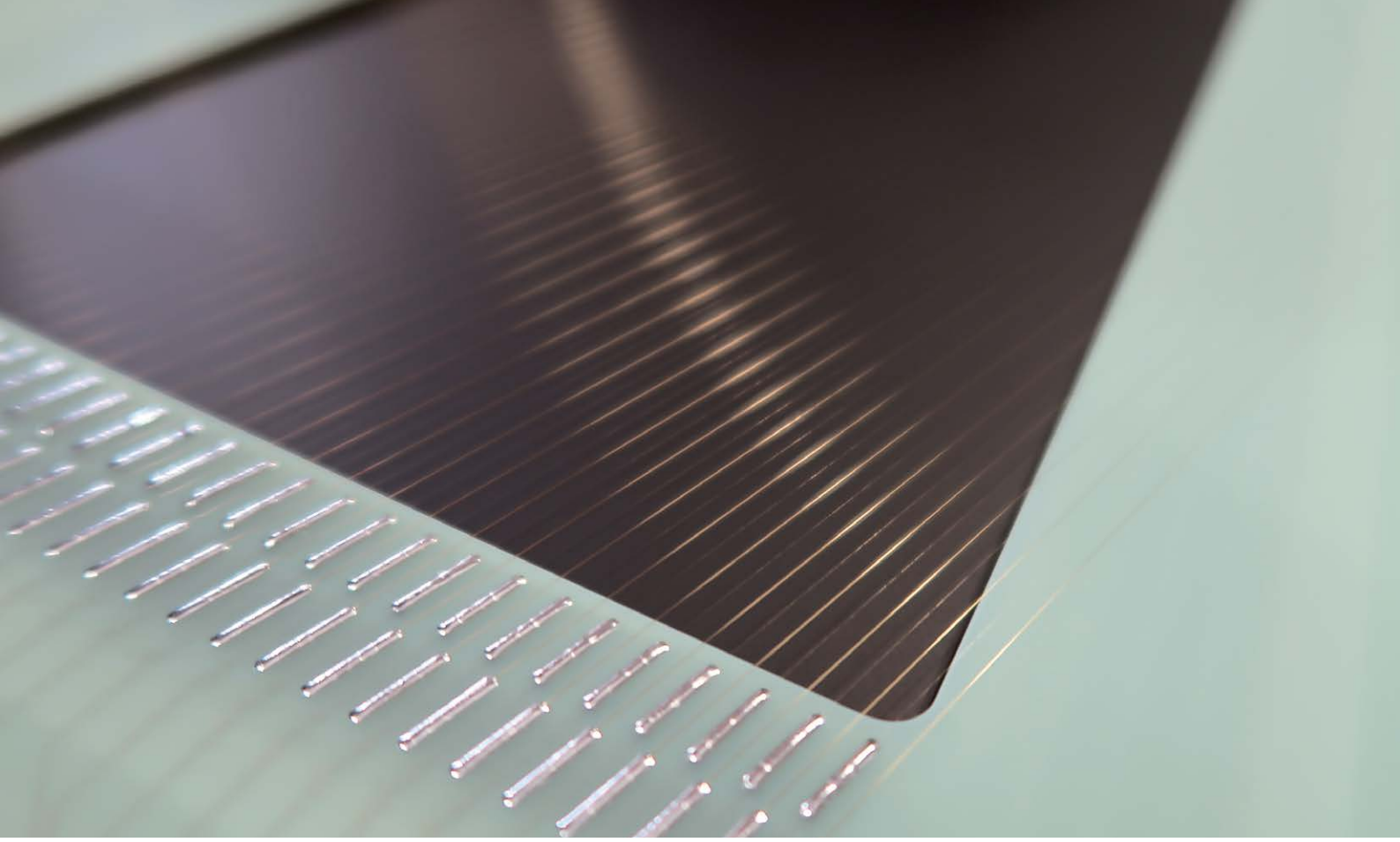

Particle and Nuclear Physics

Neutrino Experimental Facility

The Neutrino Experimental Facility sustained beam power at 810-830kW during 2024, despite interruptions caused by helium compressor failures. Beamline upgrades focused on improving horn current stability and reducing residual radiation. The Tokai-to-Kamioka (T2K) experiment completed installation of its upgraded Near Detector at 280m (ND280) detector suite: the Super Fine Grained Detector (SuperFGD) with over two million scintillator cubes, new high-angle Time Projection Chambers, and fast Time-Of-Flight (TOF) planes. These enhancements allow for better vertex resolution and tracking of low-momentum particles (Fig. 1).

T2K accumulated 4.6x10^{21} POT and continues aiming for 10^{22} POT by 2026. Analyses of oscillation and cross section data proceeded in parallel, incorporating systematic uncertainty models based on the new detector capabilities. T2K's precision in measuring δ_{CP} and θ_{23} mixing parameters improved substantially, and discussions intensified regarding synergies with Hyper-Kamiokande.

The experiment to search for sub-millicharged particles, SUBMET (E83), began commissioning the de-

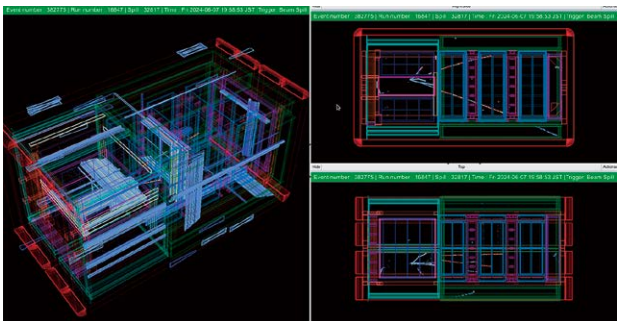

Fig. 1. Event display of a candidate neutrino interaction captured by the upgraded T2K near detector

tector system, using scintillator layers and SiPMs with low-noise electronics.

Hyper-Kamiokande construction advanced with excavation nearing completion. KEK managed production of 20-inch PMTs and finalized electronics component designs. Coordination with the Intermediate Detector proceeded, including land use applications and architectural planning. Progress was also made in joint software development for reconstruction algorithms and simulation packages between KEK and ICRR.

Hadron Experimental Facility (HEF)

The Hadron group at IPNS operates the J-PARC Hadron Experimental Facility (HEF), where high-intensity proton beams from the Main Ring (MR) are used to produce secondary beams for particle and nuclear physics experiments, alongside R&D on beam technology. In FY2024, 30GeV beam operations occurred in two periods, achieving 83kW output. Key experiments included E70/E96 (K1.8), E73/T98 (K1.8BR), and E16 (B-line), with two test runs (T105, T106) conducted for future beamline development. Radiation safety inspections followed C-line construction changes. T105 measured pion yield from embedded pipes, which T106, led by the Research Center for Nuclear Physics, Osaka University (RCNP), studied secondary pions and muons from the B-line.

Strangeness and Hadron Physics Experiments

E70 and E96 experiments began using the new S-2S spectrometer at K1.8 (Fig. 2), targeting double-strangeness hypernuclei and Ξ^--C atom spectroscopy. E73 completed lifetime measurements on ${}^{3}_{\Lambda}H$, after which the detectors in the Cylindrical Detector System (CDS) were disassembled and its solenoid transferred to RIKEN. A new larger CDS magnet was delivered to Tsukuba. The E16 experiment gathered pilot data on vector meson mass modification and detector performance was presented at the Physics Advisory Committee (PAC).

Results from previous experiments were also published. E15 measured the mesonic decay branching ratio of a quasi-bound $\overline{K}NN$ state, showing significant contributions from both isospin = 0 and 1 channels. E05 reported an 8.2-MeV resolution (FWHM) ${}^{12}C$ (K^-,K^+) spectrum, indicating Ξ^--hypernuclear states.

KOTO Experiment

The KOTO experiment, seeking the rate CP-violating decay $K^0_L \to \pi^0\nu\bar{\nu}$, set a new upper limit of 2.2x10^{-9} based on 2021 data published in Physical Review Letters. After a two-year MR shutdown for upgrades, KOTO recorded data in April-June 2024 and January-February 2025 with more than 80kW beam power. A summer workshop "Kaons @ J-PARC 2024" led to a proposal for a next-generation $K^0_L \to \pi^0\nu\bar{\nu}$ experiment.

COMET Experiment

The COMET experiment aims to detect muon-to-electron conversion with sensitivity better than 10^{-14}. In FY2024, major facility construction continued. The capture solenoid magnet was installed in October, with preparation for excitation tests ongoing (Fig. 3). The detector solenoid components were deliv-

Fig. 2. The S-2S spectrometer at K1.8

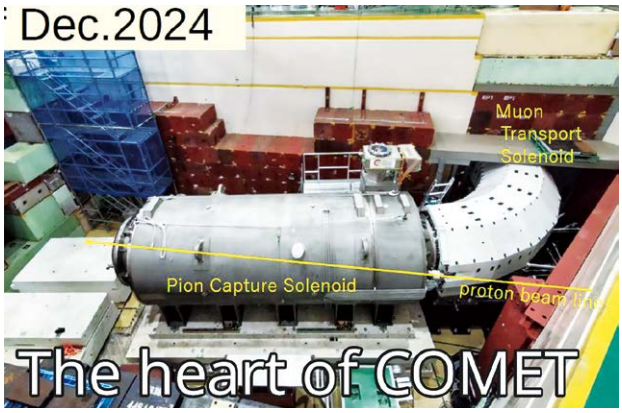

Fig. 3. COMET Pion Capture Solenoid installed in the experimental hall

ered, and the Central Drift Chamber, COMET's main tracker, began operation with optimized trigger circuits. Other detectors are being prepared. Full installation is scheduled to begin after the solenoid is in place.

Future of HEF

To accelerate the HEF extension, cost-saving and staged plans were devised and shared at a February 2025 town meeting. About 40 of 101 registered participants attended in person, including four international guests. Discussions focused on development strategies and implementation timelines.

Particle and Nuclear Physics Experiments at MLF

The experiment of the sterile neutrino search at the Material and Life science Facility (MLF) of J-PARC (JSNS^2) concluded Run 4 and entered construction of its second detector (JSNS^2-II), which will feature expanded fiducial volume and upgraded shielding (Fig. 4). Commissioning included LED calibration, Photo-Multiplier-Tube (PMT) gain characterization, and DAQ synchronization.

The anomalous magnetic moment (*g*-2) and electric dipole moment (EDM) of the muon are powerful probes for new physics beyond the Standard Model, as they can receive contributions from quantum loops involving unknown particles. The J-PARC muon *g*-2/EDM experiment, currently under preparation at the MLF, made significant progress in FY2024.

In collaboration with the Institute of Materials Structure Science, magnets for the muon beam transport line in the MLF H-line were successfully produced and installed, extending the beamline to the H2 area. The beamline was made ready for the first beam delivery in March 2025.

A major milestone was achieved as positive muons were cooled from 4MeV to 30meV and accelerated to 100keV using a Radio-Frequency Quadrupole (RFQ) in the S2 area. Building on this, construction began for a high-performance muon source featuring an intense laser system for cooling and a new diagnostic line for source monitoring. The Interdigital H-type Drift Tube Linac (IH-DTL) accelerating cavity was fabricated and passed high-power performance tests. The Disk And Washer-type (DAW-type) cavity design was optimized to ensure uniform acceleration fields, and the transport line for the Disk Loaded Structure-type (DLS-type) accelerator was finalized. System-wide simulations, covering the muon source through to final acceleration, confirmed that all design goals for the experiment will be met.

Fig. 4. Liquid scintillator filling of the JSNS2-II second detector

Work continued on detector development at the Tsukuba campus. Quarter vane components for the positron tracking detector were under fabrication. Collaborations with Kyushu University and Ibaraki University investigated potential effects of the kicker magnet field on the detector and possible countermeasures. Beam optics and muon injection techniques were further refined through systematic studies. Two collaboration meetings were held during the year: one at J-PARC in June and another at Nagoya University in December.

Theoretical scrutiny of the Standard Model prediction for muon *g*-2 intensified due to new experimental and lattice QCD results. To address this, KEK hosted an international workshop at the Tsukuba campus in September 2024, attracting approximately 180 participants (Fig. 5). Ahead of the workshop, a muon *g*-2 school for early-career researchers was held at Nagoya University's KMI.

As a part of efforts to foster international exchange, a mini-workshop titled "Exploring BSM Physics with Muons" was organized at the Paul Scherrer Institute (PSI) in collaboration with the KEK Theory Center, Hadron Group, and the University of Tokyo. Young researchers participated in a two-week research stay at PSI, exchanging knowledge on muon cooling and EDM techniques.

Fig. 5. Muon *g*-2 theory initiative workshop at KEK

Theory Group

The KEK Theory Center includes the J-PARC branch, whose mission is to investigate hadron and nuclear physics which are experimentally studied at J-PARC, in collaboration with the experimental groups at IPNS and J-PARC. At the same time, the J-PARC branch serves as a hub gathering theorists and experimentalists in these fields. In FY2024 it held an international workshop "J-PARC Hadron 2024". In the previous year, it held a workshop with the similar title, which covered all nuclear and hadron physics investigated at J-PARC. Since we received lots of favorable comments regarding the workshop from participants, we decided to hold this kind of international workshops continuously as a series of "J-PARC Hadron workshops". The second workshop of this series focused on the strangeness nuclear and hadron physics investigated at J-PARC. Many theorists and experimentalists from the Asian region as well as US and Europe attended this workshop and held lively discussions on hadron physics at J-PARC. In addition, several meetings were regularly held to discuss deeply specific fields in J-PARC hadron physics: the "Tokai meeting" for strangeness nuclear physics and related hadron physics, and the "J-PARC-HI Evening" for a future physics program with heavy-ion beams at J-PARC. It was noted that several Chinese scientists attended the Tokai meeting and visited the theory center in February, 2025. They discussed nuclear physics with clusters, hypernuclear physics and AI issues with us. That meeting strengthened our relationship and greatly promoted our collaboration on hypernuclear study. These meetings were mainly organized by the guest professors of the theory center.

ITDC-Tokai

The Instrumentation and Technology Development Center (ITDC) is developing a general-purpose trigger-less data acquisition (DAQ) system. A clock synchronization protocol that automatically adjusts the internal timestamp in an FPGA with 300ps accuracy was developed to realize this. The DAQ system with this protocol has been developed to test experiments for beamline developments in the J-PARC HEF, including the beam monitor system mentioned below. The ITDC has been constructing a superconducting magnet system and a straw tube tracker for the COMET experiment. Manufacture of all magnets has been completed, and installation work is ongoing. Conceptual design and mechanical analysis of Intermediate Water Cherenkov Detector (IWCD) for the Hyper-Kamiokande has been carried out by the ITDC.

The ITDC has started considering the construction of a hadron test beamline in the J-PARC HEF. To investigate the beam profile of the so-called π1.0 beamline near the K1.0BR beamline, a beam monitor system including a magnet, scintillators, and aerogel Cherenkov detectors have been under construction since

December 2024. The test beamline team will be involved in both upgrade of the beam monitor system and continued data analysis in FY2025.

— Research Highlight —
First successful acceleration of positive muons

Muons are elementary particles similar to electrons but approximately 200 times more massive. Despite their short lifetime of just 2.2 microseconds, muons are of significant interest in modern physics beyond the Standard Model, as well as their wide range of applications across science and engineering.

One of the most intriguing properties of the muon is its anomalous magnetic moment, commonly denoted as g-2. Theoretically, the value of g should be exactly 2 for a spin-1/2 point-like particle. However, quantum field theory predicts a small deviation from this value due to higher-order corrections involving virtual particles in loop diagrams. Closely related to g-2 is the muon's electric dipole moment (EDM). While the Standard Model predicts an extremely small EDM, many theoretical extensions suggest that the muon's EDM could lie within the sensitivity range of current or next-generation experiments.

To accurately measure the muon's g-2 and EDM, high-quality muon beams that are both highly polarized and have low emittance are essential. Emittance is a measure of how widely the particles are distributed in phase space volume. Conventional muon beams, typically produced via the decay of pions generated by proton collisions with a target, suffer from very large emittance, which limits the achievable experimental precision.

The experimental collaboration proposed an innovative solution: cooling the muons to significantly reduce beam emittance [1]. This approach, however, faces a fundamental obstacle—the muon's short lifetime prevents the use of standard cooling techniques, such as stochastic or electron cooling, which are used for protons or ions. Instead, the team adopted a novel technique involving the creation of ultra-slow muons [2]. The concept is shown in Fig. 6. The process begins with a surface muon beam that is stopped in a specially prepared silica aerogel target. Within the target, some muons capture electrons and form muonium atoms—a hydrogen-like bound state of a muon and an electron. These muonium atoms are thermalized, and a fraction is emitted from the target surface into the vacuum. By applying a carefully tuned deep-ultraviolet laser pulse, the electron is removed, freeing the muon as a slow-moving particle with thermal energies (Fig.7 (top)).

The released ultra-slow muons are then extracted using electrostatic fields and shaped using electric lenses. This beam is then injected into a radio-frequency quadrupole (RFQ) linear accelerator, where the muons are accelerated to an energy of 100keV (Fig. 7 (bottom)).

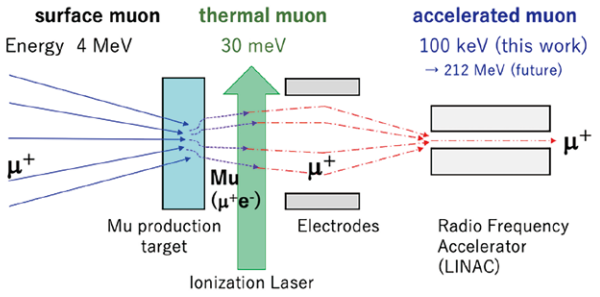

Fig. 6. Concept of positive muon cooling and acceleration

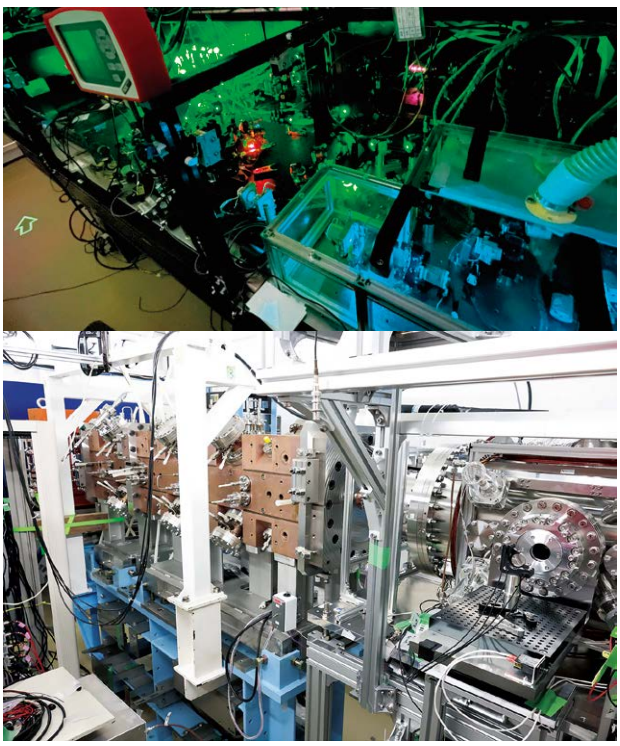

Fig. 7. The 244 nm laser system (top), and t.he cold muon source and the RFQ (bottom)

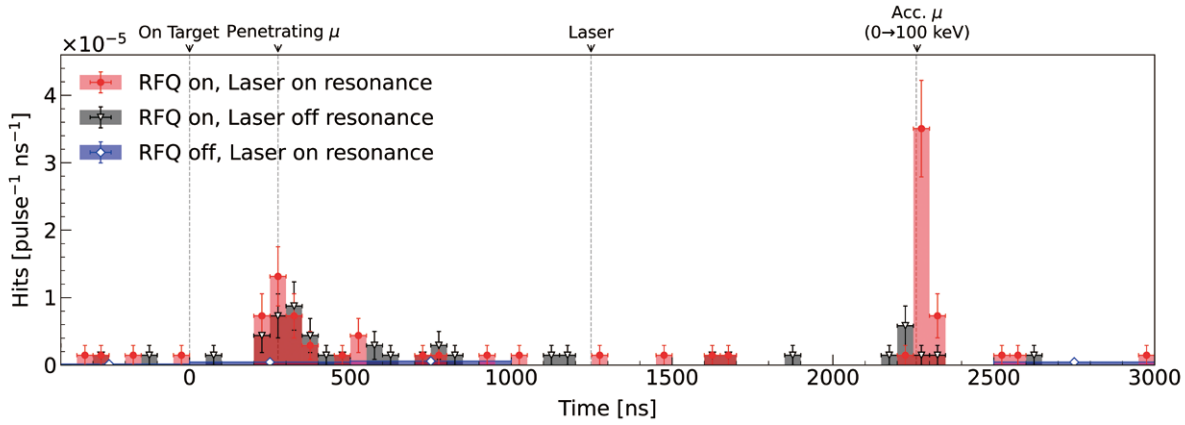

Fig. 8. The measured time-of-flight distribution at the detector after the RFQ and a bending magnet

This entire sequence was successfully demonstrated at the S2 experimental area of J-PARC MLF in 2024, marking the first successful radio-frequency acceleration of cooled muons in the world [3].

The experiment's diagnostics included beam profile monitors and time-of-flight (TOF) measurements (Fig. 8). A sharp TOF peak corresponding to the arrival of accelerated muons was observed only when the laser was tuned to the correct ionization frequency and the RFQ was powered. The measured TOF agreed with simulations, verifying the beam's identity and energy.

Additionally, the quality of the accelerated beam was evaluated through the Q-scan measurement, a technique involving varying the magnetic field strength of quadrupole magnets and observing changes in beam size downstream. The emittance of the beam was estimated to be approximately 0.85πmm•mrad horizontally and 0.32πmm•mrad vertically. This represents a reduction by factors of about 200 and 400, respectively, compared to the original uncooled surface muon beam. The results demonstrated the dramatic improvement in beam quality.

In summary, the world's first successful radio-frequency acceleration of positive muons at the J-PARC demonstrates a remarkable advance in accelerator and beam technology. This achievement, grounded in years of interdisciplinary development in beamline construction, laser systems, muonium production target, and particle diagnostics, signals the dawn of a new era in science with accelerated muons.

References

[1] M. Abe *et al.*, Prog. Theor. Exp. Phys. **2019**, 053C02 (2019).

[2] K. Nagamine et al., Phys. Rev. Lett. **74**, 4811 (1995).

[3] S. Aritomo et al., Phys. Rev. Lett. **134**, 245001 (2025).

— Research Highlight — Updating the world's best sensitivity for a CP-violating rare kaon decay

It has been 60 years since the charge conjugation and parity (CP) violation phenomenon was first observed in the decays of neutral K mesons (kaons). The Standard Model (SM) is a well-established theory that can describe the mechanism of CP violation in the quark sector, and observations thus far are consistent with the predictions of the theory. However, it is also known that the SM cannot explain the matter-antimatter asymmetry in our universe quantitatively, and other sources of CP violation must exist somewhere else. The ultra-rare decay of a long-lived neutral kaon $K_L^0 \to \pi^0\nu\bar{\nu}$ is a good probe to look for a new mechanism beyond the SM in the quark sector. The SM precisely predicts the branching ratio to be (2.94±0.15)x10^{-11}, and the deviation from the value indicates the existence of an unpredicted contribution.

KOTO, named from "K0 at Tokai", is a unique experiment dedicated to searching for $K_L^0 \to \pi^0\nu\bar{\nu}$ and is con-

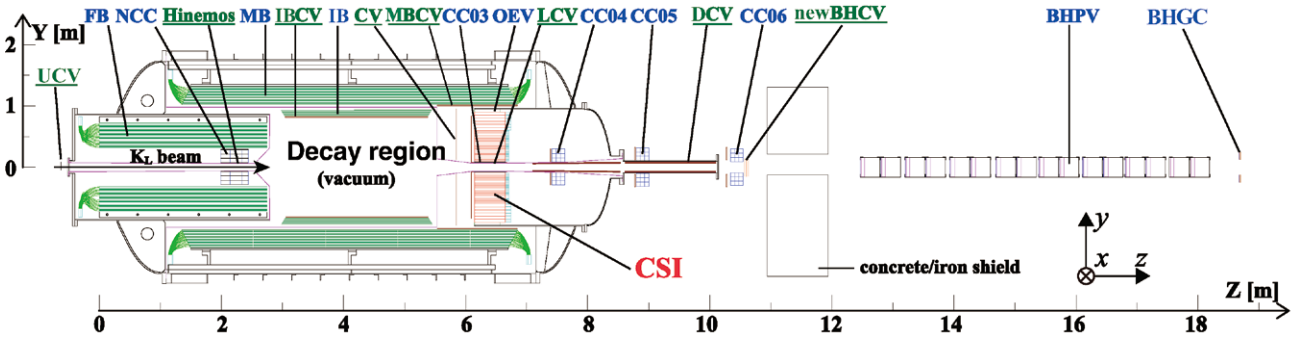

Fig. 9. Cross-sectional view of the KOTO detector in 2021

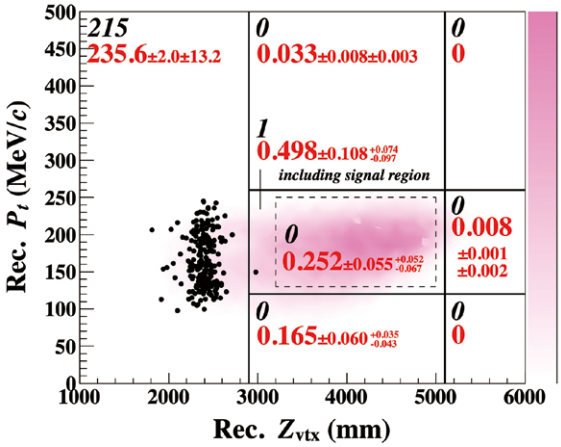

Fig. 10. Photo of the UCV used for the runs in 2021

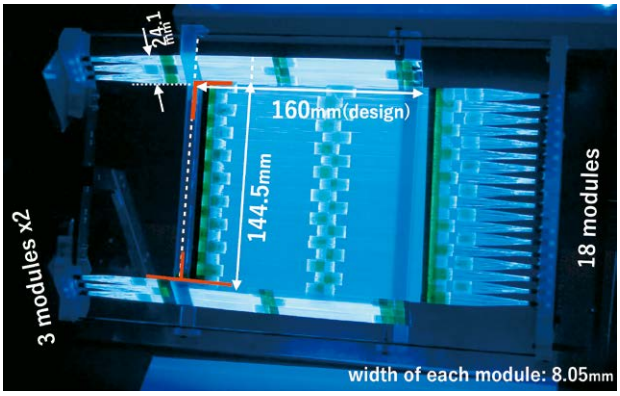

Fig. 11. Scatter plot summarizing the results of the analysis of the data accumulated in 2021 [1]

ducted at the Hadron Experimental Facility (HEF) in the J-PARC. The collaboration consists of around 40 members from four countries and regions: Japan, Korea, Taiwan, and the USA. The first major physics run was performed in 2015, and the results improved the world's best sensitivity by an order of magnitude. Since then, KOTO has gradually upgraded the detector and continues to accumulate data. Here, the latest results of the analysis of data taken in 2021, published in FY2024 [4], are introduced.

The $K_L^0 \to \pi^0\nu\bar{\nu}$ decay is identified by detecting two photons from the π^0 decay, ensuring no associated particles and requiring a large π^0 transverse momentum that reflects the missing energy taken out by two neutrinos. The KOTO beamline and detector are designed to utilize these features. A 30GeV proton beam from the Main Ring (MR) accelerator is injected into a common target in HEF, and secondary neutral particles such as K_L^0s, photons, and neutrons are transported through 4- and 5-m-long collimators and a sweeping magnet to the experimental area, located 21m downstream of the target. Figure 9 shows a schematic view of the KOTO detector in 2021. The main part is located in an 8-m-long cylindrical vacuum tank surrounding the neutral beam axis, and detects the particles from K_L^0 decays. An electromagnetic calorimeter in the endcap region, labeled CSI, measures the energies and positions of the photons, and other components are used as veto counters, rejecting events in which particles other than the two photons are detected.

A challenge in the search for a rare process is to find a genuine signal among a large number of background events. Major K_L^0 decay modes, including $K_L^0 \to 2\pi^0$, become the background if the extra particles escape the detection. A neutron coming into the beam halo region can mimic the signal by hitting the calorimeter directly and producing two photon-like hits and/or by hitting the counters near the beam and generating π^0 or η. In addition, a tiny contamination of charged kaons in the neutral beam with a fraction of 3×10^{-5} relative to the K_L^0 flux can cause a serious background, as was realized in the analysis of data collected in 2016-2018 [5]. An important feature of the detector in 2021 is a charged particle counter installed at the entrance of the KOTO detector, called the Upstream Charged Veto (UCV), which consists of 0.5-mm-square scintillating fibers, as shown in Fig. 10. The UCV detects charged particles inside the neutral beam and reduces the charged kaon background

by an order of magnitude.

Figure 11 shows a scatter plot in the plane of the reconstructed π^0 transverse momentum (P_t) and π^0 decay vertex position (Z_{VTX}) with all the selections imposed. The dashed points represent the observed distribution of the $K_L^0 \to \pi^0\nu\bar{\nu}$ signal. The numbers of observed and expected background events with statistical and systematic uncertainties are shown in black and red, respectively, in the areas separated by lines. As can be seen, no candidate was observed inside the signal region. With the single event sensitivity of 9.3×10^{-10}, the upper limit on the $K_L^0 \to \pi^0\nu\bar{\nu}$ branching ration was set to 2.2×10^{-9} at the 90% confidence level. This improved the world's best sensitivity for the search by a factor of 1.4. In addition, the results demonstrate that KOTO can successfully control the background.

After the MR shutdown for the power supply upgrade, KOTO resumed data acquisition in FY2024. KOTO plans to accumulate data over the next three-four years to achieve a sensitivity better than 10^{-10}. Furthermore, a next-generation experiment to precisely measure the $K_L^0 \to \pi^0\nu\bar{\nu}$ branching ratio is being discussed for realization in the 2030s as part of the HEF extension project, in collaboration with international partners including kaon scientists in Europe.

References

[4] J.K. Ahn *et al.*, KOTO collaboration, Phys. Rev. Lett. **134**, 081802 (2025).

[5] J.K. Ahn *et al.*, KOTO collaboration, Phys. Rev. Lett. **126**, 121801 (2021).

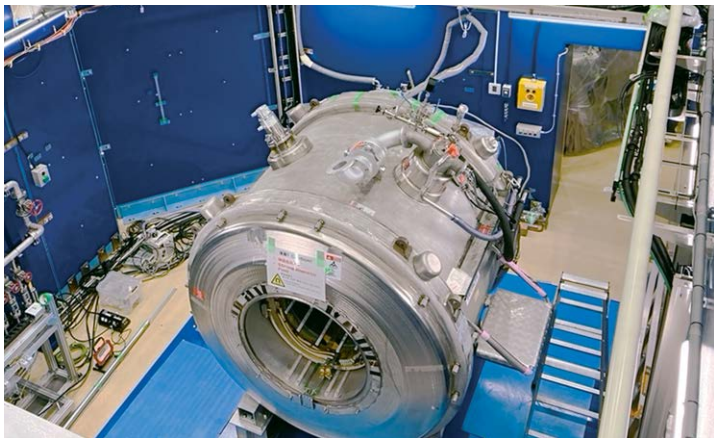

Cryogenics Section

Overview

The Cryogenics Section supports scientific activities in applied superconductivity and cryogenic engineering at J-PARC. It also supplies liquid helium and liquid nitrogen. The support work includes the maintenance and operation of superconducting magnet systems for the T2K neutrino beamline and the muon beamlines at the Materials and Life Science Experimental Facility (MLF), as well as the construction of magnet systems at the Hadron Experimental Facility (HEF). In addition, the section actively conducts R&D for future J-PARC projects.

Cryogen Supply and Technical Support

The Cryogenics Section provides liquid helium cryogen for physics experiments at J-PARC. The used helium is recycled by the helium gas recovery facility at the Cryogenics Section. Fig. 1 summarizes the liquid helium supply in FY2024.

Liquid nitrogen is also supplied to users for their convenience. The amount supplied in FY2024 is summarized in Fig. 2. The total amount of LHe was drastically decreased because the Beam Run in the MLF was stopped due to the occurrence of a water leak around the neutron target. Large amounts of LN2 were used in the hadron experiment, therefore, the amount of LN2 increased compared to 2023.

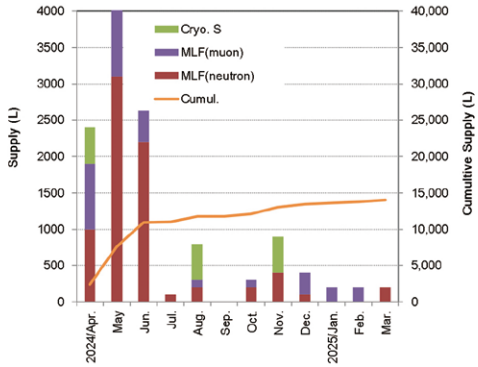

Fig. 1. Liquid helium supply at J-PARC from April 2024 to March 2025

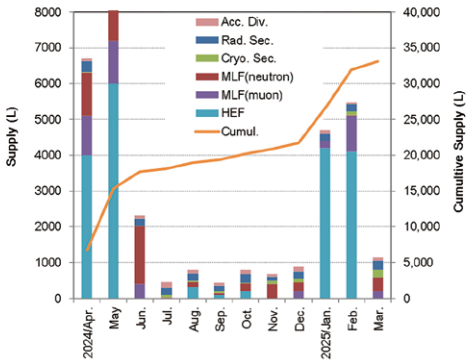

Fig. 2. Liquid nitrogen supply at J-PARC from April 2024 to March 2025

Superconducting Magnet System for T2K

The superconducting magnet system for the T2K experiments operated during the periods shown in Table 1. The system worked well without disturbing the beam time. The total operation time was 113 days and regular maintenance works were carried out in the autumn. Figure 3 summarizes the incidents in the refrigeration system from FY2009, which shows that the magnet system has been quite stable recently.

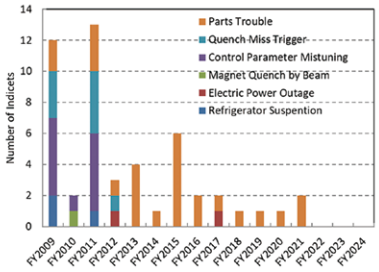

Fig. 3. Annual number of incidents in the SC Magnet system during operation

Tab 1. Operation history of the T2K superconducting magnet system

	2024									2025			
	April	May	June	July	Aug.	Sept.	Oct.	Nov.	Dec.	Jan.	Feb.	Mar	April
Operation			5/20-7/2					11/1-12/25			2/17-3/5		
Maintenance													

Superconducting Magnet Systems at the MLF

The Cryogenic Section contributes to the operation and maintenance of the superconducting magnet systems at the Muon Science Facility (MUSE) in the MLF. The superconducting solenoid in the Decay Muon Line (D-line) was operated from January 11 to June 24, 2024. Annual maintenance, was performed from July to the end of October. The filters for the third oil-separation unit were exchanged as a part of regular maintenance. The cryogenic operation was resumed from November 29, although the beam power was kept low due to the water leak issue in the neutron target.

The section also contributes to the operation of the MRI magnet for the MuSEUM experiment. The magnetic field was shimmed in August, 2024. The homogeneity reached to +/- 0.1ppm in the muon storage region, al-

Fig.4. Setup for magnetic field measurement in the MRI magnet

though without all the components of the detector. The first beam experiments were performed in January and February, 2025.

Superconducting Magnet Systems at the HEF

The COMET experiment facility is currently under construction in the Hadron South Experimental Hall (HDS) of the Hadron Experimental Facility (HEF). The Cryogenics Section has been involved in the construction of the superconducting magnets and the cryogenic system. The magnet system comprises a pion capture solenoid (PCS), a muon transport solenoid (MTS), a bridge solenoid (BS), and a detector solenoid (DS). The MTS and BS magnets have already been delivered to J-PARC.

In FY2023, the commissioning of the MTS was completed, and combined current operation for the Phase-I experiments was successfully achieved. The solenoid was energized to 210 A (3T), and the dipole to ±175 A (±0.07T). The functionality of the magnet protection system at the nominal current was verified through a current shut-off test, confirming its proper operation.

The PCS was assembled at the factory and delivered to the HDS in the fall of 2024. The results of the acceptance inspection confirmed that no damage had occurred during transportation. The PCS-to-MTS connection work, which involved horizontally moving the PCS, was carried out at the end of December 2024. Figure 5 shows the installation of the PCS at the HDS beamline, involving horizontal movement. The PCS was positioned at the target location within the allowable alignment tolerance. The vacuum connection between the PCS and MTS was completed, achieving a helium leak rate of less than 1×10^{-10}Pa·m^3/s. The next steps, including assembling the return yoke and connecting the liquid helium transfer line, will be conducted later.

The fabrication of the DS was completed, and a cryogenic excitation test was conducted at the factory in June 2024. The DS was successfully cooled to 4.2K within 14 days using three GM cryocoolers. It was then ramped up to the rated current without any training quenches. Intentional shutdown tests were conducted, and the temperature rise of the coils was verified to remain below the levels predicted by quench simulations, confirming the effectiveness of the protection system.

Magnetic field measurements were performed using a three-axis Hall probe. Figure 6 shows the setup for measuring the magnetic field of the DS using position calibration with a laser tracker. The measured distribution of B_z and the field magnitude along the z-axis showed good agreement with simulations across all scan positions. However, deviations exceeding 1% were observed in the B_y components. The z-scan peak position as a function of x for y=0 showed a flat distribution consistent with the design, indicating that the magnetic field axis is well aligned with the geometric cylinder axis.

The DS was delivered and temporarily placed at the KEK Tsukuba campus. The electrical insulation of the coils and the vacuum tightness of the cryostat were confirmed through an acceptance inspection. The DS is scheduled to be installed in the HDS experimental hall in the fall of 2025.

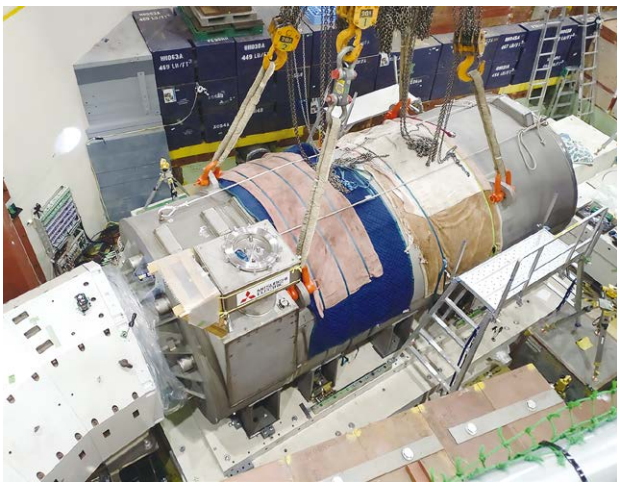

Fig. 5. Installation of the PCS at the HDS beamline

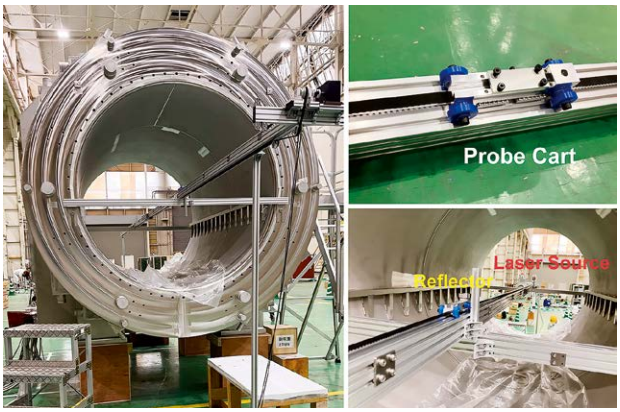

Fig. 6. Setup for measuring the magnetic field of the DS using position calibration with a laser tracker

R&D for the Future Projects at J-PARC

The g-2/EDM project aims for the precise measurement of the anomalous magnetic moment and the electric dipole moment of muons. It was proposed that this experiment would be conducted at the MUSE H-Line. A superconducting solenoid with a high field homogeneity, better than 1 ppm locally, plays a very important role as a muon storage ring. The main superconducting coils are cooled by liquid helium, and the evaporated gas was recovered by a gas bag system during quench. The design of an experimental hall is being modified to decrease the construction cost, and the gas bag design is also being modified to fit the new building design.

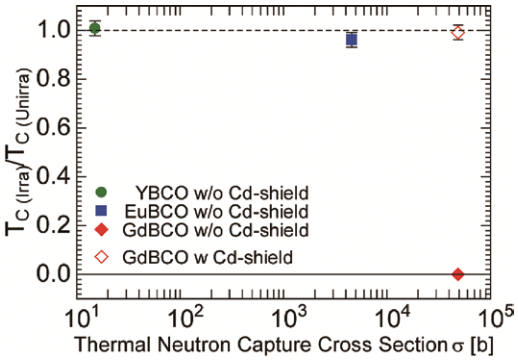

Fig. 7. Dependence of TC degradation in REBCO samples on the thermal neutron capture cross section

Applied research on REBCO (rare-earth barium copper oxide), a high-temperature superconductor, is underway to develop a solenoid system for the future muon source at the muon beamline of the MLF second target station. The solenoid will be required to operate in a high-radiation environment, where the absorbed dose may reach 100MGy. The study of neutron irradiation effects on REBCO conductors is essential, as the neutron fluence to the coil is expected to reach up to 7.8×10^{21} n/m^2.

Neutron irradiation studies have been conducted to investigate the radiation tolerance of REBCO coated conductors. To examine the effects of low-energy neutron reactions on these conductors, three types of samples—GdBCO, EuBCO, and YBCO—with significantly different neutron capture cross sections were irradiated at the Japan Research Reactor No. 3 (JRR-3) of the Japan Atomic Energy Agency (JAEA) to a fast-neutron fluence of 1.5×10^{21} n/m^2 and a thermal-neutron fluence of 8.3×10^{22} n/m^2.

Figure 7 shows how the critical temperature (T_C) of REBCO samples depends on the thermal-neutron capture cross section. Without Cd shielding, GdBCO lost superconductivity, EuBCO's T_C dropped by 3.5K, and YBCO showed no change. With Cd shielding, GdBCO showed almost no degradation. These results indicate that low-energy neutrons play a major role in (T_C) degradation.

In the next step, irradiations at different fluences will be performed with similar sample configurations at research reactors to further investigate the neutron-irradiation tolerance of each REBCO coated conductor.

Information System

Overview

The Information System Section plans, designs, manages and operates the network infrastructure of J-PARC and also provides support to ensure its information security. In terms of computing, until now, J-PARC has owed its major computer resource for analyzing and storing data from neutrinos, nuclear physics and MLF experiments to the KEK central computer system, KEKCC. The section connects the J-PARC network to KEKCC directory and helps the users to utilize the system effectively.

Status of Networking

Since 2002, the J-PARC network infrastructure, called JLAN, has been operated independently from KEK LAN and JAEA LAN in terms of logical structure and operational policy. In 2024, the total number of hosts on JLAN was 5,602, an increase of 89 hosts over the year. The growth curve of edge switches, wireless LAN access points and hosts (servers and PCs) connected to JLAN are shown in Fig. 1.

In April 2022, the National Institute of Informatics (NII) upgraded SINET (Japan Science Information Network https://www.sinet.ad.jp) from version 5 to 6. SINET is not only a gateway from JLAN to the internet but also an important connection between the Tokai and the KEK Tsukuba sites in J-PARC.

Figures 2 and 3 show the network utilization of the internet from/to JLAN. Since the bandwidth capacity for the internet through the SINET is 10 Gbps (giga-bits per second), it is clear that there is enough space for additional activity. Figures 4 and 5 show the statistics for data transfer between the Tokai and Tsukuba sites. KEKCC operates at KEK-Tsukuba campus, and most of the transferred data is archived and analyzed on KEKCC. Figure 6 shows the peak network traffic rate over the internet from/to JLAN and between the two sites in each year. The network bandwidth capacity between the two sites is 20 Gbps. This shows that the usage level has been ap-

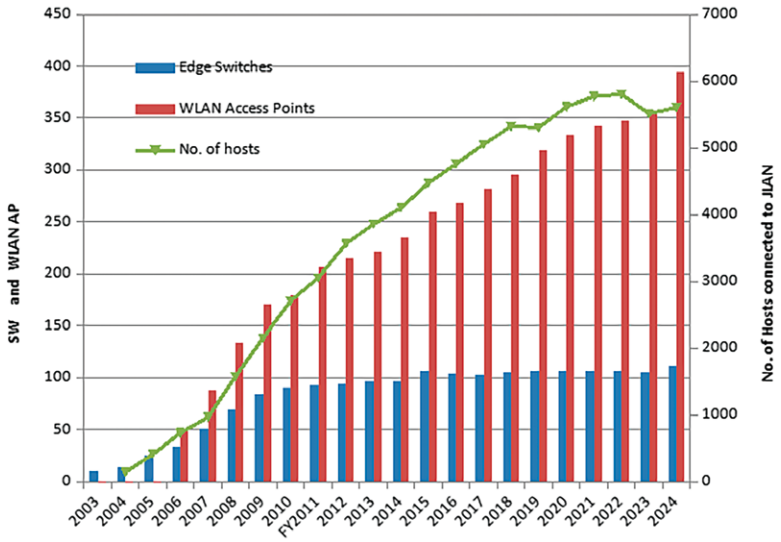

Fig. 1. Number of hosts, edge SW and wireless AP on JLAN

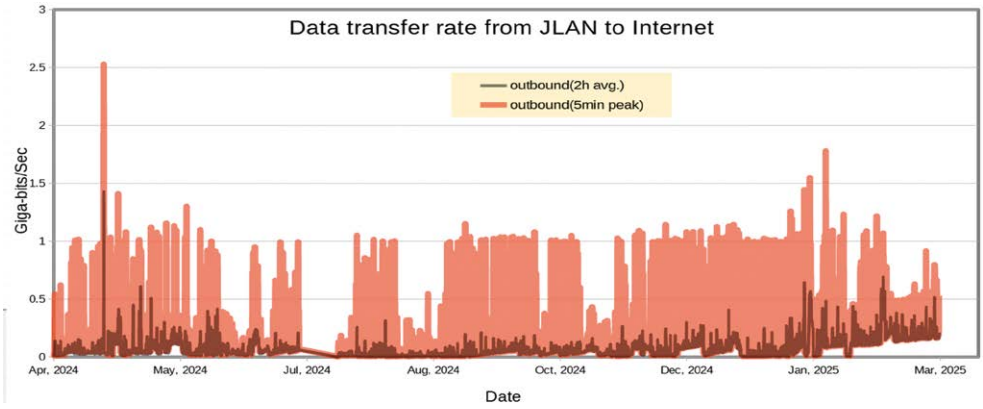

Fig. 2. Network traffic from JLAN to the internet (One-hour average and five-minute peak value)

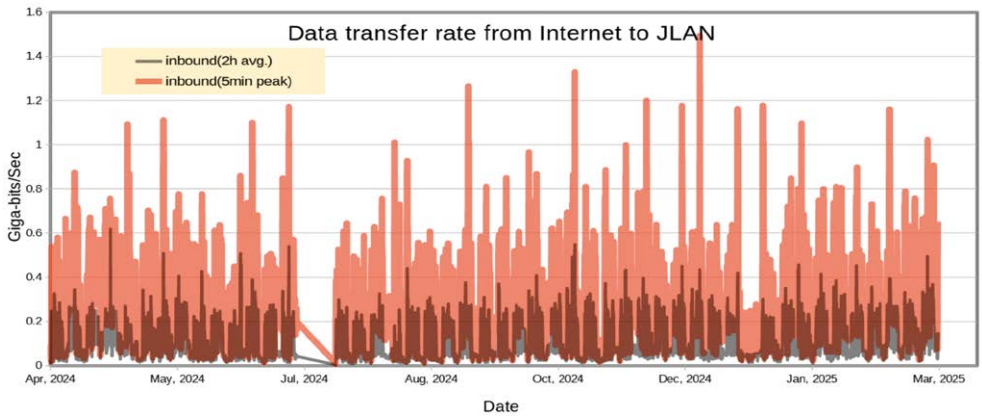

Fig. 3. Network traffic from the internet to JLAN (One-hour average and five-minute peak value)

proaching 50% capacity, especially during the period when the Hadron and g-2 facilities were running.

The replacement of the JLAN system from the third to the fourth version was carried out in July 2024. While the network architecture of JLAN remained unchanged, most components of JLAN such as switches, security systems, servers were upgraded. The network usage statistics shown in the figures could not be acquired in July 2024 due to the upgrade.

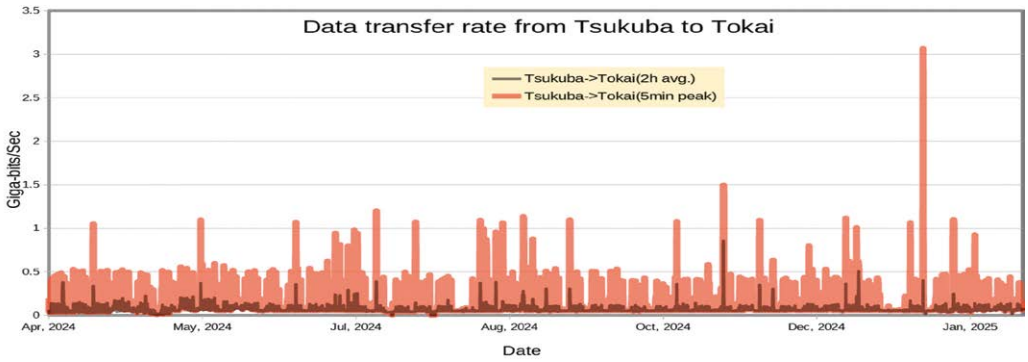

Fig. 4. Network traffic from the Tsukuba to Tokai sites

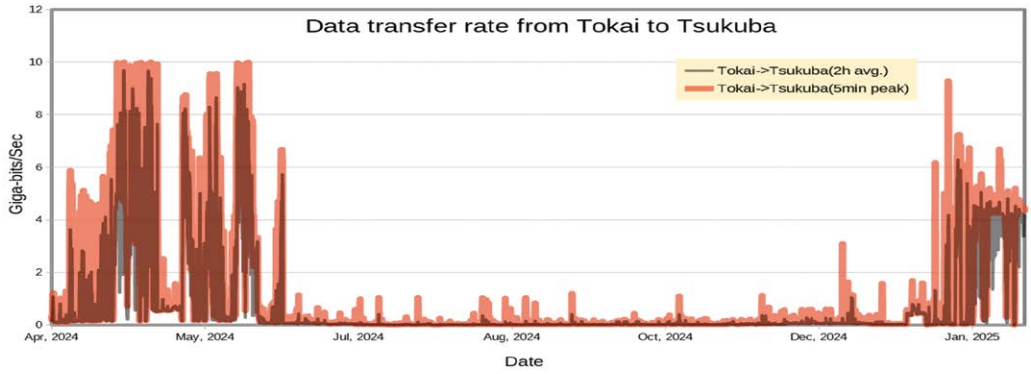

Fig. 5. Network traffic from the Tokai to Tsukuba sites

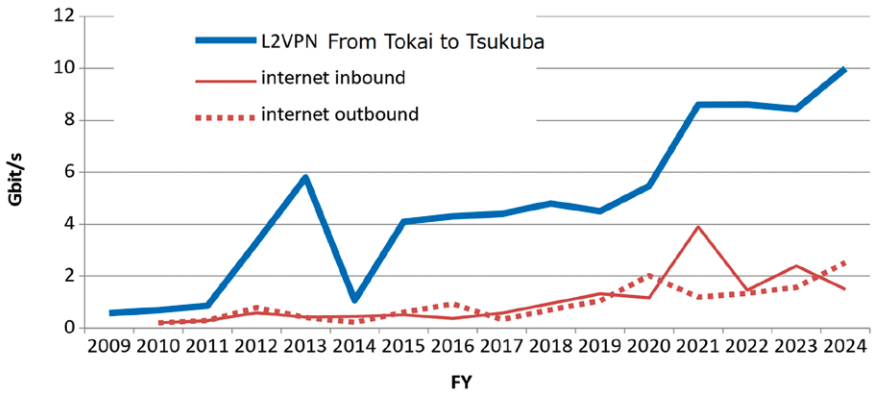

Fig. 6. Peak network traffic between Tokai and Tsukuba sites for the recent years

Internet Connection Services for Visitors and Public Users of J-PARC

Since 2009, J-PARC had offered a Guest network (GWLAN) service, which is a wireless internet connection service for short-term visitors, available in almost all J-PARC buildings. At the end of 2014, an additional network service called User LAN had started. To use the GWLAN, users are required to receive a password at the J-PARC Users Office beforehand, while in the User LAN, they are authenticated by the same ID and password for the User Support System, which is also used for dormitory reservations and so on. From March 2016, a new service called "eduroam" had been started. The eduroam (https://www.eduroam.org/) is a secure roaming access service developed for the international research and education community and mutually used among a huge number of research institutes, universities, and other institutions around the world. The eduroam service will be a convenient third option of internet connection service for J-PARC visitors. Figure 7 shows this fiscal year's usage statistics of GWLAN, User LAN and eduroam services.

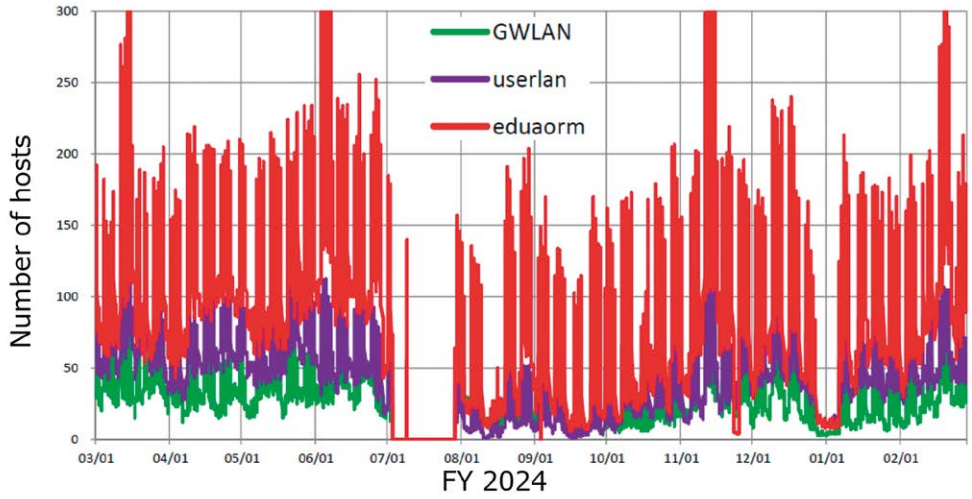

Fig. 7. Usage trends of GWLAN, User LAN and eduroam

Status of Computing

Since J-PARC does not have computing resources for physics analysis, starting from 2009, the KEK central computing system (KEKCC) at the KEK Tsukuba campus has been mainly used for that purpose. KEKCC is shared by most of the research groups of KEK, including J-PARC. At the Neutrino (T2K), Hadron and Neutron (MLF) experiments, the data recorded at J-PARC is temporarily saved at their facilities and then promptly transferred, stored, and analyzed at the system in Tsukuba. The storage of the system is also utilized as a permanent data archive for their data. The fourth upgrade of the system was completed in the summer of 2024, and the computing resources are shown in Tab. 1. Figure 8 shows the CPU usage statistics in FY2024, and Figs. 9 and 10 show the annual trends of the disk and tape usage statistics. The main users who constantly used the CPU and storage were from the Hadron and Neutrino experiment groups. The MLF group also started to store data to tapes on the system.

Tab. 1. Computing resources in the KEKCC

CPU (AMD EPYC 9534/9654)	12000 cores
RAID Disk (GPFS)	30 Peta Bytes
Tape Library (HSM)	120 Peta Bytes

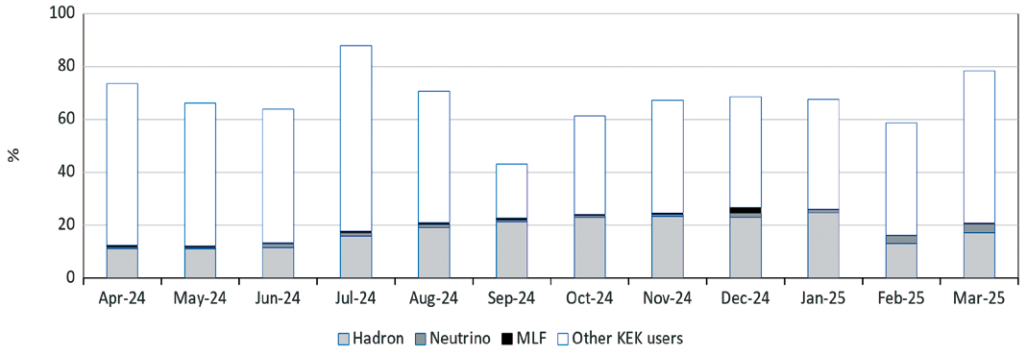

Fig.8. CPU usage statistics of KEKCC in FY2024

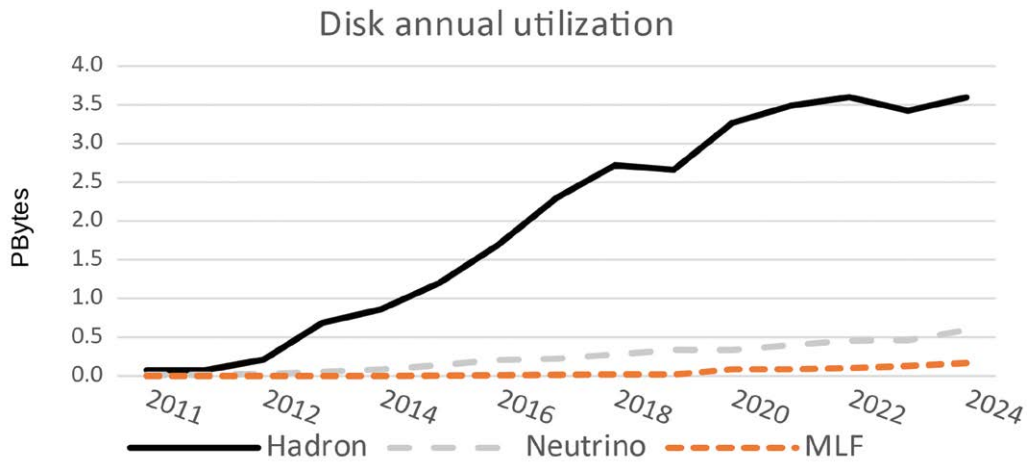

Fig. 9. Annual trend of disk usage statistics

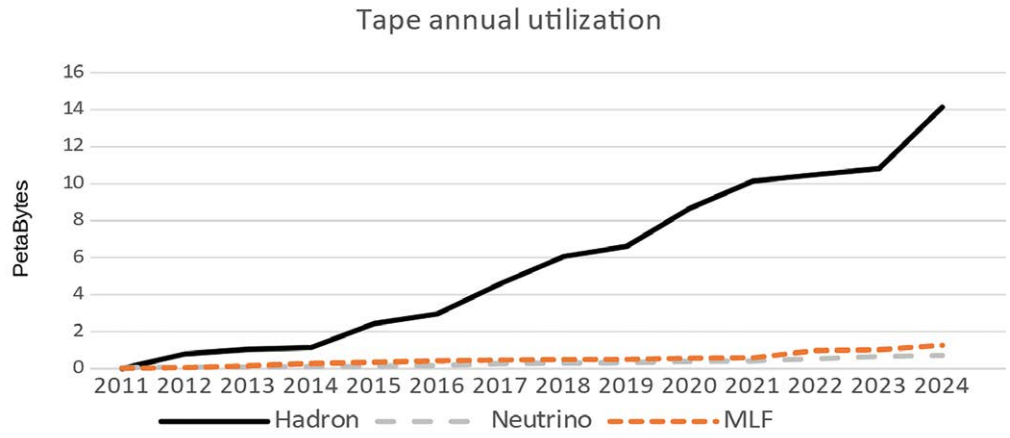

Fig.10. Annual trend of tape library usage statistics

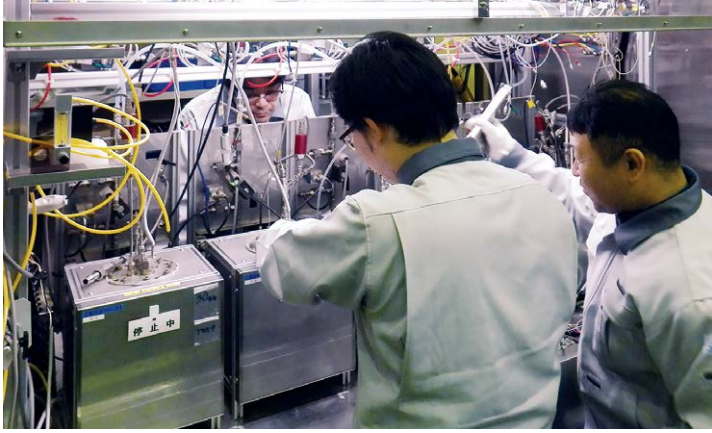

Transmutation Studies

Overview

We are developing nuclear transmutation technology with accelerator-driven systems (ADS) using the J-PARC's research resources and expertise in high-power accelerator and target technologies. The ADS are an effective nuclear system for volume reduction and mitigation of the degree of harmfulness of high-level radioactive waste produced in nuclear power reactors. We believe that the ADS are one of the most beneficial applications of high-power accelerators for contributing to the goals of society, such as carbon neutrality and SDGs.

We have developed the basic design of the ADS Target Test Facility (TEF-T) which utilizes the 400 MeV and 250 kW proton beam provided by the J-PARC Linac. The main mission of the TEF-T is irradiation of ADS's beam window materials in a flowing high-temperature lead-bismuth eutectic (LBE) alloy target. The conceptual design of the TEF-T has been published in the report entitled JAEA-Technology 2017-003. After that, the future direction of TEF-T was discussed, and the results stated in the JAEA's mid-to long-term plan (MLTP) for FY 2022-2029 were as follows: "JAEA reframes the facility plan of the TEF-T based on the results of related R&D and versatile needs to the facility in addition to nuclear transmutation research."

Now we are building up the concept of the proton beam irradiation facility, which is the advanced concept of the TEF-T, to comply with the MLTP. Fig. 1 shows the latest concept of the facility with four important application areas, i.e., (1) materials irradiation, (2) medical RI production, (3) soft-error testing of semiconductor devices and (4) proton beam applications for space technology. The conceptual design of the facility was compiled in the report JAEA-Technology 2024-026 published in March 2025. Next to the facility, the post-irradiation

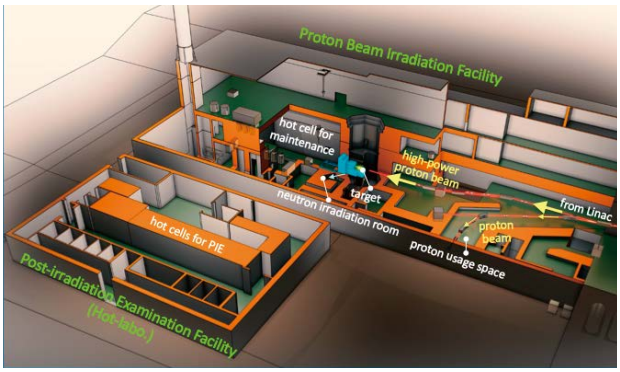

Fig. 1. The concept of the proton beam irradiation facility and the post-irradiation examination facility

Fig. 2. Group photo of the workshop on the "J-PARC Proton Beam Irradiation Facility"

examination facility is under planning, and its conceptual design has been summarized in the report JAEA-Technology 2023-025 published in March 2024.

On July 17, 2024, a workshop on the "J-PARC Proton Beam Irradiation Facility" was held. There were 131 participants, with 42 attending in person and 89 online. Expectations and needs for the facility were presented, focusing on the four important application areas. Following this, the status of the facility design, considering user needs, was presented. A key takeaway from the workshop was that deeper communication between potential users and the facility team leads to better design plans.

Regarding R&D activities on lead-bismuth target technology, a series of transient response experiments was conducted using the TEF-T lead-bismuth mockup loop, IMMORTAL, to understand the loop's behavior in the event of component failures. The transient responses obtained will be compared with simulations.

A beam chopper design has been completed for the design of a superconducting linear accelerator (linac) for ADS, which will provide a 30MW proton beam to a subcritical reactor. The chopper is a key component of the ADS linac, enabling gradual beam power ramping and making the proton pulse falling edge less than the 1 μs needed for subcriticality measurements of the reactor.

Assembling of a superconducting spoke cavity for the linac, using electron beam welding, has been completed. The resonance frequency of the cavity was confirmed to be very close to its design value of 324MHz.

Research and Development

Lead-bismuth target technology development

Management of the Lead-bismuth eutectic (LBE) is one of the key issues of the ADS. At J-PARC, various research activities, such as the operation of a corrosion test loop "OLLOCHI," the operation of a spallation target mockup loop "IMMORTAL," and the development of various sensors for LBE are underway.

1. OLLOCHI

The 4th campaign of long-term corrosion tests using Oxygen-controlled LBE LOop Corrosion tests in HIgh-temperature (OLLOCHI) shown in Fig. 3, started in March 2023 and were completed in April 2024. The target period for this campaign was 2,000 hours. The test conditions of the 4th campaign were as follows: the maximum temperature and the temperature difference were 500˚C and 100˚C, respectively. The flow rate was

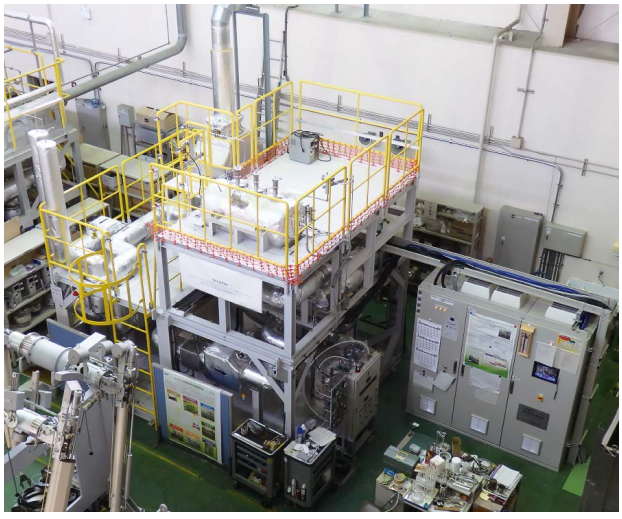

Fig. 3. Outline of OLLOCHI

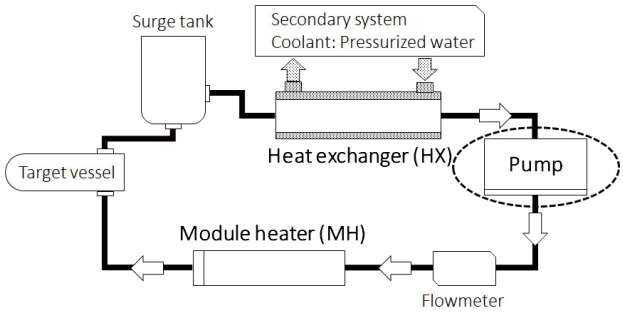

Fig.4. Schematic system diagram of IMMORTAL

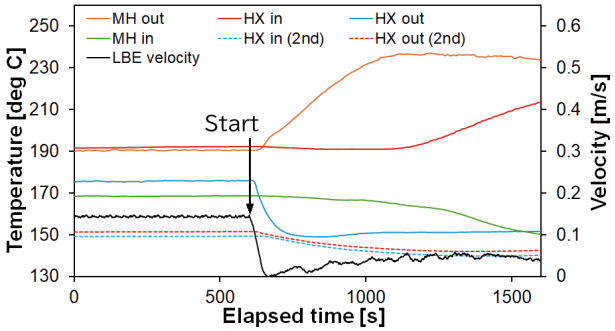

Fig.5. Measured temperature and flow velocity results of the loss-of-flow event

about 1 m/s at the specimens' position. The oxygen concentration (OC) was kept at 1×10^{-6} wt%. Preliminary oxidation by immersion in LBE under saturated oxygen for 165 hours was conducted before the corrosion test. Furthermore, preliminary oxidation using steam was performed for some test specimens. However, leakage of LBE was confirmed in the No. 3 heater, so the test was stopped at 1,911 hours. The tested specimens were removed from the specimen holders and are being observed. The third heater where the leak occurred was detached for an ongoing investigation of the cause, and the piping before and after it was shut off.

The 5th campaign began at the end of March 2025. Since oxidation film peeling was observed in test pieces in 1st and 2nd campaigns, the possibility arose that the oxygen concentration was low. Therefore, in order to find the optimal oxygen concentration for this loop, we conducted the campaign with a higher OC, 1×10^{-5} wt%. The other test conditions of the campaign were as follows: the maximum temperature and the temperature difference were 450˚C and 100˚C, respectively. The flow rate was about 1 m/s at the specimens' position. In this campaign, no pre-oxidation in LBE was performed.

The 6th campaign will be conducted under the same conditions with preliminary oxidation in LBE. Test conditions for the following 7th campaign will be determined based on the results of 5th campaign.

2. Transient response test on IMMORTAL loop

To establish a spallation target system utilizing liquid LBE as both target material and coolant, it is crucial to predict potential behavior following a malfunction and to implement necessary countermeasures. LBE, a liquid heavy metal, exhibits thermal-hydraulic properties distinct from air and water. Therefore, transient response tests were conducted on IMMORTAL (Fig. 4) to obtain experimental data for code verification and validation concerning transient behavior after malfunctions of components.

Fig.5 presents the results of a test simulating a loss-of-flow event, where the primary system pump was deactivated due to a malfunction. The temperature at the MH outlet and the HX inlet began to rise shortly after the pump was deactivated, and after approximately 500 seconds, respectively. In contrast, heat propagation from the MH outlet to the HX inlet was faster than the thermal diffusion process within static LBE. The flow path from the MH outlet to the HX inlet is approximately 12.4m. On the other hand, the distance from the MH outlet where the LBE reaches 200°C after one hour is only about 0.2m if considering only thermal diffusion. As shown in Fig.5, LBE velocity decreased to zero after the pump deactivation, subsequently increasing gradually. This suggests that natural convection occurred due to the temperature difference, indicating that convection contributes to heat transfer after the loss-of-flow event. In FY2025, the experimental data will be compared with results of a simulation code to validate prediction capability of the code.

Super-conducting linac development for ADS

1. Chopper studies at the low-energy beam transport line

The chopper is an element used in the accelerator to control the beam pulse length and, consequently, the beam power. It produces an electromagnetic kick that deflects the beam toward conical collimators, as shown in Fig. 6.

The ADS linac chopper is an electrostatic device that generates a potential difference between two plates. Its plates have a length of 120 mm, and an aperture of the same size was chosen based on the beam energy, the

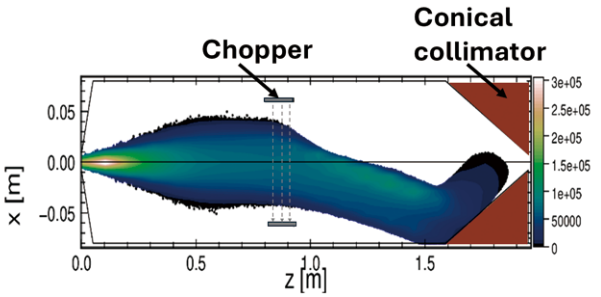

Fig. 6. Beam deflected to the collimator by the electrostatic kick provided by the chopper

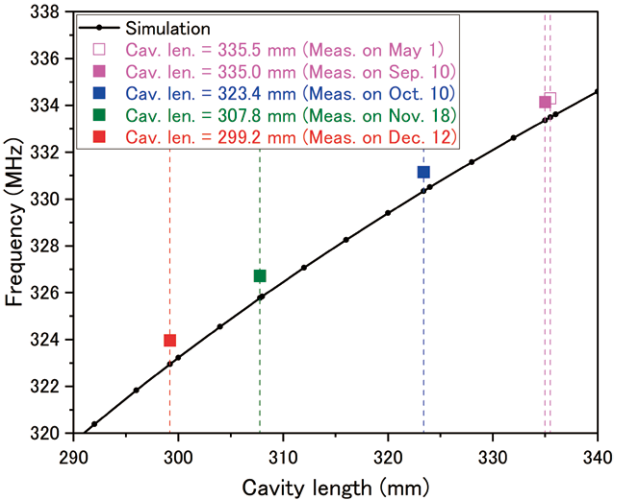

Fig. 7. Frequency adjustment during fabrication

Fig.8. [Left] After welding the body and one lid together. [Right] After welding the body and the other lid together.

chopper location in the LEBT, and the objective of operating with a difference of potential between the plates of a few kV in order to fully dump the beam. The rise and fall time of the voltage is estimated to be 15 nanoseconds based on the capacitance contribution of the chopper plates and assuming similar capacitances for the high-voltage switch and the feed-through connections reported by other choppers. Research on beam dynamics indicates that a voltage exceeding 4kV is required to completely dump the beam. This voltage level is attainable with current technology. Additionally, transient beam studies reveal that the chopper produces beam tails lasting about 180ns. This performance meets the requirements for measuring reactor subcriticality, which mandates beam tails shorter than 1μs to effectively monitor decay of the neutron population.

2. Fabrication of the prototype spoke cavity for the JAEA-ADS linac

As a first step toward the full-scale proton linac for the JAEA-ADS linac, we are currently prototyping a low-beta (around 0.2) single-spoke cavity. Since Japan has no experience in manufacturing superconducting spoke cavities, prototyping and performance-testing are essential to the feasibility of the JAEA-ADS.

The cavity fabrication began in 2020, and most parts were shaped by press-forming and machining during FY2020. In 2021, we began welding the shaped cavity parts together by electron beam welding (EBW). In FY2024, we have adjusted the resonance frequency of the cavity to the target value of 324MHz by trimming both ends of the body part (Fig. 7). And finally, we have fabricated the prototype spoke cavity by welding the body and two lids together (Fig. 8). Through the completion of the cavity's EBW-assembly, any obvious welding defects, such as unpenetrated welds and welding holes, have not been found. We will now proceed with surface treatment of the fabricated cavity. In the near future, we will conduct a Please deleted the word performance. high-field performance test of the prototype spoke cavity at liquid helium temperature.

Nuclear technology

Developing a Bayesian machine learning approach to estimating muon nuclear capture rate of a negative muon

A negative muon (μ^-) is a particle similar to the electron, but heavier and unstable. It has a negative electric charge, a mass about 200 times that of an electron (105.66MeV), and survives only about 2.2 microseconds in a vacuum before it decays. Like electrons, muons can orbit around an atomic nucleus, forming what is called a muonic atom. When a muon falls into the innermost orbit (the 1s orbital), it can be captured by the nucleus. This capture process, known as muon nuclear capture, triggers a nuclear decay.

Predicting how often this capture happens (the muon capture rate) is not easy. Yet, it is very important—for example, in developing radiation-hardened semiconductor devices and in research on reducing long-lived radioactive waste through nuclear

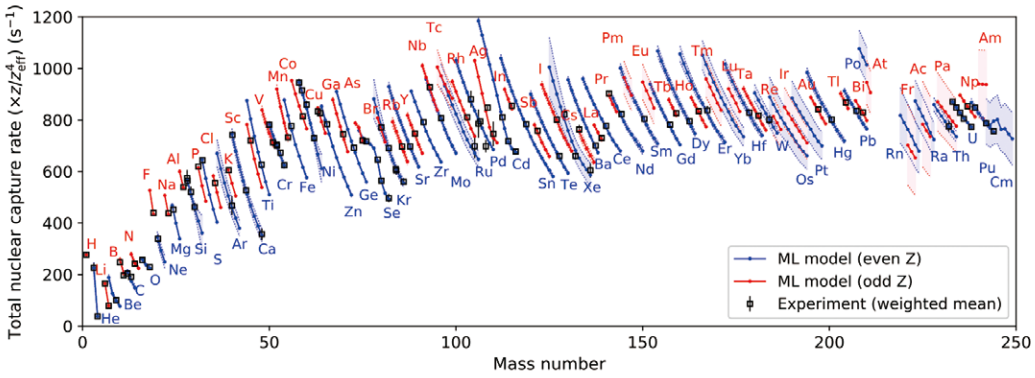

Fig. 9. Muon nuclear capture rates for respective nuclei estimated by our ML model. The band widths represent 1σ uncertainties. The experimental data represents weighted means for each element.

transmutation.

To tackle this challenge, we developed a machine learning (ML) model that estimates the muon capture rate [1]. Our model is based on Bayesian statistics, a mathematical framework that allows us to combine prior knowledge with new data. Specifically, we use a technique called Gaussian process regression. This method enables the model to make predictions by combining theoretical physics models with actual experimental data.

Figure 9 shows the capture rates estimated by our model for different atomic nuclei. The black dots represent experimental data from past studies, including recent measurements made at J-PARC [2]. Our model not only reproduces these known results, but can also predict capture rates for nuclei that have never been measured. In addition, the model provides an estimate of the uncertainty in its predictions, which is important for judging how reliable the results are.

The data obtained with our ML model will not only help develop new technologies, but also give us a better understanding of how muon capture reactions work.

References

[1] H. Iwamoto, *et al.*, Comprehensive Bayesian machine learning approach to estimating the total nuclear capture rate of a negative muon, Phys. Rev. C 111 034614 (2025).

[2] The work has been published so, please change the reference to "R. Mizuno, *et al.*, Lifetime measurement of the muonic atom of enriched Si isotopes, Phys. Rev. C 112 024307 (2025)."

International and Domestic Cooperation

We are collaborating with the Belgian Nuclear Research Centre (SCK CEN) on ADS development under the collaboration arrangement between SCK CEN and JAEA. SCK CEN is promoting the MYRRHA (Multi-purpose hYbrid Research Reactor for High-tech Application) project, which is the world's first large scale ADS project with power levels scalable to industrial systems. We held discussions with the MYRRHA accelerator team regarding the superconducting linac development.

Under the SAKURA Mobility Programme, funded by Swedish agencies, Dr. Bruce Yee-Rendon visited the European Spallation Source (ESS) to discuss high-intensity superconducting linac development, a topic of common interest to both ESS and JAEA-ADS. During the visit, beam dynamics to compensate for a single cavity failure were studied for the 810 MeV ESS linac.

We continued our collaboration with the Karlsruhe Institute of Technology in Germany on LBE technology, exchanging information regarding LBE loop operation.

We are also collaborating with domestic universities. One collaboration is with the University of Fukui on the behavior of spallation and corrosion products in LBE. We are developing the Transport of RAdionuclides In Liquid metal systems (TRAIL) code. In addition, thermodynamic calculations and metallurgical experiments on Ni-Bi oxides were conducted.

Another domestic collaboration is with the Institute of Science Tokyo. Several steel specimens were provided by the Institute and used for materials corrosion testing using the OLLOCHI loop.

Safety

Safety

1. Major events on safety culture and safety activities in the J-PARC

At J-PARC, we are actively engaged in activities to foster a safety culture to improve each individual's safety awareness, risk sensitivity, and safety-related skills.

For FY2024, we set the same safety policy as in FY2023: "Maintain safety through assertion and compliance with rules, even during routine work and before and after work; follow safety rules and share potential risks." In this context, the Japanese word "assertion" has a slightly different meaning from the English word "assertion". It refers to expressing opinions or making suggestions constructively, cooperatively and respectfully. J-PARC has continued these assertion activities since last year. Assertion activities involve encouraging participants in work meetings to freely share any questions, observations, concerns, or anxieties they may have. The meeting facilitator concludes meetings by asking if any participants have an assertion. If they do, the facilitator first expresses gratitude, responds with deference and sincerity, and ensures that the information is fully shared.

Table 1 lists the main events on safety at J-PARC.

In order not to forget the radioactive material leak incident that occurred on May 23 2013, J-PARC exchanges safety information between each section and holds a workshop for fostering safety culture around May 23 every year, which is held as the Safety Day. The Safety Day in FY2024 was held on May 23 with 352 participants at the real venue and online. In the morning, representatives from each division and section reported on case studies on fire prevention as part of the safety information exchange meeting. In the afternoon, under the title of "Workshop for Fostering a Safety Culture," we first presented the Safety Contribution Award and the Best Practices Award. Next, there was a lecture by Dr. FUKUWA Nobuo, Honorary Professor of Nagoya University and Director of the Aichi-Nagoya Resilience Co-creation Center, titled "Preparing for Large-Scale Earthquakes with Wisdom from the Past." The event concluded with the screening of the documentary film "Radioactive Material Leakage Accident: How It Was Perceived by Society."

The 2024 International Technical Safety Forum (ITSF) hosted by RIKEN and the J-PARC center was held at RIKEN Wako Campus and the J-PARC on June 10-14. The ITSF is an informal practitioner-led forum to exchange lessons learned and state-of-the-art ideas, processes, procedures, and technologies in personnel, environmental, and equipment safety. There were 104 participants in total, 86 on-site and 18 online. Fifty-one oral presentations, 24 poster presentations, five invited/summary talks, and 15 facility posters were presented.

An emergency drill was conducted on December 24 at the MR. The disaster scenario was as follows. During beam operation at the MR, a fire broke out in the hot machine room of the MR No. 2 machine building (1st class radiation-controlled area). Initial firefighting efforts were unable to extinguish the fire. Following the power shutdown, firefighting activities were conducted. The purpose of the drill was to confirm the following: (1) Initial response to a fire outbreak; (2) Public firefighters' access to the radiation-controlled area; (3) Information exchange between the fire location and the command post; and (4) Communication between the command post, JAEA Nuclear Science Research Institute (NSRI) local headquarters, and the KEK director at the TSUKUBA campus via a TV conference system.

The J-PARC Center conducts annual safety audits by external experts based on advice from the J-PARC Steering Board. Two auditors were invited to conduct the audit for FY2024. On December 2, 2024 (Day 1), a pre-audit briefing was conducted online, and on December 16, 2024 (Day 2), on-site inspections were conducted by the auditors.

The audit items were as follows: (1) Response to the fire that occurred at J-PARC during FY2024; (2) Organizational structure for safety management; (3) Safety management at work; (4) Emergency responses: and (5) Safety education and the promotion and maintenance of a safety culture.

2. Radiological license update and facility inspection

No application to update the radiological license was submitted to the Nuclear Regulation Authority during FY2024.

The facility inspection of the Hadron Experimental Facility was conducted by the Radiation Management Institute, Inc. on June 3. The items inspected were the modification of the shielding structure of the primary proton beam line (BC line area) and the measurement of radiation dose rates at the facility.

The certificate of compliance was issued on June 4.

3. Meeting of the committee on radiation safety matters

The J-PARC Radiation Safety Committee is organized as an advisory committee to both JAEA and KEK, discussing policy on radiation safety at J-PARC. Meanwhile, the Radiation Safety Review Committee was established to discuss specific subjects of radiation safety in the J-PARC.

In FY2024, the J-PARC Radiation Safety Committee met twice, and the Radiation Safety Review Committee met once. Table 2 lists the major issues discussed by the committees.

4. Radiation exposure of radiation workers

The number of persons subject to annual measurement of external exposure in FY2024 was 2784.

Table 3 lists the distribution of annual exposed doses for each category of workers. There was no exposure exceeding the dose limit specified in the local radiation protection rule for J-PARC and the administrative dose limits (7 mSv/year) specified in the detailed rules on local radiation protection for J-PARC. The total annual effective dose was 37.3 person·mSv, and the maximum effective dose was 0.9 mSv.

Tab. 1. List of major events on safety in FY2024

Day	Events
May 23, 2024	Safety Day (meeting to exchange safety information between each section, workshop on fostering safety culture)
June 10-14, 2024	The 2024 International Technical Safety Forum (ITSF)
July 3, 2024	Liaison committee on safety and health for contractors
December 2024	Refresher course on radiation safety for in-house staff (e-learning)
December 2 & 16, 2024	FY2024 J-PARC Safety Audit
December 24, 2024	Emergency drill assuming a fire accident at the MR

Tab. 2. Radiation Safety Committee (RSC) and Radiation Safety Review Committee (RSRC) in FY2024

No.	Date	Major Issues
The Radiation Safety Committee		
43th	July 30, 2024	• Report on the personal exposure situation, amount of radioactive waste released in FY2023
44th	March 14, 2025	• Report on the plan in FY2025
The Radiation Safety Review Committee		
39th	July 9, 2024	• Upgrade of the off-gas process system of MLF

Tab. 3. Annual exposure doses in FY2024

	Number of workers	Dose range x (mSv)				Collective dose (person · mSv)	Maximum dose (mSv)
		ND	0.1 ≤ x ≤ 1.0	1.0 < x ≤ 5.0	5.0 < x		
In-house staff	721	677	44	0	0	12.1	0.8
Users	949	927	22	0	0	2.2	0.1
Contractors	1123	1027	96	0	0	23.0	0.9
Total	2784	2622	162	0	0	37.3	0.9

* If the worker classification of the same worker changed during the fiscal year, the worker was counted as one worker per classification. Therefore, the total number does not match the sum of the respective classifications.

User Service

Users Office (UO)

Outline

The J-PARC Users Office (UO) was established in 2007. It opened an office on the first floor of the IBARAKI Quantum Beam Research Center in Tokai-mura, in December 2008. The UO maintains the Tokai Dormitory for J-PARC users, and provides on-site and WEB support with a one-stop service for the utilization of the J-PARC. As of March 31, 2025, the UO had 10 staff members and five WEB Support SE staff in the Users Affairs Section. After the approval of their experiments, J-PARC Users follow the administrative procedures outlined on the Users Office (UO) WEB Portal Site. These are related to registration as a J-PARC User, radiation worker registration, safety education, accommodation, invitation letters for visas and other requirements. The UO staff also provide them with support by e-mail. After their arrival at the J-PARC, the UO gives on-site assistance to J-PARC Users, like handing out J-PARC IDs, glass badges, and safety education. Since 2015, the UO has been doing its part to improve the J-PARC on-line experiment system and make it more user-friendly.

After the experiments the UO may return the experiment samples at User's cost after cooling the radioactive activity.

One stop service for J-PARC users

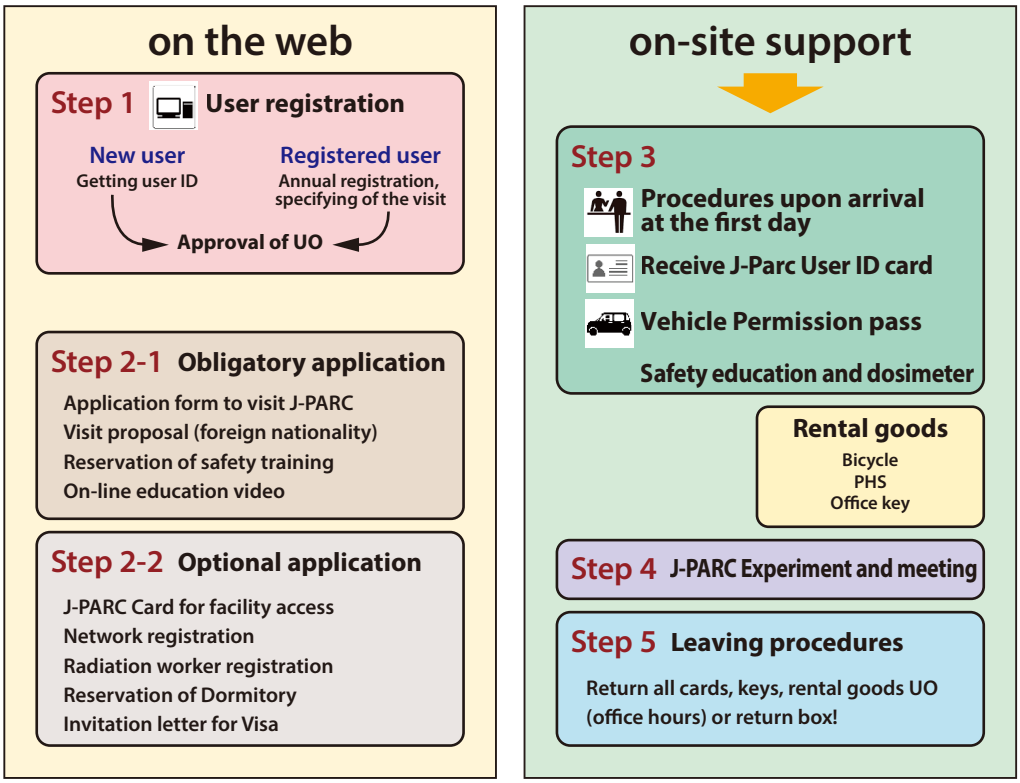

Users Office at AQBRC
Office hours
(9:00-12:00, 13:00-17:00, Mon. - Fri.)

Rental bicycle

Return box at AQBRC

User Statistics

Users in 2024 (Japanese/Foreigners, person-days)

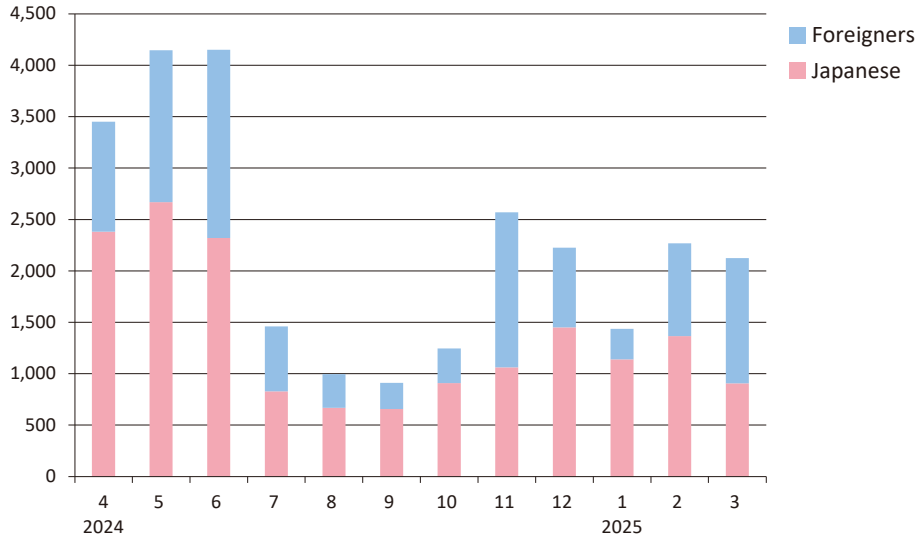

Users in 2024 (according to facilities, person-days)

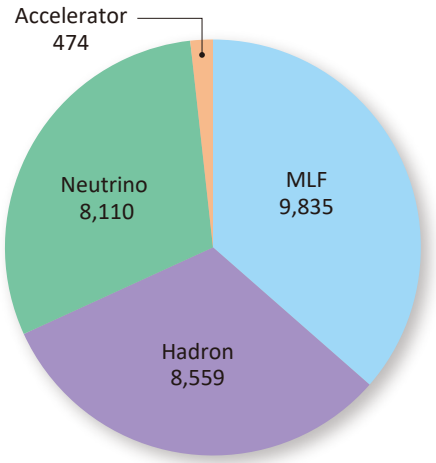

Users in 2024 (according to organizations, person-days)

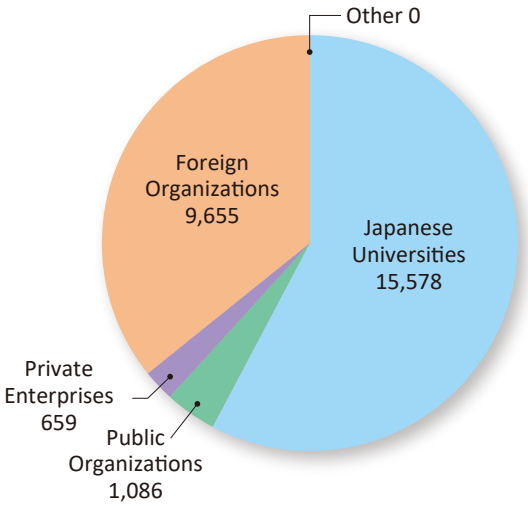

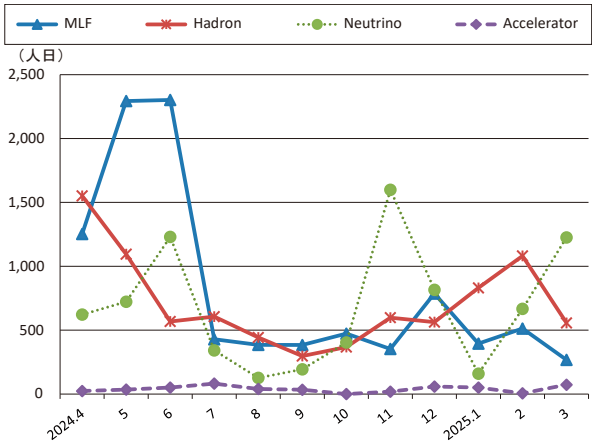

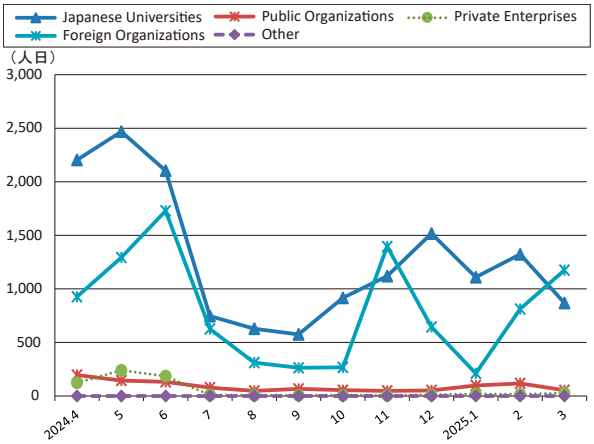

MLF Proposals Summary: FY2024

Table 1. Number of Proposals by Beamline

Beam-line	Instrument		2024A		2024B		Full Year			
			Submitted	Approved	Submitted	Approved	Submitted		Approved	
			GU	GU	GU	GU	PU/S	IU	PU/S	IU
BL01	4D-Space Access Neutron Spectrometer - ***4SEASONS***		33(1)	9(1)	29(1)	8(1)	0	2	0	2
BL02	Biomolecular Dynamics Spectrometer - ***DNA***		19(0)	8(0)	23(1)	5(1)	0	2	0	2
BL03	IBARAKI Biological Crystal Diffractometer - ***iBIX***	(100-β)‡	0	0	1	1	0	0	0	0
		(b)†	3	3	2	2	17※	0	17※	0
BL04	Accurate Neutron-Nucleus Reaction Measurement Instrument - ***ANNRI***		4	3	7	1	2	1	2	1
BL05	Neutron Optics and Physics - ***NOP***		5	5	7	4	1	1	1	1
BL06	Village of Neutron Resonance Spin Echo Spectrometers - ***VIN ROSE***		4	2	3	3	2	0	2	0
BL08	Super High Resolution Powder Diffractometer - ***SuperHRPD***		13	8	15	8	1	0	1	0
BL09	Special Environment Neutron Powder Diffractometer - ***SPICA***		2	2	6	4	1	0	1	0
BL10	NeutrOn Beam-line for Observation and Research Use - ***NOBORU***		10	7	13	9	2	1	2	1
BL11	High-Pressure Neutron Diffractometer - ***PLANET***		10(0)	8(0)	11(0)	5(0)	0	1	0	1
BL12	High Resolution Chopper Spectrometer - ***HRC***		11	7	9	3	1	0	1	0
BL14	Cold-Neutron Disk-Chopper Spectrometer - ***AMATERAS***		34	9	35	4	1	1	1	1
BL15	Small and Wide Angle Neutron Scattering Instrument - ***TAIKAN***		24(1)	11(1)	25(2)	11(2)	3	5	3	5
BL16	Soft Interface Analyzer - ***SOFIA***		11	9	19	8	1	1	1	1
BL17	Polarized Neutron Reflectometer - ***SHARAKU***		18(1)	11(1)	23(3)	10(3)	3	3	3	3
BL18	Extreme Environment Single Crystal Neutron Diffractometer - ***SENJU***		24(0)	6(0)	26(0)	6(0)	0	1	0	1
BL19	Engineering Materials Diffractometer - ***TAKUMI***		38	11	32	9	1	1	1	1
BL20	IBARAKI Materials Design Diffractometer - ***iMATERIA***	(100-β)‡	3	3	5	2	0	0	0	0
		(β)†	33	33	21	21	15	0	15	0
BL21	High Intensity Total Diffractometer - ***NOVA***		27	20	22	13	2	0	2	0
BL22	Energy Resolved Neutron Imaging System - ***RADEN***		14(0)	11(0)	17(2)	9(2)	2	2	2	2
BL23	Polarization Analysis Neutron Spectrometer - ***POLANO***		3	3	5	2	1	0	1	0
D1	Muon Spectrometer for Materials and Life Science Experiments - ***D1***		10(0)	8(0)	19(1)	6(0)	2	1	2	1
D2	Muon Spectrometer for Basic Science Experiments - ***D2***		5(1)	5(1)	5(0)	2(0)	2	1	2	1
S1	General purpose μSR spectrometer - ***ARTEMIS***		28(2)	21(2)	21(0)	13(0)	1	1	1	1
S2	Muonium Laser Physics Apparatus - ***S2***		0(0)	0(0)	0(0)	0(0)	0	1	0	1
U1A	Ultra Slow Muon Microscope - ***U1A***		0	0	0	0	0	1	0	1
U1B	Transmission Muon Microscope - ***U1B***		0	0	0	0	0	1	0	1
H1	High-intensity Muon Beam for General Use - ***H1***		0	0	2(1)	2(1)	0	1	0	1
Total			***384***	***221***	***401***	***169***	***49***	***29***	***49***	***29***

GU : General Use **PU** : Project Use or Ibaraki Pref. Project Use **S** : S-type Proposals
IU : Instrument Group Use
† : Ibaraki Pref. Exclusive Use Beamtime (β = 80% in FY2024)
‡ : J-PARC Center General Use Beamtime (100-β = 20% in FY2024)
( ) : Proposal Numbers under the New User Promotion (BL01, BL02, BL11, BL15, BL17, BL18, BL22) or P-type proposals (D1,D2, S1) in GU

※ : Operations period is held twice per year (for each of the A and B periods), with only the yearly total shown above.
The actual total number of proposals in each beamline named in the table does not match the number shown in the "Total" cell, because some proposals are submitted or approved across multiple beamlines.

Table 2. Number of Long-Term Proposals by Fiscal Year

Application FY	Submitted	Approved
2022	5	4
2023	0	0
2024	3	3

No Long-Term Proposals were called for FY2023.

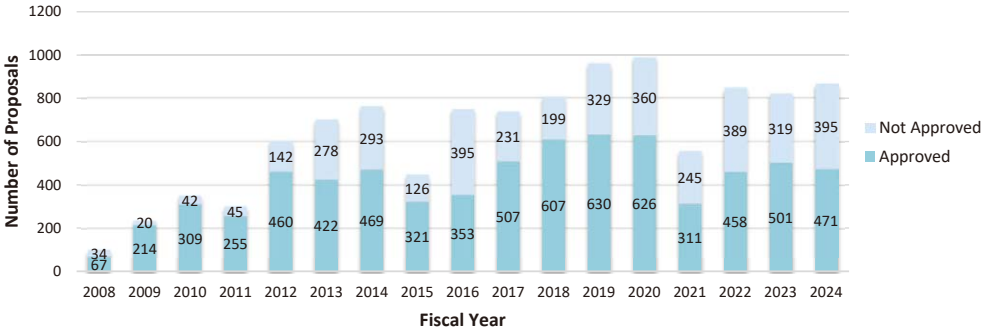

Fig. 1. Number of MLF Proposals over Time

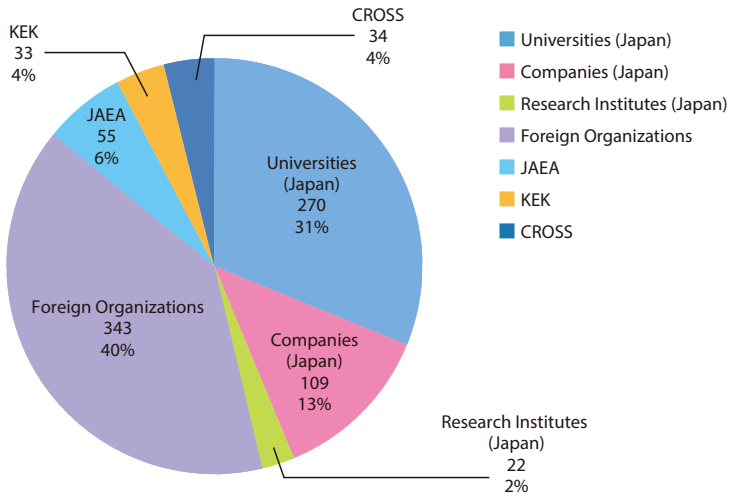

Fig. 2. Origin of Submitted Proposals by Affiliation - FY2024

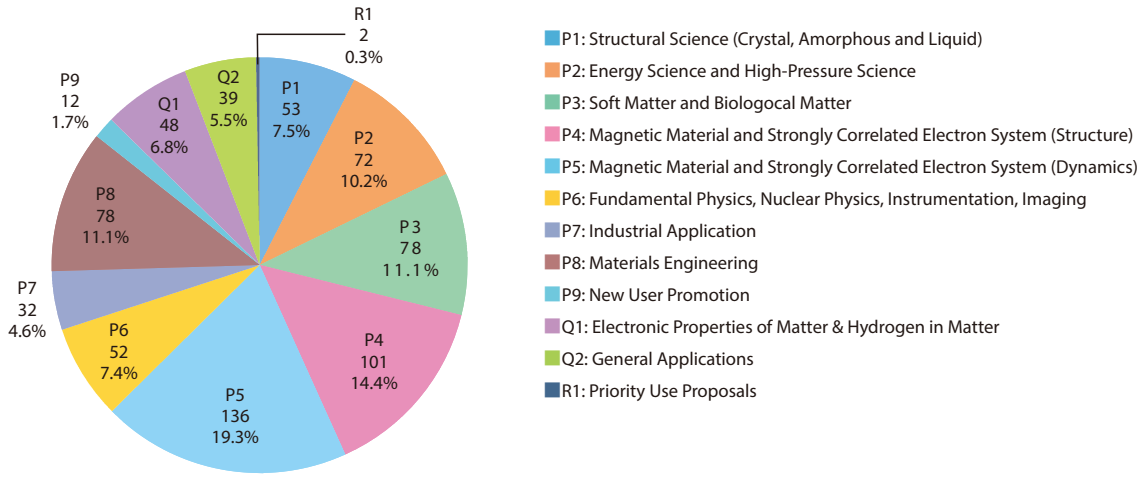

Fig. 3. Submitted Proposals by Sub-committee/Expert Panel – FY2024

J-PARC PAC Approval Summary for the 2024 Rounds

	(Co-) Spokespersons	Affiliation	Title of the experiment	Approval status (PAC recommendation)	Beamline	Status
E03	K.Tanida, T.Yamamoto	JAEA	Measurement of X rays from **X**$^-$ Atom	Stage 2	K1.8	Data taking
P04	J.C.Peng, S.Sawada	U of Illinois at Urbana-Champaign, KEK	Measurement of High-Mass Dimuon Production at the 50-GeV Proton Synchrotron	Deferred	Primary	
E05	T.Nagae	Kyoto U	Spectroscopic Study of **X**-Hypernucleus, $^{12}_{X}$Be, via the ^{12}C(K$^-$, K$^+$) Reaction	Stage 2 New experiment E70 based on the S-2S spectrometer	K1.8	Finished
E06	J.Imazato	KEK	Measurement of T-violating Transverse Muon Polarization in K$^+$ -> **p**^{0} **m**$^+$ **n** Decays	E36 as the first step	K1.1BR	
E07	K.Imai, K.Nakazawa, H.Tamura	JAEA, Gifu U, Tohoku U	Systematic Study of Double Strangeness System with an Emulsion-counter Hybrid Method	Stage 2	K1.8	Finished Data analysis
E08	A.Krutenkova	ITEP	Pion double charge exchange on oxygen at J-PARC	Stage 1	K1.8	
E10	R.Honda	KEK	Production of Neutron-Rich Lambda-Hypernuclei with the Double Charge-Exchange Reaction (Revised from Initial P10)	Stage 2	K1.8	Li run finished, Be target run with S-2S
E11	K.Sakashita, K. Mahn	KEK, Michigan State U	Tokai-to-Kamioka (T2K) Long Baseline Neutrino Oscillation Experimental Proposal	Stage 2	neutrino	Data taking
E13	H.Tamura	Tohoku U	Gamma-ray spectroscopy of light hypernuclei	Stage 2	K1.8	Finished
E14	T.Nomura	KEK	Proposal for K_L -> p^0 n n-bar Experiment at J-PARC	Stage 2	KL	Data taking
E15	M.Iwasaki, T.Nagae	RIKEN, Kyoto U	A Search for deeply-bound kaonic nuclear states by in-flight 3He(K-, n) reaction	Stage 2	K1.8BR	Finished
E16	S.Yokkaichi	RIKEN	Measurements of spectral change of vector mesons in nuclei (previously "Electron pair spectrometer at the J-PARC 50-GeV PS to explore the chiral symmetry in QCD")	Deferred for Run 1. PAC recommends to fully calibrate the detector, improve the trigger efficiency and develop the tracking procedure using the existing data.	High p	Data taking
E17	R.Hayano, H.Outa	U Tokyo, RIKEN	Precision spectroscopy of Kaonic ^{3}He 3d->2p X-rays	Registered as E62 with an updated proposal	K1.8BR	
E18	H.Bhang, H.Outa, H.Park	SNU, RIKEN, KRISS	Coincidence Measurement of the Weak Decay of $^{12}_{L}$C and the three-body weak interaction process	Stage 2	K1.8	
E19	M.Naruki	KEK	High-resolution Search for Q$^+$ Pentaquark in **p**$^-$p -> K$^-$X Reactions	Stage 2	K1.8	Finished
E21	M.Aoki	Osaka U	An Experimental Search for μ − e Conversion at a Sensitivity of 10^{-16} with a Slow-Extracted Bunched Beam	Stage 2	COMET	
E22	S.Ajimura, A.Sakaguchi	Osaka-RCNP, Osaka U	Exclusive Study on the Lambda-N Weak Interaction in A=4 Lambda-Hypernuclei	Stage 1	K1.8	
T25	S.Mihara	KEK	Extinction Measurement of J-PARC Proton Beam at K1.8BR	Test Experiment	K1.8BR	Finished
E26	K.Ozawa	KEK	Search for w-meson nuclear bound states in the p-+^{A}Z -> n+$^{(A-1)}_{w}$(Z-1) reaction, and for w mass modification in the in-medium w->p^{0}g decay	Stage 1	K1.8	
E27	T.Nagae	Kyoto U	Search for a nuclear Kbar bound state K$^-$pp in the d(p$^+$, K$^+$) reaction	Stage 2	K1.8	Fisnished
E29	H.Ohnishi	Tohoku-RAIS	Search for f-meson nuclear bound states in the pbar + ^{A}Z -> f + $^{(A-1)}_{f}$(Z-1) reaction	Stage 1	K1.1	
E31	H.Noumi	Osaka-RCNP	Spectroscopic study of hyperon resonances below KN threshold via the (K$^-$n) reaction on Deuteron	Stage 2	K1.8BR	Finished Data analysis
T32	A.Rubbia	ETH, Zurich	Towards a Long Baseline Neutrino and Nucleon Decay Experiment with a next-generation 100 kton Liquid Argon TPC detector at Okinoshima and an intensity upgraded J-PARC Neutrino beam	Test Experiment	K1.1BR	Finished
P33	H.M.Shimizu	Nagoya U	Measurement of Neutron Electric Dipole Moment	Deferred	Linac	
E34	T. Mibe	KEK	An Experimental Proposal on a New Measurement of the Muon Anomalous Magnetic Moment g-2 and Electric Dipole Moment at J-PARC	Stage 2	MLF	

	(Co-) Spokespersons	Affiliation	Title of the experiment	Approval status (PAC recommendation)	Beamline	Status
E36	M.Kohl, S.Shimizu	Hampton U, Osaka U	Measurement of $G(K^+ \to e^+ n)/G(K^+ \to m^+ n)$ and Search for heavy sterile neutrinos using the TREK detector system	Stage 2	K1.1BR	Finished Data analysis
E40	K.Miwa	Tohoku U	Measurement of the cross sections of Σp scatterings	Stage 2	K1.8	Finished Data analysis
P41	M.Aoki	Osaka U	An Experimental Search for μ – e Conversion in Nuclear Field at a Sensitivity of 10^{-14} with Pulsed Proton Beam from RCS	Deferred	MLF	Reviewed in MLF/IMSS
E42	J.K.Ahn	Pusan National U	Search for H-Dibaryon with a Large Acceptance Hyperon Spectrometer	Stage 2	K1.8	Finished
E45	K.H.Hicks, H.Sako	Ohio U, JAEA	3-Body Hadronic Reactions for New Aspects of Baryon Spectroscopy	Stage 2 PAC requests that the group further examine ways to reduce the total beam time requested and to find an efficient running scheme, including quick but careful beam tuning.	K1.8	
T46	K.Ozawa	KEK	EDIT2013 beam test program	Test Experiment	K1.1BR	Aban-donded
T49	T.Maruyama	KEK	Test for 250L Liquid Argon TPC	Test Experiment	K1.1BR	Withdrawn
E50	H.Noumi	Osaka-RCNP	Charmed Baryon Spectroscopy via the (π,D^{+*}) reaction	Stage 1 The FIFC, IPNS, and E50 should investigate the beam-line feasibility	High p	
T51	S.Mihara	KEK	Research Proposal for COMET(E21) Calorimeter Prototype Beam Test	Test Experiment	K1.1BR	had to be stopped
T52	Y.Sugimoto	KEK	Test of fine pixel CCDs for ILC vertex detector	Test Experiment	K1.1BR	not performed yet
T53	D.Kawama	RIKEN	Test of GEM Tracker, Hadron Blind Detector and Lead-glass EMC for the J-PARC E16 experiment	Test Experiment	K1.1BR	not performed yet
T54	K.Miwa	Tohoku U	Test experiment for a performance evaluation of a scattered proton detector system for the Σp scattering experiment E40	Test Experiment	K1.1BR	not performed yet
T55	A.Toyoda	KEK	Second Test of Aerogel Cherenkov counter for the J-PARC E36 experiment	Test Experiment	K1.1BR	had to be stopped
E56	T.Maruyama	KEK	A Search for Sterile Neutrino at J-PARC Materials and Life Science Experimental Facility	Stage 2	MLF	Data taking
E57	T.Hashimoto, C.Curceanu	RIKEN, INFN-LNF	Measurement of the strong interaction induced shift and width of the 1s state of kaonic deuterium at J-PARC	Stage 1	K1.8BR	in prepara-tion
P58	M. Yokoyama	U. Tokyo	A Long Baseline Neutrino Oscillation Experiment Using J-PARC Neutrino Beam and Hyper-Kamiokande	Deferred	neutrino	
T59	A. Minamino	Kyoto U	A test experiment to measure neutrino cross sections using a 3D grid-like neutrino detector with a water target at the near detector hall of J-PARC neutrino beam-line	To be arranged by IPNS and KEK-T2K	neutrino monitor bld	Finished
T60	T. Fukuda	Toho U	Proposal of an emulsion-based test experiment at J-PARC	Arranged by IPNS and KEK-T2K	neutrino monitor bld	Finished
E61	M. Wilking	Stony Brook U	NuPRISM/TITUS	Superseded. E61 has been adopted in Hyper-K as IWCD. IWCD is reviewed by HK-PAC.	neutrino	
E62	R. Hayano, S. Okada, H. Outa	U. Tokyo, RIKEN	Precision Spectroscopy of kaonic atom X-rays with TES	Stage 2	K1.8BR	Finished
E63	H. Tamura, M. Ukai	Tohoku U	Gamma-ray spectroscopy of light hypernuclei II	Stage 2	K1.1/K1.8	BL not ready yet. Exp. in preparation
T64	Y. Koshio	Okayama U	Measurement of the gamma-ray and neutron background from the T2k neutrino/anti-neutrino at J-PARC B2 Hall	Arranged by IPNS and KEK-T2K	neutrino	Finished
E65	K.Sakashita, K. Mahn	KEK, Michigan State U	Proposal for T2K Extended Run	Stage-2	neutrino	Data taking

	(Co-) Spokespersons	Affiliation	Title of the experiment	Approval status (PAC recommendation)	Beamline	Status
T66	T. Fukuda	Nagoya U	Proposal of an emulsion-based test experiment at J-PARC	Test Experiment	neutrino	Finished
P67	I. Meigo	JAEA	Measurement of displacement cross section of proton in energy region between 3 and 30 GeV for high-intensity proton accelerator facility	Carry out the experiment within the framework of facility development	MR	
T68	T. Fukuda	Nagoya U	Extension of T60/T66 Experiment: Proposal for the Run from 2017 Autumn	Test Experiment	neutrino	Finished
E69	A. Minamino	Yokohama National U	Study of neutrino-nucleus ineraction at around 1GeV using cuboid lattice neutrino detector, WAGASHI, muon range detectors and magnetized spectrometer, Baby MIND, at J-PARC neutrino monitor hall	Superseded. Merged with T2K.	neutrino	
E70	T. Nagae	Kyoto U	Proposal for the next E05 run with the S-2S spectrometer	Stage-2	K1.8	Data taking
E71	T. Fukuda	Nagoya U	Proposal for precise measurement of neutrinop-water cross-section in NINJA physics run	Stage-2	neutrino	Data taking
E72	K. Tanida	JAEA	Search for a Narrow Λ* Resonance using the p(K-, Λ)η Reaction with the hypTPC Detector	Stage-2	K1.8BR	
E73	Yue Ma	RIKEN	$^{3}_{\Lambda}$H and $^{4}_{\Lambda}$H mesonic weak decay lifetime measurement with ^{3,4}He(K$^-$,π^0)$^{3,4}_{\Lambda}$H reaction	Stage-2	K1.8BR	Data taking
E75	H.Fujioka	Inst. Science Tokyo	Decay Pion Spectroscopy of 5ΛΛH Produced by Ξ-hypernuclear Decay	Stage-2	K1.8	
P76	H.M.Shimizu	Nagoya U	Searches for the Breaking of the Time Reversal Invariance in Polarized Epithermal Neutron Optics	Deferred	MLF	
T77	Yue Ma	RIKEN	Feasibility study for 3ΛH mesonic weak decay lifetime measurement with 3,4He(K-,π0)3,4ΛH reaction	PAC supoorts the ontinuation of T77 by an explorative run with the 3He target.	K1.8BR	Finished Data analysis
T78	H.Nishiguchi	KEK	8GeV Operation Test and Extinction Measurement	Test Experiment	K1.8BR	Finished
E79	T.Ishikawa	Osaka-RCNP	Search for an I=3 dibaryon resonance	Stage-1	high-p	
E80	F.Sakuma	RIKEN	Systematic investigation of the light kaonic nuclei	Stage-2	K1.8BR	
T81	T.Fukuda	Nagoya U	Proposal of test experiment for technical improvements of neutrino measurements with nuclear emulsion detector	Test Experiment	neutrino	
E82	T.Maruyama	KEK	JSNS2-II	Stage-2	MLF	
E83	J. H. Yoo	Korea U	Search for sub-millicharged particles at J-PARC	Stage-2	neutrino	Data taking
P84	S. Nakamura	Tohoku U	High precision spectroscopy of Lambda hypernuclei with the (\pi^+, K^+) reaction at the High Intensity High Resolution beamline	Deferred. This proposal is a part of the hadron extension discussion and PAC awaits the outcome of the special committee to convene in August for more information.	HIHR	
P85	K. Shirotori	Osaka-RCNP	Spectroscopy of Omega Baryons	Deferred. This proposal is a part of the hadron extension discussion and PAC awaits the outcome of the special committee to convene in August for more information.	K10, T2 target	
E86	K. Miwa	Tohoku U	Measurement of the differential cross section and spin observables of the Λp scattering with a polarized Λ beam	Stage 1	K1.1	
P87	T. Gunji, K. Ozawa, H. Sako	Tokyo,KEK,JAEA	Proposal for dielectron measurements in heavy-ion collisions at J-PARC with E16 upgrades	Deferred. PAC encourages the proponents to think about more versatile detector enabling (for example) concurrent measurement of leptonic and hadronic measurements.	HI, high-p	
E88	H. Sako	JAEA	Study of in-medium modification of phi mesons inside the nucleus with phi->K+K- measurement with the E16 spectrometer	Stage-1	high-p	
E89	T. Yamaga	KEK	Investigation of fundamental properties of the KNN state	Stage-1	K1.8BR	
E90	Y.Ichikawa, K.Tanida	JAEA	High resolution spectroscopy of the "ΣN cusp" by using the d(K-, π-) reaction	Stage-1	K1.8	
P91	Y.Morino	KEK	Proposal for study of charm component in the nucleon via J/ψ measurement with the J-PARC E16 spectrometer	Deferred.	high-p	
P92	F.Sakuma	RIKEN	Proposal for the E80 Phase-I Experiment:Investigation of the KNNN $^-$ Bound State Focusing on the Λd Decay	Deferred.	K1.8BR	

	(Co-) Spokespersons	Affiliation	Title of the experiment	Approval status (PAC recommendation)	Beamline	Status
P93	K.Shirotori	Osaka-RCNP	Proposal of test experiment to evaluate performances of secondary beam mode at the high-momentum beam line	Deferred. PAC requests the proponent to continue discussion with the Lab/Facility management	high-p	
E94	T.Gogami	Kyoto U	New generation Λ hypernuclear spectroscopy with the (π^+, K^+) reaction by S-2S	Deferred for Stage-2. It is necessary to submit an updated TDR to FIFC.	K1.8	
E95	T.Ishikawa	Osaka-RCNP	Pion-induced phi-meson production on the proton	Stage-1	high-p	
E96	T.O.Yamamoto	JAEA	Measurement of X rays from Ξ^- C atom with an active fiber target system	Stage-2	K1.8	
E97	M.Naruki	Kyoto U	Cascade baryon spectroscopy at J-PARC high-momentum beamline	Stage-1	high-p	
T98	K.Yorita	Waseda U	Measurement of Anti-Matter Reaction in Liquid Argon Time Projection Chamber	Test-experiment. PAC recommends approval of phase-2 for 24 hours of beam time	K1.8BR	Data taking
E99	H. Shimizu	Nagoya U	Study of Discrete Symmetries in Polarized Epithermal Neutron Optics	Stage-1 for Phase-I	MLF	
E100	K. Mishima	Nagoya U	Neutron lifetime measurement with pulsed cold neutrons	Stage-1	MLF	
T101	H. Ito	Tokyo U of Science	Measurement of neutrino-induced neutron and γ-ray background for BGO-based detectors at J-PARC	Test Experiment	neutrino	Finished
P102	H. Kohri	Osaka-RCNP	Study of the peculair bump structure at 1680 MeV by the $\pi^-p \to \eta n$ reaction with momenta of p_π=0.85-1.2 GeV/c	Deferred.	K1.8	
T103	K. Shirotori	Osaka-RCNP	Proposal of a test experiment to evaluate the performance of the trigger-less data-streaming type data acquisition system	Test Experiment	K1.8BR	Finished
E104	J.K.Ahn	Korea U	Double φ Production in p-bar p Reactions near Threshold	Stage-1	K1.8BR	
T105	Y. Enari	KEK	Proposal of a test experiment for a test beam line at the K1.8 BR area	Test Experiment	K1.8BR	Finished
T106	K. Shirotori	Osaka-RCNP	Proposal for the first stage of the P93 experiment	Test Experiment	high-p	Finished
E107	H. Nanjo	Osaka U	Proposal of the KOTO II experiment	Stage-1 Discussions to grant Stage-2 Approval will be subject to the approval of the J-PARC Hadron Facility extenstion.	KL2	
T108	Y. Ma, M. Ukai	RIKEN, KEK	Test Experiment to Optimize d-bar Beam Intensity at the K1.8 Beam Line of the J-PARC Hadron Experimental Facility	Test Experiment	K1.8	
P109	S.H. Kim, Y. Ichikawa	Kyungpook National U, Tohoku U	Optimization of Low Momentum K^+ Beam Using a Beam Degrader	Test Experiment	K1.8BR	

Organization and Committees

Organization Structure

J-PARC Center Management System Chart as of April 1, 2024

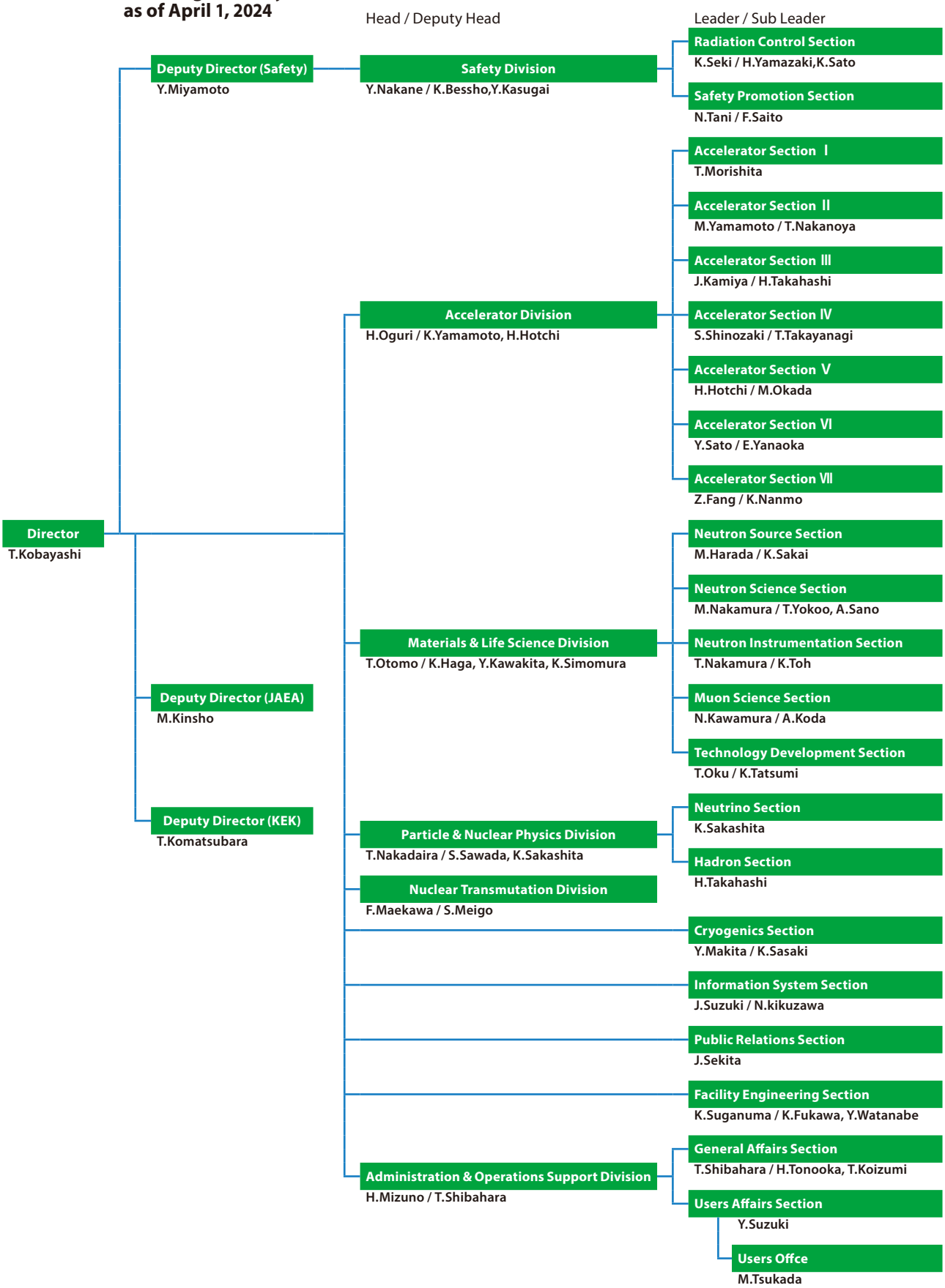

Members of the Committees Organized for J-PARC

(as of March, 2025)

1) Steering Committee

(*) Chair

Name	Affiliation
Shinichiro Michizono (*)	High Energy Accelerator Research Organization (KEK), Japan
Yuko Nagano	High Energy Accelerator Research Organization (KEK), Japan
Naohito Saito	High Energy Accelerator Research Organization (KEK), Japan
Nobumasa Funamori	High Energy Accelerator Research Organization (KEK), Japan
Tadashi Koseki	High Energy Accelerator Research Organization (KEK), Japan
Toshiyuki Momma (*)	Japan Atomic Energy Agency (JAEA), Japan
Takahiro Hayashi	Japan Atomic Energy Agency (JAEA), Japan
Kenji Nakajima	Japan Atomic Energy Agency (JAEA), Japan
Kazuhide Ajiki	Japan Atomic Energy Agency (JAEA), Japan
Toshikatsu Maeda	Japan Atomic Energy Agency (JAEA), Japan
Takashi Kobayashi	J-PARC Center, Japan

2) International Advisory Committee

(*) Chair

Name	Affiliation
Robert McGreevy (*)	Science & Technology Facilities Council (STFC), UK
Ken Andersen	Institut Laue-Langevin (ILL), France
Takeshi Egami	University of Tennessee, U.S.A.
Jie Wei	Michigan State University, U.S.A.
John Thomason	Science & Technology Facilities Council (STFC), UK
Joachim Mnich	The European Organization for Nuclear Research (CERN), Switzerland
Dmitri Denisov	Brookhaven National Laboratory, U.S.A.
Angela Bracco	Istituto Nazionale di Fisica Nucleare, Italy
Hamid Aït Abderrahim	Belgian Nuclear Research Centre（SCK CEN）, Belgium
Jamie Schulz	Australian Nuclear Science and Technology Organization (ANSTO), Australia
Klaus Kirch	ETH Zurich, Switzerland / Paul Scherrer Institute (PSI), Switzerland
Cynthia Keppel	Thomas Jefferson National Accelerator Facility, U.S.A.
Hiromi Yokoyama	The University of Tokyo, Japan
Yoko Sugawara	Kitasato University, Japan
Shinichi Kamei	Mitsubishi Research Institute, Inc., Japan
Mitsuhiro Fukuda	Osaka University, Japan

3) User Consultative Committee for J-PARC

(*) Chair

Name	Affiliation
Satoshi Nakamura	The University of Tokyo, Japan
Koji Miwa	Tohoku University, Japan
Takatsugu Masuda	The University of Tokyo, Japan
Yoshie Otake	RIKEN, Japan
Kenya Kubo (*)	International Christian University, Japan
Tadashi Adachi	Sophia University, Japan
Yuko Kojima	Mitsubishi Chemical Corporation, Japan
Kenji Ohoyama	Ibaraki University, Japan
Mitsuhiro Fukuda	Osaka University, Japan
Kazufumi Tsujimoto	Japan Atomic Energy Agency (JAEA), Japan
Kazuki Ueno	Osaka University, Japan
Tatsuya Kikawa	Kyoto University, Japan
Tsuyoshi Nakaya	Kyoto University, Japan
Megumi Naruki	Kyoto University, Japan
Tadashi Hashimoto	RIKEN, Japan
Rintaro Inoue	Kyoto University, Japan
Noriyuki Tsuchida	University of Hyogo, Japan
Yusuke Nambu	Tohoku University, Japan
Takanori Ito	Nissan Arc, Ltd., Japan
Haruo Miyadera	Toshiba Corporation, Japan
Hiroyuki Shindo	Japan Aerospace Exploration Agency, Japan

4) Accelerator Technical Advisory Committee

(*) Chair

Name	Affiliation
Wolfram Fischer	Brookhaven National Laboratory (BNL), U.S.A.
John Thomason	Science and Technology Facilities Council (STFC), UK
Sheng Wang	Institute of High Energy Physics, CAS, China
Toshiyuki Shirai	National Institutes for Quantum Science and Technology (QST), Japan
Alexander Aleksandrov	Oak Ridge National Laboratory (ORNL), U.S.A.
Jie Wei (*)	Michigan State University, U.S.A.
Alexander Valishev	Fermi National Accelerator Laboratory (FNAL), U.S.A.
Simone Gilardoni	European Organization for Nuclear Research (CERN), Switzerland
Håkan Danared	European Spallation Source, ERIC, Sweden

5) Neutron Advisory Committee

(*) Chair

Name	Affiliation
Phillip King (*)	Rutherford Appleton Laboratory, UK
Bertrand Blau	Paul Scherrer Institute (PSI), Switzerland
Michael Dayton	Oak Ridge National Laboratory (ORNL), U.S.A.
Guenter Muhrer	European Spallation Source (ESS), Sweden
Jon Taylor	Spallation Neutron Source (SNS), U.S.A.
Sungil Park	Korea Atomic Energy Research Institute (KAERI), Korea
Yoshie Otake	RIKEN, Japan
Taka-Hisa Arima	RIKEN, Japan / The University of Tokyo, Japan
Toyohiko Kinoshita	Japan Synchrotron Radiation Research Institute (JASRI), Japan
Judith Peters	University Grenoble Alpes, France / Institut Laue-Langevin (ILL), France
Kirrily Rule	Australian Nuclear Science and Technology Organization (ANSTO), Australia

6) Muon Advisory Committee

(*) Chair

Name	Affiliation
Martin Månsson	KTH Royal Institute of Technology, Sweden
Klaus Kirch (*)	ETH Zurich, Switzerland / Paul Scherrer Institute (PSI), Switzerland
Kenya Kubo	International Christian University, Japan
Nori Aoi	Osaka University, Japan
Koji Yoshimura	Okayama University, Japan
Kenji Kojima	TRIUMF, Canada
Adrian Hillier	Science and Technology Facilities Council (STFC), UK
Yoko Sugawara	Kitasato University, Japan
Makoto Fujiwara	TRIUMF, Canada

7) Radiation Safety Committee

(*) Chair

Name	Affiliation
Hiroshi Watabe (*)	Tohoku University, Japan
Kanenobu Tanaka	Institute of Physical and Chemical Research (RIKEN), Japan
Takeshi Iimoto	The University of Tokyo, Japan
Michihiro Shibata	Nagoya University, Japan
Sumi Yokoyama	Nagasaki University, Japan
Toshiya Sanami	High Energy Accelerator Research Organization (KEK), Japan
Yoshihito Namito	High Energy Accelerator Research Organization (KEK), Japan
Makoto Tobiyama	High Energy Accelerator Research Organization (KEK), Japan
Toshikatsu Maeda	Japan Atomic Energy Agency (JAEA), Japan
Tomonori Satoyama	Japan Atomic Energy Agency (JAEA), Japan
Hideki Hangai	Japan Atomic Energy Agency (JAEA), Japan

8) Radiation Safety Review Committee

(*) Chair

Name	Affiliation
Yukihiro Miyamoto (*)	Japan Atomic Energy Agency (JAEA), Japan
Yoshihiro Nakane	Japan Atomic Energy Agency (JAEA), Japan
Hirohito Yamazaki	High Energy Accelerator Research Organization (KEK), Japan
Hidetoshi Kikunaga	Tohoku University, Japan
Hiroshi Yashima	Kyoto Univaersity, Japan
Nobuyuki Chiga	National Institutes for Quantum Science and Technology (QST), Japan
Toshiro Itoga	Japan Synchrotron Radiation Research Institute (JASRI), Japan
Koji Kiriyama	Comprehensive Research Organization for Science and Society (CROSS), Japan
Masayuki Hagiwara	National Institutes for Quantum Science and Technology (QST), Japan
Makoto Kobayashi	Japan Atomic Energy Agency (JAEA), Japan
Hiroyuki Takahashi	Japan Atomic Energy Agency (JAEA), Japan
Hiroshi Miyauchi	High Energy Accelerator Research Organization (KEK), Japan
Hiroshi Iwase	High Energy Accelerator Research Organization (KEK), Japan
Hidetomo Oguri	Japan Atomic Energy Agency (JAEA), Japan
Takeshi Nakadaira	High Energy Accelerator Research Organization (KEK), Japan
Shinya Sawada	High Energy Accelerator Research Organization (KEK), Japan
Hiroshi Takada	Japan Atomic Energy Agency (JAEA), Japan

9) MLF Advisory Board

(*) Chair

Name	Affiliation
Taka-hisa Arima (*)	The University of Tokyo, Japan / RIKEN, Japan
Osamu Yamamuro	The University of Tokyo, Japan
Hiroyuki Kagi	The University of Tokyo, Japan
Takashi Kamiyama	Hokkaido University, Japan
Shigeru Kimura	Japan Synchrotron Radiation Research Institute (JASRI), Japan
Isao Watanabe	RIKEN, Japan
Yoko Sugawara	Kitasato University, Japan
Tadashi Adachi	Sophia University, Japan
Hiroyuki Kishimoto	Sumitomo Rubber Industries, Ltd., Japan
Yoshie Otake	RIKEN, Japan
Mikihito Takenaka	Kyoto University, Japan
Kenji Ohoyama	Ibaraki University, Japan
Masahiro Hino	Kyoto University, Japan
Kohzo Ito	The University of Tokyo, Japan / National Institute for Materials Science, Japan
Toshiya Otomo	High Energy Accelerator Research Organization (KEK), Japan
Yukinobu Kawakita	Japan Atomic Energy Agency (JAEA), Japan
Katsuhiro Haga	Japan Atomic Energy Agency (JAEA), Japan
Koichiro Shimomura	High Energy Accelerator Research Organization (KEK), Japan
Mitsutaka Nakamura	Japan Atomic Energy Agency (JAEA), Japan
Naritoshi Kawamura	High Energy Accelerator Research Organization (KEK), Japan
Shinichi Itoh	High Energy Accelerator Research Organization (KEK), Japan
Kenji Nakajima	Japan Atomic Energy Agency (JAEA), Japan
Masato Matsuura	Comprehensive Research Organization for Science and Society (CROSS), Japan

10) Program Advisory Committee (PAC) for Nuclear and Particle Physics Experiments at the J-PARC 50Gev Proton Synchrotron

(*) Chair

Name	Affiliation
Kenkichi Miyabayashi	Professor, Graduate School of Science, Nara Womens' University
Mayumi Aoki	Professor, College of Science and Engineering, Kanazawa University
Hirokazu Ishino	Professor, Graduate School of Natural Science and Technology, Okayama University
Kimiko Sekiguchi	Professor, School of Science, Institute of Science Tokyo
Makoto Oka	Guest Researcher, Advanced Science Research Center, Sector of Nuclear Science Research, Japan Atomic Energy Agency/ Professor Emeritus, Tokyo Institute of Technology
Yuji Yamazaki	Professor, Graduate School of Science, Kobe University
Taku Yamanaka (*)	Professor Emeritus, Osaka University
Joachim Stroth	Professor, Institute of Nuclear Physics, Goethe University
Laura Fabbietti	Professor, School of Natural Sciences, Technical University of Munich
Vincenzo Cirigliano	Professor, University of Washington/ Senior Fellow, Institute for Nuclear Theory, University of Washington
Georgia Karagiori	Associate Professor, Department of Physics, Columbia University
Xin Qian	Physicist, Physics Department, Brookhaven National Laboratory
Cristina Lazzeroni	Professor, School of Physics and Astronomy, University of Birmingham
Gabriel Orebi Gann	Associate Professor, Department of Physics,University of California, Berkeley
Horst Lenske	Professor, University of Giessen
Kyungseon Joo	Professor, Department of Physics, University of Connecticut

11) TEF Technical Advisory Committee

Name	Affiliation
Thierry Stora	European Organization for Nuclear Research (CERN), Switzerland
Kazuo Hasegawa	National Institutes for Quantum Science and Technology (QST), Japan
Mariano Tarantino	Italian National Agency for New Technologies, Energy and Sustainable Economic Development (ENEA), Italy
Michael Wohlmuther	European Spallation Source (ESS), Sweden
Tatsuya Katabuchi	Institute of Science Tokyo, Japan
Salvatore Danzeca	European Organization for Nuclear Research (CERN), Switzerland
Hiromitsu Haba	RIKEN, Japan

Main Parameters

Present main parameters of Accelerator

Linac	
Accelerated Particles	Negative hydrogen
Energy	400 MeV
Peak Current	50 mA
Pulse Width	0.50 ms for MLF 0.40 ms for MR-FX 0.20 ms for MR-SX
Repetition Rate	25 Hz
Freq. of RFQ, DTL, and SDTL	324 MHz
Freq. of ACS	972 MHz
RCS	
Circumference	348.333 m
Injection Energy	400 MeV
Extraction Energy	3 GeV
Repetition Rate	25 Hz
RF Frequency	1.23 MHz → 1.67 MHz
Harmonic Number	2
Number of RF cavities	12
Number of Bending Magnet	24
Main Ring	
Circumference	1567.5 m
Injection Energy	3 GeV
Extraction Energy	30 GeV
Repetition Rate	~0.4 Hz
RF Frequency	1.67 MHz → 1.72 MHz
Harmonic Number	9
Number of RF cavities	11
Number of Bending Magnet	96

Key parameters of Materials and Life Science Experimental Facility

Injection energy	3 GeV
Repetition rate	25 Hz
Neutron Source	
Target material	Mercury
Reflector material	Beryllium and Iron
Number of moderators	3
Moderator material	Liquid hydrogen
Moderator temperature/pressure	20 K/1.5 MPa
Number of neutron beam extraction ports	23
Muon Source	
Target material	Graphite
Number of muon beam extraction ports	4
Neutron Instruments	
Open for user program (general use)	21
Under commissioning/construction	0
Muon Instruments	
Open for user program (general use)	3
Under commissioning/construction	1/0

Events

Events

J-PARC Safety Day (May 30th)

J-PARC center has held "J-PARC Safety Day" every year around May 23rd, the day on which there was a radioactive material leakage incident at the Hadron Experimental Facility in 2013. This year, 352 people participated in the event at the physical venue and online.

In the morning session, there were reports from representatives of each division and section regarding case studies on fire prevention as part of the safety information exchange meeting. In the afternoon session, under the title of "the Workshop for Fostering a Safety Culture," we first of all presented the Safety Contribution Award and the Best Practices Award. Next, there was a lecture by Dr. FUKUWA Nobuo, Honorary Professor of Nagoya University and Director of the Aichi-Nagoya Resilience Co-creation Center, titled "Preparing for Large-Scale Earthquakes with Wisdom from the Past."

Following that, a documentary video titled "The Radioactive Material Leak Incident at J-PARC: How Society Viewed the Incident" was screened at the end of the event.

J-PARC Lecture "Accelerators - Their Principles and Application to Cancer Therapy" (July 6th).

The J-PARC Lecture 2024 was held at the Tokai Village Industrial Information Plaza (iVil) and 146 people attended.

Dr. KONDO Yasuhiro of the Accelerator Division first explained the configuration, principles, and features of the three accelerators at J-PARC. Next, Dr. SAKAE Takeji, Professor of the Institute of Medicine at the University of Tsukuba/Proton Medical Research Center, presented the current state of the art in particle therapy, comparing

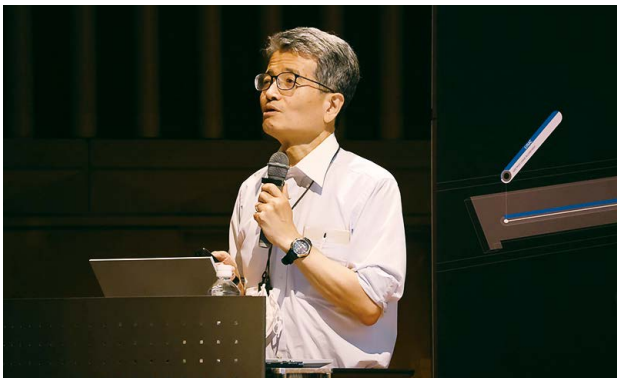

Dr. SAKAE Takeji

Dr. KUMADA Hiroaki

X-ray, proton, and heavy particle beams. Finally, Dr. KUMADA Hiroaki, Professor of the Institute of Medicine at the University of Tsukuba, and Director of the Proton Medical Research Center, explained the latest status of Boron Neutron Capture Therapy (BNCT), which can selectively destroy cancer cells, and how the source of neutrons is shifting from nuclear reactors to accelerators.

Before and after the lectures and during breaks, staff members explained the accelerators using posters in the lobby and answered questions from those interested in the accelerators at J-PARC.

Neutron Industrial Application Report Meeting for FY2024 at Akihabara Conventional Hall and partly online (July 11th- 12th)

This meeting focuses on matching industry needs to industrial applications for neutrons and muons provided by MLF and JRR-3.

A total of 247 people attended the two-day event. Special presentations were given by Dr. SHOJI Tetsuya of Toyota Motor Corporation on "Measurement Data Analysis of Materials via MI and DX Analysis Platform WAVEBASE" and Dr. HIRAYAMA Tomoko of Kyoto University on "Application of Neutron Beam Analysis for Clarification of Tribological Phenomena."

Eco-Fest Hitachi 2024 (July 20th)

This environmental event, where children learned through experiments and hands-on activities, was held at Hitachi Civic Center and other venues.

At the J-PARC Center booth, we demonstrated a superconducting coaster and introduced the facility's research. The coaster, featuring a superconductor cooled to nearly -200°C that levitates and glides along rails like a roller coaster, attracted great interest from both children and adults.

A scale model and posters were also on display, showcasing contributions to fuel cell performance and other cutting-edge technologies.

At the J-PARC booth

Summer Special Exhibition: "Science x Tokai-Village x J-PARC" (July 20th to September 29th)

The Science x Tokai-village x J-PARC Exhibition -The World is Made Up of "Particles"- was held at the Tokai Village Museum. Tokai Village and the J-PARC Center sponsored this project in which children answer riddles

At the entrance to the Particle World

and complete missions to solve the mystery of the beginning of the universe. Children can also take part in workshops with scientists and see an exhibition about the scientists who work in Tokai Village.

Children's Kasumigaseki Open Day "Let's Make a Kaleidoscope of Light" (August 7th and 8th)

The Children's Kasumigaseki Open Day offers children a chance to learn about society and strengthen parent-child bonds through tours and explanations by government ministries and agencies.

This year, 28 organizations participated. At the Japan Atomic Energy Agency (JAEA) booth in the Ministry of Education, Culture, Sports, Science and Technology (MEXT) section, children explored the nature of light—its wave properties and three primary colors —by making kaleidoscopes using spectroscope sheets.

They observed rainbow-colored light from various sources with excitement, and the J-PARC Center was also introduced.

Hello Science "Have you heard of Hadrons?"(August 30th)

Dr. UKAI Mifuyu of the Particle and Nuclear Physics Division gave a talk on the relationship between hadrons and strong force, and the prospects for research at J-PARC.

Hadrons are kept at an exquisite distance from each other by the forces of attraction and repulsion, so that they are neither too attracted to each other to be crushed, nor too far to be torn apart, thus making up this universe.

At J-PARC, researchers use high-intensity and high-purity beams of negatively charged K mesons (K^-) to create nuclei called hypernuclei, which contain strange quarks unobserved in ordinary conditions, to investigate the "strong force" acting between hadrons in nuclei. By studying this strong force, we would like to address the mysteries of the existence of nuclei, the formation of matter, and the existence of the universe.

Dr. UKAI Mifuyu

J-PARC Open House (September 28th)

The J-PARC Open House 2024 was held on a cloudy, pleasant day after the long, sizzling summer had finally come to an end.

Visitors toured the extensive site, looking closely at the experimental facilities and exhibits and asking lots of questions. There were about 1,000 visitors, 40% of whom came from outside Ibaraki Prefecture, and many of whom looked around with great interest until the very end of the tour. There was also a ceremony to mark the signing of a cooperative agreement with Tokai Village, and five presentations were given as part of the Hello Science program during the Open House.

Cooperative agreement with Tokai Village

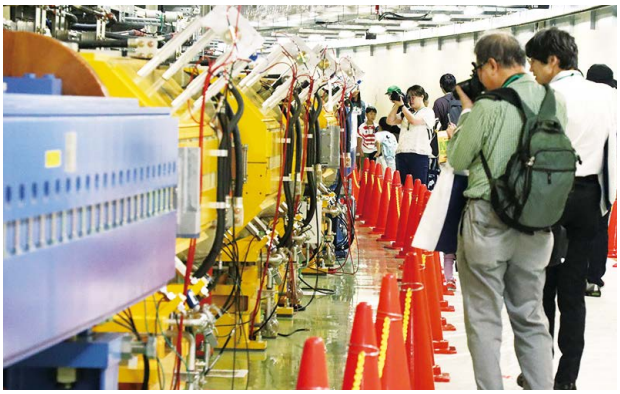

MR accelerator

Ozora Marche (October 5th)

Participation in this year's "Ozora Marche," one of the four major festivals in Tokai Village, continued from previous years.

There were various workshops, food courts, and live

stages set up in the precincts and along the approaches to the Grand Shrine and Muramatsu Kokuzoudo.

At the very back of the precincts, J-PARC gave demonstrations of a superconductive coaster and held a craft workshop to make kaleidoscopes.

Looking into the kaleidoscopes they made

Muon detector started muon measurement at Funatsuka No.2 Burial Mound (October 13th)

The muon detector "Detector for History and the Future" built with children last year, was installed at the Arayadai residential water distribution station near Funatsuka No. 2 Burial Mound.

Seventeen children watched the delicate installation process, guided by Dr. FUJII from the J-PARC Center. After helping to cover the device with a waterproof sheet, the children celebrated as muon signals appeared on the computer screen when the detector was activated.

Installed "Detector for History and the Future"

J-PARC Symposium (October 14th-18th)

The 4th J-PARC Symposium was held at the Mito Civic Center under the theme "Futures of J-PARC, Futures by J-PARC," marking 15 years since all J-PARC facilities became fully operational.

- October 14th: A public lecture titled "The future created by J-PARC, the mysteries explored by J-PARC - from Next-Generation Energy to Space" featured five researchers presenting cutting-edge work in particle and nuclear physics, neutron science, and industrial applications.
- October 15th-17th: Plenary, parallel, and poster sessions highlighted achievements over the past 15 years, future prospects, and the global impact of J-PARC technologies. The symposium included 93 oral presentations and 290 poster presentations, with over 400 participants from Japan and abroad.
- October 18th: Facility tours were held, including visits to the Linac, MLF, Hadron Experimental Facility, and Neutrino Monitoring Building.

Group photo

The Youngsters' Science Festival (October 20th)

The Youngster's Science Festival was held at the Hitachi Civic Center with the aim of enabling many children to experience the fun of science. The J-PARC Center hosted a workshop to build a unipolar motor using copper wire, dry batteries and neodymium magnets. The children's eyes lit up with excitement when their hand-made heart- and spiral-shaped copper wires started spinning. Many children also tried their hand at the Irritating Maze, a maze of the three accelerators at J-PARC, created by Dr. TAKAYANAGI Tomohiro of the Accelerator Division, in which a buzzer sounds when a stick hits the maze frame.

J-PARC Photo Contest 2024

Dr. Wu GONG from the Neutron Science Section won the Grand Prize in the 11th J-PARC Photo Contest for his photo of a magnesium alloy undergoing high tem-

perature tensile deformation during in situ neutron diffraction measurement at the engineering materials diffractometer "TAKUMI" in MLF. The jury praised the image for its beautiful red gradation, dynamic feel, and stable composition.

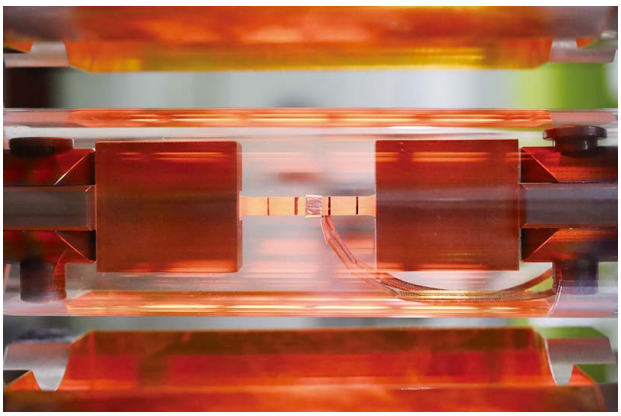

Grand Prize

J-PARC Workshop (October 28th-30th)

The J-PARC Workshop titled "Explore Small Wonders in Non-crystalline Materials with 1 MW J-PARC Beam: A Concerto of Freedom and Constraint," was held jointly by the J-PARC Center, Metallic Glass Research Group of the Society of Materials Science, Japan, and CROSS.

The event focused on structural fluctuations in non-crystalline materials like liquids and glasses, driven by the interplay of atomic freedom and constraint. It attracted 58 participants, including one online speaker, and featured 27 oral and 10 poster presentations. A tour of the MLF was also conducted for 22 attendees, fostering active discussions and collaboration.

FC-Cubic Open Symposium (November 1st)

The 15th FC-Cubic Open Symposium was held at the Tokai Village Industry and Information Plaza, aiming to address technical challenges in the fuel cell industry through shared knowledge. A J-PARC tour was conducted for 40 participants, showcasing neutron beamline experiments. The symposium attracted about 120 attendees, including remote participants. Highlights included a presentation by Dr. KISHIMOTO Hiromichi (Sumitomo Rubber Industries) on neutron-based tire rubber research, and lectures on neutron applications, global trends in analytical facilities, and fuel cell technologies by experts from Mizuho Research & Technologies and Toyota Central R&D Labs.

Symposium on the Fusion of the Humanities and Sciences (November 1st and 2nd)

The Institute for Materials Structure Research (IMS) at KEK held its 9th annual interdisciplinary symposium at Akihabara Convention Hall, focusing on non-destructive research methods for cultural heritage using negative muon beams from J-PARC. The event featured 12 oral presentations on topics such as underwater archaeology, archaeological astronomy, and artifacts. It concluded with three public lectures attended by approximately 220 participants both in person and online, highlighting the growing interest in quantum beam-based cultural heritage research.

Hello Science "The world is made up of particles ~ an introduction to J-PARC~" (December 20th)

Dr. KOMATSUBARA Takeshi, Deputy Director of J-PARC, introduced the mechanisms and principles of J-PARC incorporating the contents of the special exhibition held this summer at the Tokai Village Museum.

He explained the physical laws on which the J-PARC apparatuses are based on, how the accelerators can bend the direction of the moving protons, and the units and numerical values often heard at J-PARC, such as megawatts for beam power and their order of magnitude.

Takamatsu Campus of the National Institute of Technology, Kagawa College (January 6th)

Dr. OTANI Masashi from J-PARC's Accelerator Division gave a lecture to about 100 fourth-year students titled "The Mechanism of Accelerators that Reveal the Microscopic World." Dr. OTANI explained the principles and applications of accelerators, including medical uses, and introduced muons—elementary particles used in exploring pyramids and volcanoes. He also discussed the latest research at J-PARC using artificially produced muons. The lecture began with songs from the creative label *Academimic*, which blends science and pop culture, and concluded with insights into how the College's education contributes to real-world technologies like accelerators. Students expressed strong interest, and indicated that they want to learn more about the connection between space and accelerators.

Katsuta Third Junior High School, Hitachinaka City (February 4th)

A lecture and workshop to build a "cloud chamber" was held for about 120 students in four ninth grade

classes to deepen their understanding of basic knowledge related to space, energy and radiation.

First, Director KOBAYASHI gave a lecture on the theme 'Secrets of the Big Universe, Microscopic World and Accelerators,' in which he talked about the size of the universe and the smallness of the microscopic world, and also about the research being conducted at J-PARC on space.

Next, in the theme "How to 'see' small things" by Mr. TAKAHASHI Kazutoshi, Radiation Control Section, gave a presentation. The students tried to make a "cloud chamber" through group work, which allowed alpha radiation to be visualized in supersaturated ethanol.

Shirakata Elementary School in Tokai Village (February 7th)

The MLF Outreach Circle "Protons" conducted a hands-on science class for about 80 fourth-grade students across three classes, themed "You are a researcher, too! Let's observe creatures of various sizes." Students explored three topics: dissecting dried sardines, observing water fleas, and investigating the secrets of fermented soy beans. Using magnifying glasses and microscopes, they made new discoveries through close observation. Dr. SHIBAZAKI, the class leader, encouraged students to enjoy science and consider careers as "researchers" in the future.

Hyper-Kamiokande Collaboration Meeting (February 17th-22nd)

Around 120 researchers from Japan and abroad gathered at the AYA'S LABORATORY Quantum Beam Research Center (AQBRC) for the Hyper-Kamiokande Collaboration Meeting. This international project, involving approximately 600 researchers from 22 countries, is preparing for the launch of experiments in 2027. Active discussions were held both in person and online to address key issues in detector development. Participants also toured the J-PARC beamlines and visited the planned site for the Intermediate Water Cherenkov Detector (IWCD) in Tokai Village.

Tokai Forum (February 19th)

The 19th Tokai Forum was held at the Tokai Cultural Center, co-hosted by the Nuclear Fuel Cycle Engineering Laboratories, the Nuclear Science Research Institute, and J-PARC to promote public understanding of JAEA's activities.

The event drew 125 in-person visitors and a record 198 online registrants. Director Dr. KOBAYASHI Takashi presented an overview of J-PARC, and Dr. KAWASAKI Takuro of the Neutron Science Section discussed neutron-based research on structural materials. A panel session featuring university students from Ibaraki Prefecture, moderated by Ms. SUGITA Moe of the Accelerator Division, added a fresh perspective. Feedback highlighted an increased awareness of nuclear energy's role in daily life and appreciation for the student-led discussion.

The International Advisory Committee (IAC2025) (February 24th and 25th)

The International Advisory Committee (IAC2025) met to review J-PARC's research and development activities for fiscal year 2024. Based on the Fundamental Collaboration Agreement, all 16 members — including 12 from overseas and 4 from Japan — participated. The committee, chaired by Dr. Robert McGreevy from the U.K., provided recommendations for future operations. Young researchers also presented their recent work in parallel sessions. A reception featured open dialogue with Tokai Village Mayor Mr. YAMADA Osamu and executive directors from KEK and JAEA. The final day included a facility tour of MLF, the Hadron Experimental Facility, and the Neutrino Monitoring Building.

Group photo

2024 Quantum Beam Science Festa (March 12-14)

The 2024 Quantum Beam Science Festa was held at the Tsukuba International Congress Center, bringing together 565 participants, including 142 students. This annual event fosters collaboration between the Photon Factory (PF) and the Materials and Life Science Experimental Facility (MLF) at J-PARC.

Day 1: The MLF Symposium featured facility updates, user discussions, and improvement requests.

Day 2: The main Festa included 276 poster presentations, with 75 student entries for the Student

Encouragement Award, which was awarded to MLF participants.

Day 3: The PF Symposium saw strong participation from MLF members, reflecting the deepening ties between the two facilities.

Sakurie Science Festival (March 15th)

The J-PARC Center participated in the Sakurie Science Festival at the Hitachi Civic Center Science Museum, themed *"Let's have lots of fun with science and learn to love it even more!"* The center hosted a hadron accessory class, a cloud chamber class, and a superconducting coaster demonstration. The hadron class was highly popular, with tickets selling out quickly. In the cloud chamber class, participants successfully observed radiation trails. The superconducting coaster booth attracted a wide range of visitors, from preschoolers to adults, who enjoyed hands-on experiments with magnetic levitation.

Making accessories using hadron-themed materials

Koshien of Science National Competition (March 21st-24th)

The 14th Koshien of Science National Competition was held in Tsukuba, bringing together high school students from across Japan to compete in science proficiency. On March 23, J-PARC joined 16 other organizations in an exhibition organized by the Ibaraki Prefectural Office to showcase local science and technology. J-PARC presented a 3D mockup of ion sources, RFQ vanes, a tabletop high-pressure device, and a site model, attracting interest from about half of the 400 participating students.

New "Research Developing Building" Completed (March 31th)

A large hall in the J-PARC site that is available to develop and assemble equipment for accelerators, beamlines and experiments had been a long-standing issue. There had also been a lack of dedicated space for graduate students of KEK doing their research at the Tokai campus. To solve these issues, the Graduate University for Advanced Studies, with the abbreviated Japanese name of SOKENDAI, submitted a proposal in cooperation with KEK to MEXT's Program for Facility Enhancement for Industry-Academia-Government Collaboration and Joint Research by Regional Core and Specialized Research Universities. SOKENDAI, found in 1988, operates in close partnership with MEXT-based Inter-University Research Institutes, and KEK provides three programs in Accelerator Science, Materials Structure Science, and Particle and Nuclear Physics. The proposal was approved in April 2023; construction of the new building started on a site across the road from MLF and was completed in March 2025. The building was officially named the SOKENDAI Joint Research Center/ J-PARC Experimental Equipment Development, abbreviated to the "Research Development Building."

Research Development Building in March 2025

It is a two-story building with an area of 2,853 square meters and a height of 15.4 meters. The first-floor area is 2,353 square meters including the entrance, a large "open space" for the development and assembly of equipment by research teams, and a "closed space" for specific uses. The second-floor area is 500 square meters including a common space, two rooms for graduate students, and three rooms for laboratories. The operation of the building is currently managed by a volunteer-based committee whose members are from J-PARC facilities, and its usage will be annually reviewed. Thirty applications were received, and their preparations for use are underway.

More information will be provided in the 2025 Annual Report.

Visitors

KONOMOTO Shingo, Chairman, Member of the Board, Nomura Research Institute, Ltd. (May 8th)

NAKAJIMA Hiroki, Executive Vice President, Member of the Board of Directors (Representative Director), Toyota Motor Corporation (June 6th)

YAMADA Osamu, Mayor, Tokai Village (August 26th)

KIUCHI Minoru, Minister of State for Special Missions (November 1st)

MASUDA Naohiro, Executive President and CEO, Representative Member of the Board (December 5th)

ABE Toshiko
Minister of Education, Culture, Sports and Technology (January 16th)

KOYASU Shigeo, President, National Institute for Quantum Science and Technology (January 29th)

IWASHITA Yasuyoshi, Deputy Governor, Ibaraki Prefecture (February 17th)

There were 3,095 visitors to J-PARC for the period from April 2024 to the end of March 2025.

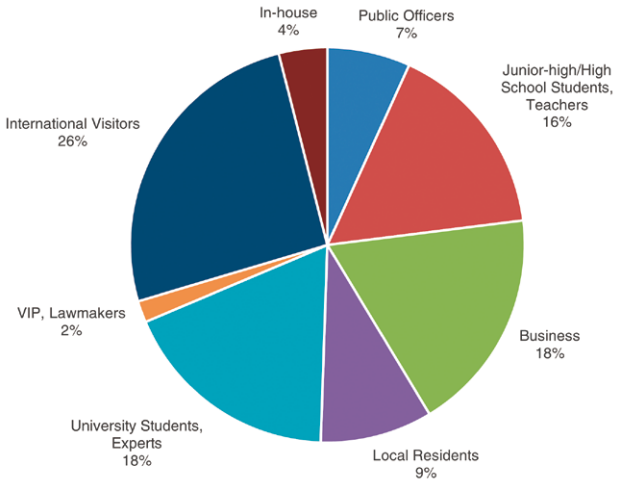

Publications

Publications in Periodical Journals

A-001
T. Katase, et al.
Simultaneous Realization of Single-Crystal-Like Electron Transport and Strong Phonon Scattering in Polycrystalline SrTiO3–xHx,
ACS Appl. Electron. Mater., 6 7424–7429 (2024).

A-002
K. Uchida, et al.
Stability Enhancement by Hydrophobic Anchoring and a Cross-Linked Structure of a Phospholipid Copolymer Film for Medical Devices
ACS Appl. Mater. Interfaces, 16 39104–39116 (2024).

A-003
K. Yamamoto, et al.
Surface Depth Analysis of Chemical Changes in Random Copolymer Thin Films Composed of Hydrophilic and Hydrophobic Silicon-
Based Monomers Induced by Plasma Treatment as Studied by Hard X-Ray Photoelectron Spectroscopy and Neutron Reflectivity Measurements
ACS Appl. Mater. Interfaces, 16 66782–66791 (2024).

A-004
S. Asano, et al.
Formation Processes of a Solid Electrolyte Interphase at a Silicon/Sulfide Electrolyte Interface in a Model All-Solid-State Li-Ion Battery
ACS Appl. Mater. Interfaces, 16 7189–7199 (2024).

A-005
T. Ikami, et al.
Lamellar Microphase Separation and Phase Transition of Hydrogen-Bonding/Crystalline Statistical Copolymers: Amide Functionalization at the Interface
ACS Macro Lett., 13 446–452 (2024).

A-006
J. Kim, et al.
Suppression of Segmental Chain Dynamics on a Particle's Surface in Well-Dispersed Polymer Nanocomposites
ACS Macro Lett., 13 720–725 (2024).

A-007
R. Sujita, et al.
Universal Access to Water-Compatible and Nanostructured Materials via the Self-Assembly of Cationic Alternating Copolymers
ACS Macro Lett., 13 747–753 (2024).

A-008
K. Yamashita, et al.
Crystal Structure and Compressibility of Magnesium Chloride Heptahydrate Found under High Pressure
Acta Crystallogr. Sect. B Struct. Sci. Cryst. Eng. Mater., 80 695–705 (2024).

A-009
W. Guo, et al.
Significantly Enhanced Reversibility and Mechanical Stability in Grain-Oriented MnNiGe-Based Smart Materials
Acta Mater., 263 119530 (2024).

A-010
B. Guo, et al.
Direct Observations of Dynamic and Reverse Transformation of Ti-6Al-4V Alloy and Pure Titanium
Acta Mater., 268 119780 (2024).

A-011
Y. Ma, et al.
Microscopic Insights of the Extraordinary Work-Hardening Due to Phase Transformation
Acta Mater., 270 119822 (2024).

A-012
W. Mao, et al.
Martensitic Transformation-Governed Lüders Deformation Enables Large Ductility and Late-Stage Strain Hardening
in Ultrafine-Grained Austenitic Stainless Steel at Low Temperatures
Acta Mater., 278 120233 (2024).

A-013
K. V. Werner, et al.
Experimental and Computational Assessment of the Temperature Dependency of the Stacking Fault Energy in Face-Centered Cubic High-Entropy Alloys
Acta Mater., 278 120271 (2024).

A-014
H. Zhong, et al.
Design of Excellent Mechanical Performances and Magnetic Refrigeration via in situ Forming Dual-Phase Alloys
Adv. Mater., 36 2402046 (2024).

A-015
A. Åhl, et al.
Moisture-Dependent Vibrational Dynamics and Phonon Transport in Nanocellulose Materials
Adv. Mater., 37 2415725 (2024).

A-016
R. Kadono, et al.
Ambipolarity of Hydrogen in Matter Revealed by Muons
Adv. Phys., 72 409–476 (2023).

A-017
M. Ai, et al.
Significantly Promoting the Thermal Conductivity and Machinability of Negative Thermal Expansion Alloy via in situ Precipitation of Copper Networks
Adv. Sci., 11 2404838 (2024).

A-018
K. Koruza, et al.
Botryococcus Braunii Autolysate for the Production of Deuterium-Labeled Recombinant Protein
Algal Res., 79 103459 (2024).

A-019
T. Ji, et al.
Development of an FeII Complex Exhibiting Intermolecular Proton Shifting Coupled Spin Transition
Angew. Chem. Int. Ed., 63 e202404843 (2024).

A-020
T. Hanashima, et al.
Temperature- and Magnetic Field-Induced Magnetic Structural Changes
in the Fe3 Si/FeSi2 Superlattice
Appl. Phys. Express, 17 035002 (2024).

A-021
S. Shamoto, et al.
Inelastic Neutron Scattering Study of Magnon Excitation by Ultrasound Injection in Yttrium Iron Garnet
Appl. Phys. Lett., 124 112402 (2024).

A-022
Y. Kawamoto, et al.
Understanding Spin Currents from Magnon Dispersion and Polarization: Spin-Seebeck Effect and Neutron Scattering Study on Tb3Fe5O12
Appl. Phys. Lett., 124 132406 (2024).

A-023
J. Li, et al.
Crystal-Liquid Duality Driven Ultralow Two-Channel Thermal Conductivity in α-MgAgSb
Appl. Phys. Rev., 11 011406 (2024).

A-024
M. Yoshida, et al.
Evidence of a Rod-like Structure for Hydroxypropyl Cellulose Samples in Aqueous Solution
Biomacromolecules, 25 4255–4266 (2024).

A-025
Y. Kameda, et al.
Experimental Determination of Relationship between Intramolecular Bond Lengths and Their Stretching Vibrational Frequencies of N,N -Dimethylformamide and Acetonitrile Molecules in the Liquid State
Bull. Chem. Soc. Jpn., 97 uoad006 (2024).

A-026
Y. Kameda, et al.
Experimental Determination of the Relationship between S=O Bond Length and Its Stretching Frequency of the DMSO Molecule
Bull. Chem. Soc. Jpn., 97 uoae120 (2024).

A-027
C. Wang, et al.
Enhanced Storage Performance of a Low-Cost Hard Carbon Derived from Biomass
Carbon Trends, 17 100415 (2024).

A-028
T. Katsumata, et al.
Existence of Local Polar Domains in Perovskite Oxyfluoride, BaFeO2F
Chem. Mater., 36 3697–3704 (2024).

A-029
A. E. Baumann, et al.
Measuring the Influence of CO2 and Water Vapor on the Dynamics in Polyethylenimine To Understand the Direct Air Capture of CO2 from the Environment
Chem. Mater., 36 6130–6143 (2024).

A-030
Y. Kajita, et al.
Ferroaxial Transitions in Glaserite-Type Na2BaM(PO4)2 (M = Mg, Mn, Co, and Ni)
Chem. Mater., 36 7451–7458 (2024).

A-031
Y. Masubuchi, et al.
Average Cubic BaTaO2N Crystal Structure Formed by 50 Nm Size Domains with Polar Nanoregions Consisting of Cis-TaO4 N2 Octahedral Chains
Chem. Mater., 36 7504–7513 (2024).

A-032
T. Ichikawa, et al.
Surface Proton Hopping Conduction Mechanism Dominant Polymer Electrolytes Created by Self-Assembly of Bicontinuous Cubic Liquid Crystals
Chem. Sci., 15 7034–7040 (2024).

A-033
R. Liu, et al.
Low-Energy Spin Excitations in Detwinned FeSe
Chin. Phys. Lett., 41 067401 (2024).

A-034
A. Yamaguchi, et al.
Quasielastic Neutron Scattering Study on Low-Hydrated Myoglobin inside Silica Nanopores
Colloids Surf. Physicochem. Eng. Asp., 698 134559 (2024).

A-035
T. Miyazaki, et al.
Adsorption Isotherm and Kinetics of Diffusion of Water Accumulated between Polypropylene Thin Film and Si Substrate: Neutron Reflectivity Investigation
Colloids Surf. Physicochem. Eng. Asp., 701 134928 (2024).

A-036
T. Ishii, et al.
Synthesis, Crystal Structure and Investigation of Ion-Exchange Possibility for Sodium Tellurate NaTeO3(OH)
Dalton Trans., 53 5373–5381 (2024).

A-037
Y. Mori, et al.
Hydrogenation of Silicon-Bearing Hexagonal Close-Packed Iron and Its Implications for Density Deficits in the Inner Core
Earth Planet. Sci. Lett., 634 118673 (2024).

A-038
J. Kamiya, et al.
SRPES and XPS analysis of activation and deterioration processes for Ti-Zr-V NEG coating
e-Journal of Surface Science and Nanotechnology (Internet), 22(4), p.316 - 326, 2024/08

A-039
N. Kitamura, et al.
Effect of Intermediate-Range Structure on Negative Electrode Properties of Wadsley–Roth Phase Ti2Nb10O29
Electrochemistry, 92 087002–087002 (2024).

A-040
Y. Idemoto, et al.
Operating-Temperature Dependence of the Average and Electronic Structures of 0.4Li2MnO3–0.6Li(Mn1/3Ni1/3Co1/3)O2
Electrochemistry, 92 107003–107003 (2024).

A-041
L. Zheng, et al.
Decoupling of the Onset of Anharmonicity between a Protein and Its Surface Water around 200 K
eLife, 13 RP95665 (2024).

A-042
F. Hu, et al.
Gradient Residual Strain Determination of Surface Impacted Railway S38C Axles by Neutron Bragg-Edge Transmission Imaging
Eng. Fract. Mech., 306 110267 (2024).

A-043
S. Kumano
Parton distribution functions and fragmentation functions of spin-1 hadrons
Eur. Phys. J. A 60, 205 (2024)

A-044
X. Chen, et al.
Pion-production cross section in neutrino reactions for studying generalized parton distributions of the nucleon
Eur. Phys. J. A 60, 208 (2024)

A-045
G. Rovira, et al.
Neutron Capture Cross Section Measurement of 129I and 127I Using the NaI(Tl) Spectrometer of the ANNRI Beamline at J-PARC
Eur. Phys. J. A, 60 120 (2024).

A-046
D. Lee, et al.
Study on the accidental background of the JSNS^2 experiment
Eur. Phys. J. C 84, 409 (2024)

A-047
H. Iwase, et al.
Structural Analysis of Polyglycerol Fatty Acid Ester-Coenzyme Q10 Aggregates in Solution
Food Res. Int., 175 113741 (2024).

A-048
N. Yamashita, et al.
A Method for Simultaneously Measuring Friction and Gap at Metal–Lubricant

Interface by Combined Use of Atomic Force Microscopy and Line-and-Space Patterned Metal Films
Front. Mech. Eng., 10 1470775 (2024).

A-049
K. Suzuki , et al.
Test Results of the First Series Magnet of Beam Separation Dipole for the HL-LHC Upgrade
IEEE Trans. Appl. Supercond., 34 4001805 (2024).

A-050
M. Sugano, et al.
Cold Mass Assembly of First Full-Scale Prototype of Beam Separation Dipole Magnet for the High-Luminosity LHC Upgrade
IEEE Trans. Appl. Supercond., 34 4002106 (2024).

A-051
L. Bottura, et al.
Magnets for a Muon Collider -- Needs and Plans
IEEE Trans. Appl. Supercond., 34 4005708 (2024).

A-052
T. Yanagi, et al.
Design and Demonstration of Al-Stabilized MgB_2 Conductor for Higher-Sensitivity Particle Detection Magnet
IEEE Trans. Appl. Supercond., 34 4500706 (2024).

A-053
M. Dhakarwal , et al.
Development and Testing of HTS Coil With Ceramic Coated REBCO Conductor for High Radiation Tolerance
IEEE Trans. Appl. Supercond., 34 4603805 (2024).

A-054
M. Nakamoto, et al.
Internal Strain Measurement by Neutron Diffraction Under Transverse Compressive Stress for Nb3Sn Wires With and Without Cu-Nb Reinforcement
IEEE Trans. Appl. Supercond., 34 8400806 (2024).

A-055
Y. Arimoto, et al.
Magnetic Field Measurement of Superconducting Transport Solenoid for COMET
IEEE Trans. Appl. Supercond., 34 9000205 (2024).

A-056
K. Suzuki , et al.
Evaluation of the Parallel-Scheme Varistors as Energy-Extraction System for a Test Facility of Superconducting Accelerator Magnet
IEEE Trans. Appl. Supercond., 34 9501407 (2024).

A-057
Y. Deng, et al.
Impact of Irradiation Side on Muon-Induced Single-Event Upsets in 65-Nm Bulk SRAMs
IEEE Trans. Nucl. Sci., 71 912–920 (2024).

A-058
T. D. Vu, et al.
Application of Energy-Resolving Neutron Imaging to Major-Component Analyses of Materials Using Four-Channel Superconducting Detector
IEEJ Trans. Electr. Electron. Eng., 19 1888–1894 (2024).

A-059
X. He, et al.
High-Pressure Behaviors of Hydrogen Bonds in Fluorine-Doped Brucite
Inorg. Chem., 63 22349–22360 (2024).

A-060
K. Arai, et al.
Promoted Hydride Substitution in BaTiO3 Cubes
Inorg. Chem., 63 23260–23266 (2024).

A-061
K. Ikeda, et al.
Local Structural Changes in V–Ti–Cr Alloy Hydrides with Hydrogen Absorption/Desorption Cycling
Int. J. Hydrog. Energy, 51 79–87 (2024).

A-062
K. Shimizu, et al.
Novel Approach to Explore Hydrogen Trapping Sites in Aluminum: Integrating Muon Spin Relaxation with First-Principles Calculations
Int. J. Hydrog. Energy, 95 292–299 (2024).

A-063
K. Hagihara, et al.
Contributions of Multimodal Microstructure in the Deformation Behavior of Extruded Mg Alloys Containing LPSO Phase
Int. J. Plast., 173 103865 (2024).

A-064
M. Fujihala, et al.
μSR Studies on Copper Minerals
Interactions, 245 13 (2024).

A-065
K. Shimomura, et al.
Pulsed Muon Facility of J-PARC MUSE,
Interactions, 245 31 (2024).

A-066
C. M. Wensrich, et al.
Direct Inversion of the Longitudinal Ray Transform for 2D Residual Elastic Strain Fields
Inverse Probl., 40 075011 (2024).

A-067
M. Watanabe, et al.
Thermal Stability of Retained Austenite with Heterogeneous Composition and Size in Austempered Fe-2Mn-1.5Si-0.4C Alloy
ISIJ Int., 64 1464–1476 (2024).

A-068
T. Yamashita, et al.
Role of Retained Austenite and Deformation-Induced Martensite in 0.15C-5Mn Steel Monitored by in-situ Neutron Diffraction Measurement during Tensile Deformation
ISIJ Int., 64 2051–2060 (2024).

A-069
Y. Zhang, et al.
Multi-Aspect Characterization of Low-Temperature Tempering Behaviors in High-Carbon Martensite
ISIJ Int., 64 245–256 (2024).

A-070
N. Tsuchida, et al.
Change in Mechanical Properties of High-Strength Martensitic Steel by the Combination of Pre-Strain and Deformation Temperature
ISIJ Int., 64 354–360 (2024).

A-071
S. Uranaka, et al.
Effects of Retained Austenite upon Softening during Low-Temperature Tempering in Martensitic Carbon Steels
ISIJ Int., 64 449–458 (2024).

A-072
R. Ueji, et al.
Deformation-Induced Martensitic Transformation at Tensile and Compressive Deformations of Bainitic Steels with Different Carbon Contents
ISIJ Int., 64 459–465 (2024).

A-073
K. Matsuda, et al.
Reverse Transformation Behavior in Multi-Phased Medium Mn Martensitic Steel

Analyzed by in-situ Neutron Diffraction
ISIJ Int., 64 486–490 (2024).

A-074
K. Edalati, et al.
Severe Plastic Deformation for Producing Superfunctional Ultrafine-Grained and Heterostructured Materials: An Interdisciplinary Review
J. Alloys Compd., 1002 174667 (2024).

A-075
Y. Zhou, et al.
Probing Deformation Behavior of a Refractory High-Entropy Alloy Using in Situ Neutron Diffraction
J. Alloys Compd., 971 172635 (2024).

A-076
C. González-Guillén, et al.
Microstructural and Mechanical Behavior of Second-Phase Hardened Porous Refractory Ti-Nb-Zr-Ta Alloys
J. Alloys Compd., 980 173605 (2024).

A-077
K. Matsuzaki, et al.
High Proton Conduction in the Octahedral Layers of Fully Hydrated Hexagonal Perovskite-Related Oxides
J. Am. Chem. Soc., 146 18544–18555 (2024).

A-078
T. Nagai, et al.
Ferroelectricity Induced by a Combination of Crystallographic Chirality and Axial Vector
J. Am. Chem. Soc., 146 23348–23355 (2024).

A-079
W. Yi, et al.
La2SrSc2O7 : A-Site Cation Disorder Induces Ferroelectricity in Ruddlesden–Popper Layered Perovskite Oxide
J. Am. Chem. Soc., 146 4570–4581 (2024).

A-080
K.-H. Lu, et al.
Modulating Phase Segregation during Spin-Casting of Fullerene-Based Polymer Solar-Cell Thin Films upon Minor Addition of a High-Boiling Co-Solvent
J. Appl. Crystallogr., 57 1871–1883 (2024).

A-081
J. Abe, et al.
A High-Temperature High-Pressure Small-Angle Neutron Scattering Cell for Studying Hydrothermal Reactions in Supercritical Water
J. Appl. Crystallogr., 57 306–313 (2024).

A-082
T. Kumada, et al.
Low-Background Ultrahigh-Purity Aluminium Window for Small-Angle Neutron Scattering Using Monochromatic Cold Neutrons
J. Appl. Crystallogr., 57 728–733 (2024).

A-083
S. Takeshita, et al.
Slow Polymer Dynamics in Poly(3-Hexylthiophene) Probed by Muon Spin Relaxation
J. Appl. Phys., 136 034701 (2024).

A-084
Z. Zhang, et al.
Giant Barocaloric Effects in Sodium Hexafluorophosphate and Hexafluoroarsenate
J. Appl. Phys., 136 035105 (2024).

A-085
Y. Matsumoto, et al.
Nondestructive Analysis of Internal Crystallographic Structures of Japanese Swords Using Neutron Imaging
J. Archaeol. Sci. Rep., 58 104729 (2024).

A-086
N. Yano, et al.
Charge Neutralization and β-Elimination Cleavage Mechanism of Family 42 L-Rhamnose-α-1,4-D-Glucuronate Lyase Revealed Using Neutron Crystallography
J. Biol. Chem., 300 105774 (2024).

A-087
S. Sato, et al.
Synthesis of Hyperordered Permanently Densified Silica Glasses by Hot Compression above the Glass Transition Temperature,
J. Ceram. Soc. Jpn., 132 427–433 (2024).

A-088
T. Kikuchi, et al.
Detailed Dynamical Features of the Slow Hydration Water in the Vicinity of Poly(Ethylene Oxide) Chains
J. Chem. Phys., 160 064902 (2024).

A-089
R. Inoue, et al.
Dynamics of Side Chains in Poly(Quinoxaline-2,3-Diyl)s Studied via Quasielastic Neutron Scattering
J. Chem. Phys., 161 054905 (2024).

A-090
F. Nemoto, et al.
Difference in Structural Changes of Surfactant Aggregates near Solid Surface under Shear Flow versus Those in the Bulk
J. Chem. Phys., 161 164902 (2024).

A-091
F. Lin, et al.
Correlation between Viscoelastic Response and Frictional Properties of Hydrated Zwitterionic Polymer Brush Film in Narrowing Shear Gap
J. Colloid Interface Sci., 655 253–261 (2024).

A-092
A. Murmiliuk, et al.
Polyelectrolyte-Protein Synergism: pH-Responsive Polyelectrolyte/Insulin Complexes as Versatile Carriers for Targeted Protein and Drug Delivery
J. Colloid Interface Sci., 665 801–813 (2024).

A-093
T. Kämäräinen, et al.
Multiscale Structure Analysis of a pH-Responsive Gelatin/Hydroxypropyl Methylcellulose Phthalate Blend Using Small-Angle Scattering
J. Colloid Interface Sci., 669 975–983 (2024).

A-094
K. Kawai, et al.
Effect of Water Activity on the Mechanical Glass Transition and Dynamical Transition of Bacteria-Solute Systems
J. Food Eng., 375 112066 (2024).

A-095
K. Saito, et al.
High Proton Conduction by Full Hydration in Highly Oxygen Deficient Perovskite
J. Mater. Chem. A, 12 13310–13319 (2024).

A-096
L. Romero Reséndiz, et al.
Mechanical and Electrochemical Properties Comparison of Additively Manufactured Ti-6Al-4V Alloys by Electron Beam Melting and Selective Laser Melting
J. Mater. Eng. Perform., 33 9028–9038 (2024).

A-097
T.-D. Nguyen, et al.
Mechanical Properties of Base Metal and Heat-Affected Zone in Friction-Stir-Welded AA6061-T6 at Ultra-Low Temperature of 20 K
J. Mater. Res. Technol., 31 1547–1556 (2024).

A-098
J. Ge, et al.
Evolution of Medium-Range Order and Its Correlation with Magnetic Nanodomains in Fe-Dy-B-Nb Bulk Metallic Glasses
J. Mater. Sci. Technol., 176 224–235 (2024).

A-099
W. Mao, et al.
In situ Neutron Diffraction Revealing the Achievement of Excellent Combination of Strength and Ductility in Metastable Austenitic Steel by Grain Refinement
J. Mater. Sci. Technol., 176 69–82 (2024).

A-100
S. Wang, et al.
Dual Nanoprecipitation and Nanoscale Chemical Heterogeneity in a Secondary Hardening Steel for Ultrahigh Strength and Large Uniform Elongation
J. Mater. Sci. Technol., 185 245–258 (2024).

A-101
K.-D. Liss, et al.
Recrystallization of Bulk Nanostructured Magnesium Alloy AZ31 after Severe Plastic Deformation: An in situ Diffraction Study
J. Mater. Sci., 59 5831–5853 (2024).

A-102
M. Takano, et al.
Low Reactivity of Stoichiometric FeS with Hydrogen at High-Pressure
and High-Temperature Conditions
J. Mineral. Petrol. Sci., 119 240122 (2024).

A-103
C. Micheau, et al.
Organization of Malonamides from the Interface to the Organic Bulk Phase
J. Mol. Liq., 401 124372 (2024).

A-104
H. Abe, et al.
Probing Water-Driven Nanostructures in an Ionic Liquid Using Small- and Wide-Angle Neutron Scattering:
1-Dodecyl-3-Methylimidazolium Iodide
J. Mol. Liq., 404 124952 (2024).

A-105
H. Liu, et al.
X-Ray Diffraction and Quasielastic Neutron Scattering Studies of the Structure and Dynamic Properties of Water Confined in Ordered Microporous Carbon Pores
J. Mol. Liq., 415 126316 (2024).

A-106
X. He, et al.
Hydroxyl Group/Fluorine Disorder in Deuterated Magnesium Hydroxyfluoride and Behaviors of Hydrogen Bonds under High Pressure
J. Mol. Struct., 1310 138271 (2024).

A-107
M. K. Ahmed Patwary, et al.
Measurement of the Thermal Neutron Capture-Cross Section of 191Ir at ANNRI MLF J-PARC
J. Nucl. Sci. Technol., 61 1385–1396 (2024).

A-108
Nguyen Thi Hong Thuong, et al.
Experimental study of photoneutron spectra from tantalum, tungsten, and bismuth targets for 16.6 MeV polarized photons
J. Nucl. Sci. Technol., 61, 261-268 (2024)

A-109
M. Segawa, et al.
Development of Neutron Self-Indication Thermometry at J-PARC
J. Nucl. Sci. Technol., 62 268–277 (2024).

A-110
H. Li, et al.
Role of Exchange Cations and Layer Charge on the Dynamics of Confined Water
J. Phys. Chem. A, 128 261–270 (2024).

A-111
Y. Kameda, et al.
Structure of Ion Pair Receptor Combined with Li+Cl– in Concentrated Acetonitrile Solutions Studied by Neutron Diffraction with6Li/7Li Isotopic Substitution Method
J. Phys. Chem. B, 128 12533–12539 (2024).

A-112
Y. Shinohara, et al.
Proton Diffusion in Liquid 1,2,3-Triazole Studied by Incoherent Quasi-Elastic Neutron Scattering
J. Phys. Chem. B, 128 1544–1549 (2024).

A-113
T. Takamuku, et al.
Alcohol-Induced Denaturation of Hen Egg White Lysozyme Studied by Infrared, Circular Dichroism, and Small-Angle Neutron Scattering
J. Phys. Chem. B, 128 4076–4086 (2024).

A-114
K. Chai, et al.
Structure, Microheterogeneity, and Transport Properties of Ethaline Decoded by X-Ray/Neutron Scattering and MD Simulation
J. Phys. Chem. B, 128 7445–7456 (2024).

A-115
T. Takamuku, et al.
Effects of Heterogeneous Mixing of Imidazolium-Based Ionic Liquids with Alcohols on Complex Formation of Ni(II) Ion
J. Phys. Chem. B, 128 8567–8577 (2024).

A-116
T. Kumada, et al.
Interpenetration of Rubber and Silane Coupling Agent on an Inorganic Substrate Revealed by Spin-Contrast-Variation Neutron Reflectivity
J. Phys. Chem. C, 128 8797–8802 (2024).

A-117
C. Yu, et al.
Atomic Structure and Dynamics of Organic–Inorganic Hybrid Perovskite Formamidinium Lead Iodide
J. Phys. Chem. Lett., 15 329–338 (2024).

A-118
K. Nawa, et al.
Magnetism of Pseudospin-1/2 Pyrochlore Antiferromagnet Na3Co(CO3)2Cl
J. Phys. Condens. Matter, 36 495801 (2024).

A-119
S. Hosokawa, et al.
Local- and Intermediate-Range Partial Structure Study of As–Se Glasses
J. Phys. Soc. Jpn., 93 014601 (2024).

A-120
T. Miyatake, et al.
Neutron Diffraction Study of Layered Nickelates Pr4Ni3–x CoxO8 for High-Temperature Superconductor Candidate
J. Phys. Soc. Jpn., 93 024709 (2024).

A-121
T. U. Ito, et al.
Distinguishing Ion Dynamics from Muon Diffusion in Muon Spin Relaxation
J. Phys. Soc. Jpn., 93 044602 (2024).

A-122
T. Nakajima, et al.
Polarized and Unpolarized Neutron Scattering for Magnetic Materials at the Triple-Axis Spectrometer PONTA in JRR-3
J. Phys. Soc. Jpn., 93 091002 (2024).

A-123
T. Higuchi, et al.
Polarized Cold-Neutron Reflectometry at JRR-3/MINE2 for the Development of Ultracold-Neutron Spin Analyzers for a Neutron EDM Experiment at TRIUMF
J. Phys. Soc. Jpn., 93 091009 (2024).

A-124
K. Yamakawa, et al.

Atomic Imaging of BaTiO3 by Multiple-Wavelength Neutron Holography
J. Phys. Soc. Jpn., 93 104601 (2024).

A-125
T. Taniguchi, et al.
Field-Induced Criticality in YbCu4Au
J. Phys. Soc. Jpn., 93 124706 (2024).

A-126
Z. Liu, et al.
Inelastic Neutron Scattering Study on Skyrmion Host Compound GaV4Se8
J. Phys. Soc. Jpn., 93 124707 (2024).

A-127
K. Ninomiya, et al.
Development of a Non-Destructive Carbon Quantification Method in Iron by Negative Muon Lifetime Measurement
J. Radioanal. Nucl. Chem., 333 3445–3450 (2024).

A-128
K. Matsuzaki, et al.
Structural and Electrical Properties of Bi3GaSb2O11 at High Temperatures
J. Solid State Chem., 329 124380 (2024).

A-129
K. Hikima, et al.
Structure and Particle Surface Analysis of Li2S–P2S5–LiI-Type Solid Electrolytes Synthesized by Liquid-Phase Shaking
J. Solid State Electrochem., 28 4377–4387 (2024).

A-130
Y. Yamaguchi, et al.
Preliminary experiment for measurement of radionuclide yield from nuclear capture reaction of negative muon
JAEA-Conf, 2023–001 (2024).

A-131
T. SHIBATA, et al.
Discoloration of RF antenna coil surface after long-term operation of J-PARC ion source
Journal of Instrumentation, 19 C01009 (2024)

A-132
K. Shimokita, et al.
Neutron Reflectivity Study on the Adsorption Layer of Polyethylene Grown on Si Substrate
Langmuir, 40 15758–15766 (2024).

A-133
Y. Ueda, et al.
Fluorous and Organic Extraction Systems: A Comparison from the Perspectives of Coordination Structures, Interfaces, and Bulk Extraction Phases
Langmuir, 40 24257–24271 (2024).

A-134
T. Hirayama, et al.
Adsorption Characteristics and Mechanical Responses of Lubricants Containing Polymer Additives under Fluid Lubrication with a Narrow Gap
Langmuir, 40 6229–6243 (2024).

A-135
R. Kanno, et al.
Thermoresponsive Gelation and Phase Transition of PEG/Cation Random Terpolymer Micelles in Water in the Presence of Salts
Macromolecules, 57 10071–10082 (2024).

A-136
K. Yoshimura, et al.
Effects of Functional Graft Polymers on Phase Separation and Ion-Channel Structures in Anion Exchange Membranes Analyzed by SANS Partial Scattering Function
Macromolecules, 57 1998–2007 (2024).

A-137
Y. Nakamura, et al.
Spatial Dynamics of Water Molecules Confined in Deuterated Epoxies by Quasi-Elastic Neutron Scattering
Macromolecules, 57 4254–4262 (2024).

A-138
M. Kawano, et al.
In-Plane Movement of Isolated Poly(Methacrylate) Chains on a Hydrophilic Solid Surface
Macromolecules, 57 6625–6633 (2024).

A-139
W. Zhang, et al.
The Effect of Productive and Quality Deposition Strategies on Residual Stress for Directed Energy Deposition (DED) Process
Manuf. Lett., 41 868–878 (2024).

A-140
P. Thirathipviwat, et al.
In situ Neutron Diffraction Study and Electron Microscopy Analysis of Microstructure and Texture Evolution during Annealing of Rolled CoCrFeNi Alloy Doped with 1 at.%C
Mater. Charact., 212 113980 (2024).

A-141
Z. Pan, et al.
Mixed Anion Control of Enhanced Negative Thermal Expansion in the Oxysulfide of PbTiO3
Mater. Horiz., 11 5394–5401 (2024).

A-142
K. Yamanaka, et al.
Effect of Matrix Dislocation Strengthening on Deformation-Induced Martensitic Transformation Behavior of Metastable High-Entropy Alloys
Mater. Res. Lett., 12 1–9 (2024).

A-143
Y. S. Kim, et al.
In-situ Neutron Diffraction Study of Serration-Involved Ultra-Cryogenic Deformation Behavior at 15K
Mater. Sci. Eng. A, 899 146453 (2024).

A-144
M. Naeem, et al.
Enhanced Cryogenic Mechanical Properties of Heterostructured CrCoNi Multicomponent Alloy: Insights from in-situ Neutron Diffraction
Mater. Sci. Eng. A, 916 147374 (2024).

A-145
S. Futami, et al.
Search for Significant Short-Range Ordering in Medium-Entropy Alloys Tr-Co-Ni (Tr = Cr, Mn, and Fe)
Mater. Trans., 65 995–1000 (2024).

A-146
H. Chae, et al.
Mechanical Stability of Retained Austenite and Texture Evolution in Additively Manufactured Stainless Steel
Met. Mater. Int., 30 1321–1330 (2024).

A-147
Y.-J. Zhang, et al.
Pearlite Growth Kinetics in Fe-C-Mn Eutectoid Steels: Quantitative Evaluation of Energy Dissipation at Pearlite Growth Front Via Experimental Approaches
Metall. Mater. Trans. A, 55 3921–3936 (2024).

A-148
X. Yang, et al.
High-Pressure Polymerization of Phenol toward Degree-4 Carbon Nanothread
Nano Lett., 25 1028–1035 (2025).

A-149
A. A. Kaharudin, et al.
Unified Interpretations of Two Kinds of

Needle-Shaped Precipitates Using Transmission Electron Microscopy and Small-Angle Neutron Scattering in Aged Al–Mg2Si(-Cu) Alloys
Nanomaterials, 14 176 (2024).

A-150
S. Hasegawa, et al.
Field Control of Quasiparticle Decay in a Quantum Antiferromagnet
Nat. Commun., 15 125 (2024).

A-151
Z. Song, et al.
Promoting High-Voltage Stability through Local Lattice Distortion of Halide Solid Electrolytes
Nat. Commun., 15 1481 (2024).

A-152
E. Fogh, et al.
Field-Induced Bound-State Condensation and Spin-Nematic Phase in SrCu2(BO3)2 Revealed by Neutron Scattering up to 25.9T
Nat. Commun., 15 442 (2024).

A-153
K. Komatsu, et al.
Hydrogen Bond Symmetrisation in D2O Ice Observed by Neutron Diffraction
Nat. Commun., 15 5100 (2024).

A-154
Q. Yang, et al.
Brightening Triplet Excitons Enable High-Performance White-Light Emission in Organic Small Molecules via Integrating n–Π*/π–Π* Transitions
Nat. Commun., 15 7778 (2024).

A-155
X.-G. Zheng, et al.
Unique Magnetic Transition Process Demonstrating the Effectiveness of Bond Percolation Theory in a Quantum Magnet
Nat. Commun., 15 9989 (2024).

A-156
H. Yoshimochi, et al.
Multistep Topological Transitions among Meron and Skyrmion Crystals in a Centrosymmetric Magnet
Nat. Phys., 20 1001–1008 (2024).

A-157
Z. Zeng, et al.
Spectral Evidence for Dirac Spinons in a Kagome Lattice Antiferromagnet
Nat. Phys., 20 1097–1102 (2024).

A-158
P.-F. Liu, et al.
Strong Low-Energy Rattling Modes Enabled Liquid-like Ultralow Thermal Conductivity in a Well-Ordered Solid
Natl. Sci. Rev., 11 nwae216 (2024).

A-159
N. Kitamura, et al.
Relationship between Network Topology and Negative Electrode Properties in Wadsley–Roth Phase TiNb2O7
NPG Asia Mater., 16 62 (2024).

A-160
T.N. Murakami, et al.
Construction of gas electron multiplier tracker for the J-PARC E16 experiment
Nucl. Instr. Meth. A 1058, 168817 (2024)

A-161
Y.C. Tung, et al.
Suppression of neutron background using deep neural network and Fourier frequency analysis at the KOTO experiment
Nucl. Instr. Meth. A 1059, 169010 (2024)

A-162
K. Abe, et al.
Second gadolinium loading to Super-Kamiokande
Nucl. Instr. Meth. A 1065, 169480 (2024)

A-163
Y. Fujii, et al.
Particle identification using plastic scintillators in the COMET Phase-I experiment
Nucl. Instr. Meth. A 1067, 169665 (2024)

A-164
A. Sato, et al.
Design and construction of the cylindrical drift chamber for the COMET Phase-I experiment
Nucl. Instr. Meth. A 1069, 169926 (2024)

A-165
T. Matsumura, et al.
Measurement of muon flux behind the beam dump of the J-PARC Hadron Experimental Facility
Nucl. Instr. Meth. A 1069, 169990 (2024)

A-166
Y. Yang, et al.
Magnetic properties of a non-oriented electrical steel at cryogenic temperature for rapid-cycling accelerator superconducting magnets
Nucl. Instrum. Methods Phys. Res. A, 1068 169781 (2024).

A-167
Y. Iwamoto , et al.
Measurements of displacement cross sections of metals for 120-GeV proton beam irradiation
Nucl. Instrum. Methods Phys. Res. B, 557 165543 (2024).

A-168
K. Sugihara, et al.
Measurement of Nuclide Production Cross Sections for GeV-region Proton-induced Reactions on ^{nat}Mg, ^{nat}Si, ^{nat}Fe, ^{nat}Cu, and ^{nat}Zn
*Nucl. Instrum. Methods Phys. Res. **B549**, 165299 (2024).*

A-169
T. Hattori, et al.
Development of 0.5 Mm Gauge Size Radial Collimators for High-Pressure Neutron Diffraction Experiments at PLANET in J-PARC
Nucl. Instrum. Methods Phys. Res. Sect. Accel. Spectrometers Detect. Assoc. Equip., 1059 168956 (2024).

A-170
T. Kanno, et al.
Development of Instruments for Imaging of Local Magnetic Structure by Magnetic Neutron Holography
Nucl. Instrum. Methods Phys. Res. Sect. Accel. Spectrometers Detect. Assoc. Equip., 1064 169349 (2024).

A-171
R. Iwai, et al.
Dual-Mode Rectangular Microwave Cavity for Precision Spectroscopy of Hyperfine Structure in Muonium
Nucl. Instrum. Methods Phys. Res. Sect. Accel. Spectrometers Detect. Assoc. Equip., 1064 169434 (2024).

A-172
K. Horie, et al.
Measurement of Residual μ+ Polarization in a LaF3 Scintillating Material for a New μ+ Polarimeter System
Nucl. Instrum. Methods Phys. Res. Sect. Accel. Spectrometers Detect. Assoc. Equip., 1066 169606 (2024).

A-173
M. Teshigawara, et al.
In-situ Measurement of Radiation Driven Back-Conversion from Para to Ortho Liquid Hydrogen State in Cold Moderators at J-PARC
Nucl. Instrum. Methods Phys. Res. Sect. B Beam

Interact. Mater. At., 557 165534 (2024).

A-174
Y. Xu, et al.
Development of a scintillating-fiber-based beam monitor for the coherent muon-to-electron transition experiment
Nucl. Sci. Tech., 35, 79 (2024)

A-175
W. Yoshimune, et al.
Neutron Imaging for Automotive Polymer Electrolyte Fuel Cells during Rapid Cold Starts
Phys. Chem. Chem. Phys., 26 29466–29474 (2024).

A-176
G. Che, et al.
Pressure-Induced Polymerization of 1,4-Difluorobenzene towards Fluorinated Diamond Nanothreads
Phys. Chem. Chem. Phys., 27 1112–1118 (2025).

A-177
T. Yamanaka, et al.
Anisotropic Electrical Conductivity Changes in FeTiO3 Structure Transition under High Pressure
Phys. Chem. Miner., 51 4 (2024).

A-178
Z. Huang, et al.
Microscopic Origin of the Spin-Reorientation Transition in the Kagome Topological Magnet TbMn6Sn6
Phys. Rev. B, 109 014434 (2024).

A-179
S. Zheng, et al.
Interplay between Crystal Field and Magnetic Anisotropy in the Triangular-Lattice Antiferromagnet NaTmTe2
Phys. Rev. B, 109 075159 (2024).

A-180
M. Hase, et al.
Inelastic Neutron Scattering Studies on the Eight-Spin Zigzag-Chain Compound KCu4P3O12: Confirmation of the Validity of a Data-Driven Technique Based on Machine Learning
Phys. Rev. B, 109 094434 (2024).

A-181
A. Shimoda, et al.
Antiferromagnetic Ordering and Chiral Crystal Structure Transformation in Nd3Rh4Sn13
Phys. Rev. B, 109 134425 (2024).

A-182
P. Miao, et al.
Persistent Spin Dynamics in Magnetically Ordered Honeycomb-Lattice Cobalt Oxides
Phys. Rev. B, 109 134431 (2024).

A-183
S. Holm-Janas, et al.
Magnetic Structure and Magnetoelectric Properties of the Spin-Flop Phase in LiFePO4
Phys. Rev. B, 109 174413 (2024).

A-184
D. Ueta, et al.
Neutron Scattering Study on Dimerized 4f1 Intermetallic Compound Ce5Si3
Phys. Rev. B, 109 205127 (2024).

A-185
T. Yamaguchi, et al.
Mechanism of Intermetallic Charge Transfer and Bond Disproportionation in BiNiO3 and PbNiO3 Revealed by Hard X-Ray Photoemission Spectroscopy
Phys. Rev. B, 109 205131 (2024).

A-186
K. Yadav, et al.
Coexistence of Antiferromagnetism and Glassy Magnetic State and Signature of Quantum Interference Effects in the Frustrated Ternary Silicides HoScSi and ErScSi
Phys. Rev. B, 109 224409 (2024).

A-187
J. Liao, et al.
Spin and Lattice Dynamics in the van Der Waals Antiferromagnet MnPSe3
Phys. Rev. B, 109 224411 (2024).

A-188
P. Park, et al.
Composition Dependence of Bulk Properties in the Co-Intercalated Transition Metal Dichalcogenide Co1/3TaS2
Phys. Rev. B, 109 L060403 (2024).

A-189
Y. Gu, et al.
In-Plane Multi-q Magnetic Ground State of Na3Co2SbO6
Phys. Rev. B, 109 L060410 (2024).

A-190
K. Lee, et al.
High-Spin Co3+ as a Trigger of Weak Ferromagnetism in Co-Substituted BiFeO3
Phys. Rev. B, 110 024422 (2024).

A-191
T. Taniguchi, et al.
Fermi Liquid State in T* -Type La1−x/2Eu1−x/2SrxCuO4 Revealed via Element Substitution Effects on Magnetism
Phys. Rev. B, 110 085116 (2024).

A-192
S. Araki, et al.
Ferrimagnetic Structure in the High-Pressure Phase of α−Mn
Phys. Rev. B, 110 094420 (2024).

A-193
A. D. Pant, et al.
Formation and Structure of MuOH in Ice Studied by Muon Spin Rotation
Phys. Rev. B, 110 104104 (2024).

A-194
B. Hu, et al.
Absence of Magnetoelastic Deformation in the Spin-Chain Compound CuBr2
Phys. Rev. B, 110 115142 (2024).

A-195
K. Kimura, et al.
Ca-Induced Phonon Softening in BaTiO3 Revealed by Inelastic X-Ray and Neutron Scattering
Phys. Rev. B, 110 134314 (2024).

A-196
S. Yano, et al.
Spin Reorientation and Interplanar Interactions of the Two-Dimensional Triangular-Lattice Heisenberg Antiferromagnets h−(Lu, Y) MnO3 and h−(Lu, Sc) FeO3
Phys. Rev. B, 110 134444 (2024).

A-197
W. Lee, et al.
Quasistatic Magnetism in the Breathing Pyrochlore Antiferromagnets LiGa1−xInxCr4O8 (x = 0.2, 0.5)
Phys. Rev. B, 110 144435 (2024).

A-198
J. Kumar, et al.
YbTaO4: A Quasi-Two-Dimensional Frustrated Magnet Possessing Spin Orbit Entangled Kramers Doublet Ground State
Phys. Rev. B, 110 174420 (2024).

A-199
M. Ma, et al.
Ferromagnetic Interlayer Coupling in FeSe1−xSx Superconductors Revealed by Inelastic Neutron Scattering
Phys. Rev. B, 110 174503 (2024).

A-200
Y. Ishii, et al.
Nonferroelectric Phase with Loss of Cycloidal Magnetic Structure in Tb0.515Gd0.485Mn2O5
Phys. Rev. B, 110 184404 (2024).

A-201
J. C. Jiao, et al.
μ SR Study on the Noncentrosymmetric Superconductor NbGe2
Phys. Rev. B, 110 214516 (2024).

A-202
T. Okudaira, et al.
Spin dependence in the p-wave resonance of 139La+n
Phys. Rev. C 109 44606 (2024).

A-203
R. Nakabe, et al.
High sensitivity of a future search for effects of P-odd/T-odd interactions on the 0.75 eV p-wave resonance in n + 139La forward transmission determined using a pulsed neutron beam
Phys. Rev. C 109 L041602 (2024).

A-204
T. Yamaga , et al.
Measurement of the mesonic decay branch of the K-NN quasibound state
Phys. Rev. C 110 14002 (2024).

A-205
T. Yamaga, et al.
Measurement of the mesonic decay of the K-barNN quasibound state
Phys. Rev. C 110, 14002 (2024)

A-206
T. Okudaira, et al.
Spin Dependence in the p-Wave Resonance of 139 $^{\rightarrow}$ La + n $^{\rightarrow}$
Phys. Rev. C, 109 044606 (2024).

A-207
H. Iwamoto, et al.
Comprehensive estimation of nuclide production cross sections using a phenomenological approach
*Phys. Rev. C, **109** 054610 (2024).*

A-208
R. Nakabe, et al.
High Sensitivity of a Future Search for Effects of P-Odd/T-Odd Interactions on the 0.75 eV p-Wave Resonance in n $^{\rightarrow}$ + 139La $^{\rightarrow}$ Forward Transmission Determined Using a Pulsed Neutron Beam
Phys. Rev. C, 109 L041602 (2024).

A-209
M. Aoki, et al.
Search for quantum black hole production in lepton + jet final states using proton-proton collisions at $\sqrt{s}$ = 13 TeV with the ATLAS detector
Phys. Rev. D 109 32010 (2024).

A-210
S. Navas, et al.
REVIEW OF PARTICLE PHYSICS
Phys. Rev. D 110 30001 (2024).

A-211
K. Sakai, et al.
Search for Antideuterons of Cosmic Origin Using the BESS-Polar II Magnetic-Rigidity Spectrometer
Phys. Rev. Lett. 132 131001 (2024).

A-212
T. Fujiie, et al.
Development of Neutron Interferometer Using Multilayer Mirrors and Measurements of Neutron-Nuclear Scattering Length with Pulsed Neutron Source
Phys. Rev. Lett., 132 023402 (2024).

A-213
M. Hiraishi, et al.
Nonmagnetic Ground State in RuO2 Revealed by Muon Spin Rotation
Phys. Rev. Lett., 132 166702 (2024).

A-214
Y. Gu, et al.
Signatures of Kitaev Interactions in the van Der Waals Ferromagnet VI3
Phys. Rev. Lett., 132 246702 (2024).

A-215
L. Zhu, et al.
Antiferromagnetism and Phase Stability of CrMnFeCoNi High-Entropy Alloy
Phys. Rev. Lett., 133 126701 (2024).

A-216
M. Matsuura, et al.
Singular Continuous and Nonreciprocal Phonons in Quasicrystal AlPdMn
Phys. Rev. Lett., 133 136101 (2024).

A-217
Z. Liu, et al.
Chiral Split Magnon in Altermagnetic MnTe
Phys. Rev. Lett., 133 156702 (2024).

A-218
M. Zhu, et al.
Continuum Excitations in a Spin Supersolid on a Triangular Lattice
Phys. Rev. Lett., 133 186704 (2024).

A-219
N. Subotić, et al.
Single Crystal Growth of FeRh from AuPb Flux
Phys. Rev. Mater., 8 023401 (2024).

A-220
K. Taniguchi, et al.
Tuning of Spin-Orbit Coupling in Chiral Molecule-Incorporated Two-Dimensional Organic-Inorganic Hybrid Perovskite Copper Halides with Ferromagnetic Exchange Interactions
Phys. Rev. Mater., 8 024409 (2024).

A-221
H. Okabe, et al.
Nanoscale Dynamics of Hydrogen in VO2 Studied by μSR
Phys. Rev. Mater., 8 024602 (2024).

A-222
H. Yamamoto, et al.
Continuous Structural Phase Transition and Antiferromagnetic Order in Ilmenite-Type NiVO3
Phys. Rev. Mater., 8 094402 (2024).

A-223
M. Kofu, et al.
Magnetic Boson Peak in Classical Spin Glasses
Phys. Rev. Res., 6 013006 (2024).

A-224
H. Yamauchi, et al.
Quantum Critical Behavior of the Hyperkagome Magnet Mn3CoSi
Phys. Rev. Res., 6 013144 (2024).

A-225
T. Nakajima, et al.
Stroboscopic Time-of-Flight Neutron Diffraction in Long Pulsed Magnetic Fields
Phys. Rev. Res., 6 023109 (2024).

A-226
D. Sarenac, et al.
Cone Beam Neutron Interferometry: From Modeling to Applications
Phys. Rev. Res., 6 023260 (2024).

A-227
J. Nagl, et al.
Excitation Spectrum and Spin Hamiltonian of the Frustrated Quantum Ising Magnet Pr3BWO9
Phys. Rev. Res., 6 023267 (2024).

A-228
S. Shamoto, et al.
Magnetic Excitation in the Hyperkagome Antiferromagnet Mn3RhSi
Phys. Rev. Res., 6 033303 (2024).

A-229
Y. Ye, et al.
Dynamic Entity Formed by Protein and Its Hydration Water
Phys. Rev. Res., 6 033316 (2024).

A-230
D. Sarenac, et al.
Phase and Contrast Moiré Signatures in Two-Dimensional Cone Beam Interferometry
Phys. Rev. Res., 6 L032054 (2024).

A-231
S. Fukumura, et al.
Present Status of Spectroscopy of the Hyperfine Structure and Repolarization of Muonic Helium Atoms at J-PARC
Physics, 6 877–890 (2024).

A-232
T. Komiya, et al.
Salt Concentration Dependency of the Hydrated Swollen Structure of Cholinephosphate-Type Polyzwitterion Brushes
Polym. J., (2024).

A-233
F. Kaneko, et al.
Microstructural Investigation of the Cooperative Gelation of Syndiotactic Polystyrene and High MW Polyethylene Glycol Di-Methyl
Ether in Common Solution in THF
Polymer, 295 126771 (2024).

A-234
Y. Shiraki, et al.
Adhesion to Untreated Polyethylene by Diffusion: Effect of Polyurethane Adhesive Molecular Weight on Polyethylene Penetration
Polymer, 302 127073 (2024).

A-235
D. Cortis, et al.
Functionally Graded Material via L-PBF: Characterisation of Multi-Material Junction between Steels (AISI 316L/16MnCr5), Copper (CuCrZr) and Aluminium Alloys (Al-Sc/AlSi10Mg)
Prog. Addit. Manuf., (2024).

A-236
K. Mishima, et al.
Performance of the Fully Equipped Spin Flip Chopper for the Neutron Lifetime Experiment at J-PARC
Prog. Theor. Exp. Phys., 2024 093G01 (2024).

A-237
T. Honjo, et al.
Performance Evaluation of Electron Multiplier Tubes as a High-Intensity Muon Beam Monitor of Accelerator Neutrino Experiments
Prog. Theor. Exp. Phys., 2024, 123H01 (2024)

A-238
P. Xu, et al.
Principal Preferred Orientation Evaluation of Steel Materials Using Time-of-Flight Neutron Diffraction
Quantum Beam Sci., 8 7 (2024).

A-239
K. Sakashita, et al.
Measurement of Gaseous Radioactivity Concentration of Short-Lived Nuclides Produced by Air Activation in the Spallation Neutron Source Facility of J-PARC
Radiation Safety Management, 23 7-15 (2024).

A-240
I. Yamada, et al.
Response function measurement for a non-destructive gas-sheet beam profile monitor
Rev. Sci. Inst., 95(12), 123308_1-12338_11(2024)

A-241
O. Sans-Planell, et al.
Redifining RADEN's High-Resolution Neutron Imaging Capabilities
Rev. Sci. Instrum., 95 113702 (2024).

A-242
K. Ninomiya, et al.
Development of a Non-Destructive Depth-Selective Quantification Method for Sub-Percent Carbon Contents in Steel Using Negative Muon Lifetime Analysis
Sci. Rep., 14 1797 (2024).

A-243
K. Watanabe, et al.
Comparison between Carrier Transport Property and Crystal Quality of TlBr Semiconductors
Sci. Rep., 14 25224 (2024).

A-244
K. Oikawa, et al.
Energy-Resolved Neutron Imaging Study of a Japanese Sword Signed by Bishu Osafune Norimitsu
Sci. Rep., 14 27990 (2024).

A-245
H. Masai, et al.
Combinatorial Characterization of Metastable Luminous Silver Cations
Sci. Rep., 14 4638 (2024).

A-246
K. Shimizu, et al.
Combining Muon Spin Relaxation and DFT Simulations of Hydrogen Trapping in Al6Mn
Scr. Mater., 245 116051 (2024).

A-247
H. Ying, et al.
Anomalous Dislocation Response to Deformation Strain in CrFeCoNiPd High-Entropy Alloys with Nanoscale Chemical Fluctuations
Scr. Mater., 250 116181 (2024).

A-248
K. Watanabe, et al.
Comparison Between Neutron Bragg Dip and Electron Backscatter Diffraction Images of TlBr Semiconductors
Sens. Mater., 36 149 (2024).

A-249
K. Matsumura, et al.
Comprehensive Investigation of the Crystal Structure of Cation-Disordered Li3 VO4 as a High-Rate Anode Material: Unveiling the Dichotomy between Order and Disorder
Small, 20 2405259 (2024).

A-250
H. Takagi, et al.
Tracer Diffusion Coefficient Measurements on NASICON-Type Lithium-Ion Conductor LAGP Using Neutron Radiography between 25°C and 500°C
Solid State Ion., 417 116716 (2024).

A-251
S. Tomone, et al.
Strain Analysis by Neutron Diffraction on Nb3Sn Strands in ITER Central Solenoid Conductors of Short and Long Twist Pitch
Supercond. Sci. Technol., 38 015008 (2025).

A-252
K. Nagase, et al.
Temperature-Dependent Behavior of Poly(N-Isopropylacrylamide) Brushes via Neutron Reflectometry
Surf. Interfaces, 54 105268 (2024).

A-253
E. Nocerino, et al.
Na-Ion Dynamics in the Solid Solution NaxCa1−xCr2O4 Studied by Muon Spin Rotation and Neutron Diffraction
Sustain. Energy Fuels, 8 1424–1437 (2024).

A-254
M. Koyama, et al.
Microstructure and Plasticity Evolution During Lüders Deformation in an Fe-5Mn-0.1C Medium-Mn Steel
Tetsu-to-Hagane, 110 197–204 (2024).

A-255
M. Koyama, et al.
Hierarchical Deformation Heterogeneity during Lüders Band Propagation in an Fe-5Mn-0.1C Medium Mn Steel Clarified through in situ Scanning Electron Microscopy
Tetsu-to-Hagane, 110 205–216 (2024).

A-256
T. Yamashita, et al.
Role of Retained Austenite and Deformation Induced Martensite in 0.15C-5Mn Steel Monitored by in-situ Neutron Diffraction Measurement during Tensile Deformation
Tetsu-to-Hagane, 110 241–251 (2024).

A-257
S. Uranaka, et al.
Effects of Retained Austenite upon Softening during Low-Temperature Tempering in Martensitic Carbon Steels
Tetsu-to-Hagane, 110 621–631 (2024).

A-258
K. Matsuda, et al.
Reverse Transformation Behavior in Multi-Phased Medium Mn Martensitic Steel Analyzed by in-situ Neutron Diffraction
Tetsu-to-Hagane, 110 83–88 (2024).

A-259
F. Lin, et al.
Hydration–Lubrication Performance Improvement via Synergistic Effects of Free Polymers and Polymer Brushes
Tribol. Int., 191 109189 (2024).

A-260
R. Dronskowski, et al.
Neutron Diffraction: A Primer
Z. Für Krist. - Cryst. Mater., 239 139–166 (2024).

Conference Reports and Books

B-001
Y. Gomi, et al.
Muon-Induced SEU Cross Sections of 12-nm FinFET and 28-nm Planar SRAMs
2023 23rd Eur. Conf. Radiat. Its Eff. Compon. Syst. RADECS, 1-4, (2024).

B-002
T. Nakamura, et al.
Detector Performances of Large Area Scintillator / Wavelength Shifting Fiber Neutron Detectors for SENJU Upgrade at J-PARC MLF
2024 IEEE Nucl. Sci. Symp. NSS Med. Imaging Conf. MIC Room Temp. Semicond. Detect. Conf. RTSD, (2024).

B-003
K. Toh, et al.
Measurement of pulsed neutrons using real-time data display and storage module in neutron reflectometer at J-PARC MLF
2024 IEEE Nucl. Sci. Symp. NSS Med. Imaging Conf. MIC Room Temp. Semicond. Detect. Conf. RTSD, (2024).

B-004
A. Kimura, et al.
Total and Double Differential Scattering Cross-Section Measurements of Isotropic Graphite
EPJ Web Conf., 294 01002 (2024).

B-005
S. Nakayama, et al.
Evaluation of Thermal Neutron Scattering Law of Nuclear-Grade Isotropic Graphite
EPJ Web Conf., 294 07001 (2024).

B-006
H. Noumi, et al.
Measurement of K-bar N scattering below the K-bar N mass threshold
EPJ web of Conf., 291, 5011 (2024)

B-007
V. Mikola
Results from the T2K+NOvA Joint Analysis
EPJ web of Conf., 312, 2002 (2024)

B-008
H. Noumi , et al.
Measurement of K$^-$N scattering below the K$^-$N mass threshold
EPJ Web of Conferences, 291 5011 (2024).

B-009
T. Takayanagi , et al.
Development of a Fast-Rising Short-Pulse High-Voltage Power Supply using SiC-MOSFETs for the J-PARC Kicker System
IEEE EAPPC 2024 1 (2024).

B-010
Y. Fuwa , et al.
Development of a prototype Marx generator module for a klystron power-supply in J-PARC linear accelerator
IEEE EAPPC 2024 2 (2024).

B-011
P. Jaikaew, et al.
Surface Muon Production at J-PARC Muon Facility
Interactions, 245 24 (2024).

B-012
T. U. Ito, et al.
Muon Spin Relaxation in Mixed Perovskite (LaAlO3)x(SrAl0.5Ta0.5O3)1-x with X≃0.3
Interactions, 245 25 (2024).

B-013
R. Pudasaini, et al.
Muonium Behavior in Derivatives of Hemoglobin: A First-Principles Study
Interactions, 245 34 (2024).

B-014
S. Takeshita, et al.
Negative Muon Beam Status at the D-Line of MUSE, J-PARC
Interactions, 245 38 (2024).

B-015
M. Tampo, et al.
Developments on Muonic X-Ray Measurement System for Historical-Cultural Heritage Samples in Japan Proton Accelerator Research Complex (J-PARC)
Interactions, 245 39 (2024).

B-016
S. Tsutsui, et al.
149Sm Synchrotron-Radiation-Based Mössbauer and μ+SR Studies of Sm3Ru4Ge13
Interactions, 245 55 (2024).

B-017
P. Xie, et al.
Annealing and Doping Effects on Magnetism for T*-Type (La, Eu, Sr)2CuO4-yFy Cuprates
Interactions, 245 66 (2024).

B-018
Y. Goto, et al.
New Muonic He Atom HFS Measurements at J-PARC MUSE
Interactions, 245 75 (2024).

B-019
S. Kanda
Hexapole State Selector for Focusing and Polarizing Muonium
Interactions, 245 78 (2024).

B-020
T. Ishida, et al.
Neutron Transmission CB-KID Imager Using Samples Placed at Room Temperature
J. Low Temp. Phys., 214 152–157 (2024).

B-021
M. Nirei, et al.
Neutron Flux and Energy Resolution of Direct-Geometry Disk-Chopper Spectrometer AMATERAS at J-PARC
J. Neutron Res., 26 75–82 (2024).

B-022
R. Kitamura, et al.
Beam profile measurement using the highly-oriented pyrolytic graphite
J. Phys. Conf. Ser. 2687 072006 (2024).

B-023
H. Okita, et al.
Improvement of the Longitudinal Phase Space Tomography at the J-PARC Synchrotrons
J. Phys. Conf. Ser., 2687, 072005_1-072005_6 (2024)

B-024
I. Yamada, et al.
Observation of Beam Emittance Reduction due to Gas Sheet Injection for Beam Profile Measurement
J. Phys. Conf. Ser., 2687, 072018_1-072018_6 (2024)

B-025
H. Iinuma, et al.
Precise control of a strong X-Y coupling beam transportation for J-PARC muon g-2/EDM experiment
J. Phys. Conf. Ser., 2687, 22034 (2024)

B-026
R. Matsushita, et al.
Demonstration of Three-dimensional Spiral Injection for the J-PARC Muon g-2/EDM Experiment
J. Phys. Conf. Ser., 2687, 22035 (2024)

B-027
K. Shinto, *et al.*
Development of a new J-PARC-made internal antenna for the J-PARC RF-driven H^- ion source
J. Phys. Conf. Ser., 2743 012023 (2024).

B-028
M. Wada, T. Shibata, K. Shinto
Factors influencing the fluctuation amplitude of the H^- ion beam extracted from an RF wave excited ion source plasma
J. Phys. Conf. Ser., 2743 012031 (2024).

B-029
T. Dang Vu, et al.
Neutron Transmission Imaging System with a Superconducting Kinetic Inductance Detector
J. Phys. Conf. Ser., 2776 012009 (2024).

B-030
J. Tamura, et al.
Fabrication progress of the prototype spoke cavity for the JAEA-ADS linac
J. Phys.: Conf. Ser. 2687 052008 (2024).

B-031
J. Tamura , et al.
Fabrication progress of the prototype spoke cavity for the JAEA-ADS linac
Journal of Physics: Conference Series 2687 52008 (2024).

B-032
P.K.Saha , et al.
High Intensity Beam Operation of J-PARC RCS With Minimum Beam Loss
Journal of Physics: Conference Series 2687 52020 (2024).

B-033
Y. SUGIYAMA , et al.
Estimation of the Anode Power Supply Current of the J-PARC MR RF system for 1.36s cycle operation
Journal of Physics: Conference Series 2687 52022 (2024).

B-034
T. SHIBATA , et al.
The Leakage Field of the New High-Field Septum Magnets for Fast Extraction in Main Ring of J-PARC
Journal of Physics: Conference Series 2687 52030 (2024).

B-035
R. MUTO , et al.
Simulation study on the slow extraction for the improvement of the beam shill structure at J-PARC Main Ring
Journal of Physics: Conference Series 2687 52032 (2024).

B-036
H.Okita , et al.
Improvement of the longitudinal phase space tomography at the J-PARC synchrotrons
Journal of Physics: Conference Series 2687 72005 (2024).

B-037
R. Kitamura , et al.
Beam Profile Measurement Using the Highly-Oriented Pyrolytic Graphite
Journal of Physics: Conference Series 2687 72006 (2024).

B-038
T. SHIBATA , et al.
Simple 3D PIC Analysis for Beam Phase Space Oscillation in RF Driven Negative Hydrogen Ion Source
Journal of Physics: Conference Series 2743 12007 (2024).

B-039
K. Shinto , et al.
Development of a new J-PARC-made internal antenna for the J-PARC RF-driven H- ion source
Journal of Physics: Conference Series 2743 12023 (2024).

B-040
M. Wada , et al.
Factors Influencing the Fluctuation Amplitude of the H- Ion Beam Extracted from an RF Wave Excited Ion Source Plasma
Journal of Physics: Conference Series 2743 12031 (2024).

B-041
H. Iinuma , et al.
Precise control of a strong X-Y coupling beam transportation for J-PARC muon g-2/EDM experiment
Journal of Physics: Conference Series, 2687 22034 (2024).

B-042
P. K. Saha, et al.
High intensity beam operation of J-PARC

RCS with minimum beam loss
Journal of Physics; Conference Series, 2687(5), p.052020_1 - 052020_7, 2024/01

B-043
H. Takahashi, et al.
Development of new synchronized data system for J-PARC RCS
Journal of Physics; Conference Series, 2687(7), p.072019_1 - 072019_5, 2024/01

B-044
A. Ueno, et al.
Innovative cesiation deriving incredible 145 mA beam from J-PARC cesiated RF-driven H$$^{-}$$ ion source
Journal of Physics; Conference Series, 2743(1), p.012001_1 - 012001_8, 2024/05

B-045
T. KOBAYASHI
Research with J-PARC Beams
Kasokuki 21 272 (2024).

B-046
K. FUTATSUKAWA , et al.
Upgrade of Low-Level Radio-Frequency Control System at J-PARC LINAC
Kasokuki 21 3 (2024).

B-047
S. IGARASHI
Beam Power Upgrade of the J-PARC Main Ring
Kasokuki 21 305 (2024).

B-048
T. TOYAMA
Beam Coupling Impedance Effects and Countermeasures in J-PARC Accelerators
Kasokuki 21 314 (2024).

B-049
C. OHMORI
History and Prospects of Magnetic Alloy Cavity Developments
Kasokuki 21 323 (2024).

B-050
T. SHIBATA , et al.
Operation Status of J-PARC H- Ion Source
Kasokuki 21 94 (2024).

B-051
T. Kobayashi
Research with J-PARC Beams
Kasokuki, 21, 272 (2024)

B-052
W. Gong, et al.
Cryogenic Deformation Behavior of a Dual-Phase Mg–Li Alloy Investigated by in-situ Neutron Diffraction
Magnes. Technol. 2024, 89–90(2024).

B-053
Y. Shobuda, et al.
Calculation of space-charge tune shift in a cylindrical chamber for bunched beams employing Green's function formalism
Physical Review Accelerators and Beams, 27(1), p.011001_1 - 011001_25, 2024/01

B-054
T. Morikawa, et al.
Development of Polarization Analysis at TAIKAN under Magnetic Field at Low Temperature
Proc. 11th Int. Workshop Sample Environ. Scatt. Facil. ISSE Workshop Nasu 2022, J. Phys. Soc. Jpn., (2024).

B-055
J. G. Nakamura, et al.
Sample Environment for Low Temperature μSR Experiments at MLF, J-PARC
Proc. 11th Int. Workshop Sample Environ. Scatt. Facil. ISSE Workshop Nasu 2022, J. Phys. Soc. Jpn., (2024).

B-056
S. Takada, et al.
Study of Magnetic Environment for Neutron Spin Filters Using Polarized 3He at J-PARC and JRR-3
Proc. 11th Int. Workshop Sample Environ. Scatt. Facil. ISSE Workshop Nasu 2022, J. Phys. Soc. Jpn., (2024).

B-057
D. Ueta, et al.
Sample Environment of the HRC Spectrometer at J-PARC
Proc. 11th Int. Workshop Sample Environ. Scatt. Facil. ISSE Workshop Nasu 2022, J. Phys. Soc. Jpn., (2024).

B-058
S. Zhang, et al.
Advanced Biaxial Tensile State Evaluation Method Using Neutron Bragg-Edge Imaging
Proc. 11th Int. Workshop Sample Environ. Scatt. Facil. ISSE Workshop Nasu 2022, J. Phys. Soc. Jpn., (2024).

B-059
T. Tominaga
Network Devices Development at BL02 in J-PARC MLF
Proc. 11th Int. Workshop Sample Environ. Scatt. Facil. ISSE Workshop Nasu 2022, J. Phys. Soc. Jpn., (2024).

B-060
B. Yee-Rendon, et al.
Design and Beam Dynamics Studies of a Chopper for the JAEA-ADS LEBT
Proc. 20th Ann. Mtg. PASJ, 205-209 (2024).

B-061
S. Meigo, et al.
Proton Beam Utilization for Space Development Equipment at J-PARC
Proc. 20th Ann. Mtg. PASJ, 32-37 (2024).

B-062
S. Meigo, et al.
SiC Sensor Wire Test by Heavy Ion Beam Irradiation (2)
Proc. 20th Ann. Mtg. PASJ, 853-858 (2024).

B-063
Y. Yamaguchi et al.
Investigation of solenoid fringe field based on change in 3-GeV proton beam orbit and the orbit correction
Proc. 21st Ann. Mtg. PASJ (internet), 239-243 (2024)

B-064
K. Suganuma
Start-up of a test equipment for corrosion evaluation using copper thin film
Proc. 21th Ann. Mtg. PASJ (internet), 738-740 (2024)

B-065
K. Adachi, et al.
Benchmarking GPU Backend of Longitudinal Simulation Code BLOND
Proc. 21th Ann. Mtg. PASJ, 543-546(2024)

B-066
H. Okita, et al.
Circuit Simulation Model for the RF System of J-PARC RCS
Proc. 21th Ann. Mtg. PASJ, 765-769(2024)

B-067
B. Yee-Rendon, et al.
Beam Transient Studies for the JAEA-ADS LEBT
Proc. 32nd International Linear Accelerator Conference 2024 (LINAC 2024), pp. 488-491 (2024).

B-068
B. Yee-Rendon, et al.
The LINACs Simulation Framework
Proc. 32nd International Linear Accelerator Conference 2024 (LINAC 2024), pp. 492-495

(2024).

B-069
J. Tamura, et al.
Progress of the Spoke Cavity Prototyping for the JAEA-ADS Linac
Proc. 32nd International Linear Accelerator Conference 2024 (LINAC 2024), pp. 496-498 (2024).

B-070
A. Plaçais, et al.
Automatic Retuning of Superconducting Linacs Using LightWin
Proc. 32nd International Linear Accelerator Conference 2024 (LINAC 2024), pp. 563-568 (2024).

B-071
M. SHIRAKATA , et al.
EQUIPMENT COOLING WATER UPGRADE PLAN AT J-PARC MR D1 POWER SUPPLY BUILDING
Proc. Ann. Mtg Part. Accel. Soc. Jpn 2024 1015 (2024).

B-072
K. FUTATSUKAWA , et al.
CURRENT STATUS OF LLRF SYSTEM FOR J-PARC LINAC
Proc. Ann. Mtg Part. Accel. Soc. Jpn 2024 1030 (2024).

B-073
M. UOTA
MEASUREMENT OF RESIDUAL GAS MOLECULE DURING BEAM OPERATION IN J-PARC MR RING I
Proc. Ann. Mtg Part. Accel. Soc. Jpn 2024 1058 (2024).

B-074
F. MIYAHARA , et al.
DEVELOPMENT OF A HIGH-SENSITIVITY BEAM POSITION MONITOR CAPABLE OF MUON IDENTIFICATION
Proc. Ann. Mtg Part. Accel. Soc. Jpn 2024 110 (2024).

B-075
Y. SUGIYAMA , et al.
BEAM LONGITUDINAL DYNAMICS SIMULATION FOR HIGH-POWER UPGRADE OF J-PARC MR
Proc. Ann. Mtg Part. Accel. Soc. Jpn 2024 166 (2024).

B-076
K. Sumi , et al.
DEMONSTRATION OF RF LINEAR ACCELERATION OF COOLED MUON BY LASER IONIZATION
Proc. Ann. Mtg Part. Accel. Soc. Jpn 2024 171 (2024).

B-077
C. OHMORI
50-80MHz RF CAVITY FOR EMITTANCE CONTROL OF J-PARC MR BEAM
Proc. Ann. Mtg Part. Accel. Soc. Jpn 2024 210 (2024).

B-078
P.K.Saha , et al.
5-YAER PROGRESS OF H- LASER STRIPPING AT J-PARC RCS
Proc. Ann. Mtg Part. Accel. Soc. Jpn 2024 218 (2024).

B-079
M. TOMIZAWA , et al.
LONGITUDINAL BEAM SIMULATION FOR A HIGH REPETITION CYCLE J-PARC SLOW EXTRACTION
Proc. Ann. Mtg Part. Accel. Soc. Jpn 2024 223 (2024).

B-080
R. Kitamura , et al.
MEASUREMENT OF LEAKAGE BEAM FROM RF CHOPPER
Proc. Ann. Mtg Part. Accel. Soc. Jpn 2024 233 (2024).

B-081
T. MIYAO , et al.
MEASUREMENT OF NOISE ORIGINATING FROM WIRE SCANNER MONITOR DRIVE SYSTEM IN THE J-PARC LINAC
Proc. Ann. Mtg Part. Accel. Soc. Jpn 2024 248 (2024).

B-082
Min YANG , et al.
UPGRADE OF VACUUM CONTROL SYSTEM FOR J-PARC MAIN RING
Proc. Ann. Mtg Part. Accel. Soc. Jpn 2024 310 (2024).

B-083
H. Takahashi , et al.
UPDATE OF BLM MPS MODULE FOR J-PARC LINAC
Proc. Ann. Mtg Part. Accel. Soc. Jpn 2024 314 (2024).

B-084
Y. Tajima , et al.
VISUALIZATION OF MPS ALARMS USING TRIGGERED SCALER MODULE
Proc. Ann. Mtg Part. Accel. Soc. Jpn 2024 324 (2024).

B-085
S. YAMADA , et al.
DAMAGE TO FIBRE OPTIC COMMUNICATIONS IN THE J-PARC MAIN RING CAUSED BY SMALL WILDLIFE
Proc. Ann. Mtg Part. Accel. Soc. Jpn 2024 332 (2024).

B-086
T. SHIBATA , et al.
THE RECOVER AND PERFORMANCE EVALUATION OF A NEW HIGH FIELD SEPTUM MAGNET SM32 FOR FAST EXTRACTION IN J-PARC MR
Proc. Ann. Mtg Part. Accel. Soc. Jpn 2024 372 (2024).

B-087
Yulian TAN , et al.
THE DATA ACQUISITION SYSTEM BASED ON SoC FPGA FOR THE MAGNET POWER SUPPLIES IN J-PARC MR
Proc. Ann. Mtg Part. Accel. Soc. Jpn 2024 386 (2024).

B-088
T. YASUI , et al.
RESONANCES IN J-PARC MR AND FUTURE STRATEGY
Proc. Ann. Mtg Part. Accel. Soc. Jpn 2024 492 (2024).

B-089
K. Shinto , et al.
OPERATION STATUS OF THE J-PARC HIGH-INTENSITY RF-DRIVEN NEGATIVE HYDROGEN ION SOURCE IN 2023/2024
Proc. Ann. Mtg Part. Accel. Soc. Jpn 2024 525 (2024).

B-090
S. IWATA , et al.
EVALUATION OF BEAM ORBIT SIMULATION FOR FAST EXTRACTION IN J-PARC MAIN RING
Proc. Ann. Mtg Part. Accel. Soc. Jpn 2024 532 (2024).

B-091
S. Nagayama , et al.
DEVELOPMENT OF THE BEAM SEPARATION EXAM DEVICE FOR THE NON-DESTRUCTIVE ELECTROSTATIC SEPTUM
Proc. Ann. Mtg Part. Accel. Soc. Jpn 2024 538 (2024).

B-092
K. HASEGAWA , et al.
PREPARATION STATUS 2024 OF RF SYSTEM FOR J-PARC MR UPGRADE
Proc. Ann. Mtg Part. Accel. Soc. Jpn 2024 547

(2024).

B-093
H. Sakai , et al.
A DEVELOPMENT OF APPLICATION ON BEAM PROFILE MONITOR FOR INJECTION BEAM IN J-PARC MR
Proc. Ann. Mtg Part. Accel. Soc. Jpn 2024 558 (2024).

B-094
H. Nakano , et al.
STATUS AND EQUIPMENT CONFIGURATION OF BEAM LOSS MONITORS AT J-PARC LINAC
Proc. Ann. Mtg Part. Accel. Soc. Jpn 2024 582 (2024).

B-095
T. Takayanagi , et al.
LTD PULSE POWER SUPPLY FOR KICKER MAGNETS USING SiC-MOSFETS
Proc. Ann. Mtg Part. Accel. Soc. Jpn 2024 61 (2024).

B-096
K. SATO , et al.
THE THIRD PHASE UPDATE OF CONTROL NETWORK IN J-PARC MR
Proc. Ann. Mtg Part. Accel. Soc. Jpn 2024 655 (2024).

B-097
T. KIMURA
UPDATE OF MACHINE PROTECTION SYSTEM AND OPTICALIZATION OF INTERLOCK SIGNALS IN J-PARC MAIN RING
Proc. Ann. Mtg Part. Accel. Soc. Jpn 2024 659 (2024).

B-098
S. SHITARA , et al.
ESTIMATION OF RADIATION LEVEL FOR THE MUON LINEAR ACCELERATOR
Proc. Ann. Mtg Part. Accel. Soc. Jpn 2024 746 (2024).

B-099
F. Tamura , et al.
MITIGATION OF CAVITY VOLTAGE JUMP DUE TO HIGH INTENSITY BEAM EXTRACTION IN J-PARC RCS
Proc. Ann. Mtg Part. Accel. Soc. Jpn 2024 774 (2024).

B-100
T. SHIBATA , et al.
BEAM OPERATION OF 5%-DUTY FACTOR LaB6 ION SOURCE
Proc. Ann. Mtg Part. Accel. Soc. Jpn 2024 813 (2024).

B-101
R. MUTO , et al.
INVESTIGATION OF THE CAUSE OF THE BEAM LOSS BEFORE THE START OF THE SLOW EXTRACTION AT THE J-PARC MAIN RING
Proc. Ann. Mtg Part. Accel. Soc. Jpn 2024 839 (2024).

B-102
M. Nomura , et al.
APPLYING A DEEP GENERATIVE MODEL TO MOUNTAIN PLOT IMAGES
Proc. Ann. Mtg Part. Accel. Soc. Jpn 2024 85 (2024).

B-103
K. SATOU , et al.
CALIBRATION OF BEAM CURRENT MONITORS AT J-PARC ACCELERATOR FACILITY
Proc. Ann. Mtg Part. Accel. Soc. Jpn 2024 859 (2024).

B-104
H. Iinuma , et al.
EVALUATION OF MAGNETIC FIELD LINEARITY IN IRON YOKE CHANNEL AND CENTER ORBIT DESIGN OF MUON g-2/EDM EXPERIMENTAL STORAGE MAGNET
Proc. Ann. Mtg Part. Accel. Soc. Jpn 2024 863 (2024).

B-105
T. SASAKI , et al.
DEVELOPMENT OF A WIDE DYNAMIC-RANGE BEAM PROFILE MONITOR USING OTR AND FLUORESCENCE FOR INJECTED BEAMS IN J-PARC MAIN RING (5)
Proc. Ann. Mtg Part. Accel. Soc. Jpn 2024 875 (2024).

B-106
T. NAKAMURA , et al.
DEVELOPMENT OF NEW RFSoC BASED INTRA-BUNCH TRANSVERSE FEEDBACK SYSTEM AT J-PARC MR : DESIGN AND INITIAL EVALUATION
Proc. Ann. Mtg Part. Accel. Soc. Jpn 2024 881 (2024).

B-107
K. Watanabe , et al.
UPGRADE OF ACQUISITION AND MONITORING SYSTEM FOR J-PARC ACCELERATOR PPS(II) : AUTOMATIC GENERATION OF GUI
Proc. Ann. Mtg Part. Accel. Soc. Jpn 2024 929 (2024).

B-108
H. Watanabe, et al.
Development of a rotating-disk-type production target at J-PARC Hadron Experimental Facility
Proc. Ann. Mtg Part. Accel. Soc. Jpn, 2024, 507 (2024)

B-109
H. Watanabe
Evaluation of Tungsten made with 3D printer for secondary-particle production target
Proc. Ann. Mtg Part. Accel. Soc. Jpn, 2024, 513 (2024)

B-110
Y. Sato, et al.
Measurement of duty factor of slow-extraction proton beams with a residual gas ionization current monitor in J-PARC Hadron Experimental Facility
Proc. Ann. Mtg Part. Accel. Soc. Jpn, 2024, 551 (2024)

B-111
A. Toyoda, et al.
Development of B Line intensity monitor for J-PARC Hadron Beamline
Proc. Ann. Mtg Part. Accel. Soc. Jpn, 2024, 555 (2024)

B-112
R. Matsushita, et al.
Demonstration of beam assumulation by three-dimensional spiral injection scheme
Proc. Ann. Mtg Part. Accel. Soc. Jpn, 2024, 585 (2024)

B-113
M. Abe, et al.
Design of passive shimming structures for precision magnetic field shimming on muon storage volume in the superconducting muon storage magnet for g-2/EDM measurements
Proc. Ann. Mtg Part. Accel. Soc. Jpn, 2024, 66 (2024)

B-114
S. Ogawa, et al.
Design of beam phase space distribution to realize precise three-dimensional beam injection at J-PARC muon g-2/EDM experiment
Proc. Ann. Mtg Part. Accel. Soc. Jpn, 2024, FRP010 (2024)

B-115
K. Kurihara, et al.
Development of 3D-printed beam windows for J-PARC/COMET phase-1 bridge solenoid part
Proc. Ann. Mtg Part. Accel. Soc. Jpn, 2024,

FRP081 (2024)

B-116
S. Nishi , et al.
APPLICATION OF THE PARALLEL-SCHEME ``VARISTOR'' TO THE SUPERCONDUCTING ACCELERATOR MAGNET AS THE ENERGY EXTRACTION SYSTEM
Proc. Ann. Mtg Part. Accel. Soc. Jpn., 2024 983 (2024).

B-117
S. Ogawa , et al.
Design of beam phase space distribution to realize precise three-dimensional beam injection at J-PARC muon g-2/EDM experiment
Proc. Ann. Mtg Part. Accel. Soc. Jpn., 2024 FRP010 (2024).

B-118
K. Kurihara , et al.
Development of 3D-printed beam windows for J-PARC/ COMET phase-1 bridge solenoid part
Proc. Ann. Mtg Part. Accel. Soc. Jpn., 2024 FRP081 (2024).

B-119
K. Sumi, et al.
Demonstration of rf linear acceleration of cooled muon by laser ionization
Proc. Ann. Mtg PASJ, 171 (2024).

B-120
M. Sugita, et al.
Waveform pattern control system of paint bump power supply for J-PARC RCS
Proc. Ann. Mtg PASJ, 730 (2024).

B-121
S. Shitara, et al.
Estimation of radiation level for the muon linear accelerator
Proc. Ann. Mtg PASJ, 746 (2024).

B-122
R. Kitamura, et al.
Measurement of leakage beam from RF chopper
Proc. Ann. Mtg. Part. Accel. Soc. Jpn. (2024), 233

B-123
K. Shinto, *et al.*
Operation status of the J-PARC high-intensity RF-driven negative hydrogen ion source in 2023/2024
Proc. Ann. Mtg. Part. Accel. Soc. Jpn. (2024), 525

B-124
H. Nakano, et al.
Status and equipment configuration of beam loss monitors in the J-PARC linac
Proc. Ann. Mtg. Part. Accel. Soc. Jpn. (2024), 582

B-125
T. Ito, K. Hirano
Study on inner wall geometry to suppress multipactor discharge occurring on the inner wall of SDTL cavity
Proc. Ann. Mtg. Part. Accel. Soc. Jpn. (2024), 959

B-126
R.P. Litchfield
Latest activities and results from T2K
Proc. EW, 2024, 8720 (2024)

B-127
T. NAKAMURA
BUNCH BY BUNCH FEEDBACK SYSTEM REVIEW
Proc. IBIC 2024 235 (2024).

B-128
Y. HASHIMOTO , et al.
A DEVELOPMENT OF WIDE DYNAMIC-RANGE HALO MONITOR FOR 8 GeV PROTON BEAMS AT FNAL
Proc. IBIC 2024 274 (2024).

B-129
T. TOYAMA
TRANSVERSE FEEDBACK TO DAMP COLLECTIVE BEAM INSTABILITIES, PAST, PRESENT AND FUTURE
Proc. IBIC 2024 35 (2024).

B-130
S. Takada , et al.
Strange Behavior of Boiling Around Wire Heater at The Pressure Condition Very Close to The Lambda Point
Proc. ICEC-ICMC., 2024 1 (2024).

B-131
R. Ueji, et al.
Microstructure and Plastic Deformation Behavior of Si-Bearing Bainitic Steels with Different Carbon Contents
Proc. Int. Symp. Steel Sci., 2024 119–128 (2024).

B-132
S. Harjo, et al.
Deformation Behavior of Ultrafine-Grained TRIP Steel Observed by Neutron Diffraction
Proc. Int. Symp. Steel Sci., 2024 205–208 (2024).

B-133
H. Dannoshita, et al.
Role of Dislocation Characteristics on Deformation Behavior of Martensitic Steel Analyzed by Neutron Diffraction
Proc. Int. Symp. Steel Sci., 2024 209–212 (2024).

B-134
T. Ito, et al.
In situ Neutron Diffraction Study to Elucidate Hydrogen Effect on the Deformation Mechanism in Type 310S Austenitic Stainless Steel
Proc. Int. Symp. Steel Sci., 2024 237–240 (2024).

B-135
Y. Zhang, et al.
In-situ Characterization of Tempering Behaviors and Alloying Effects on Tempering Kinetics in High-Carbon Martensitic Steels
Proc. Int. Symp. Steel Sci., 2024 81–87 (2024).

B-136
K. SEIYA , et al.
RF SYSTEM UPGRADE FOR 1.3 MW OPERATION OF J-PARC MAIN RING
Proc. IPAC 2024 1017 (2024).

B-137
M. TOMIZAWA , et al.
TRACKING ERROR ANALYSIS ON THE POWER SUPPLY CURRENTS OF J-PARC MAIN RING MAIN MAGNETS
Proc. IPAC 2024 1665 (2024).

B-138
R. MUTO
STATUS AND OUTLOOK ON SLOW EXTRACTION OPERATION AT J-PARC MAIN RING
Proc. IPAC 2024 1905 (2024).

B-139
H.Iinuma , et al.
BEAM ALIGNMENT STRATEGY AT THE BEAM TRANSPORT LINE FOR J-PARC MUON g-2/EDM EXPERIMENT
Proc. IPAC 2024 2323 (2024).

B-140
S. OGAWA , et al.
BEAM STORAGE MONITOR TO ACHIEVE 3-D SPIRAL INJECTION IN MUON G-2/EDM EXPERIMENT AT J-PARC
Proc. IPAC 2024 2922 (2024).

B-141
M. YOSHII , et al.
EQUIPMENT PROTECTION SYSTEM AGAINST UNEXPECTED ABNORMALITIES

DURING HIGH-INTENSITY PROTON BEAM OPERATION AT J-PARC MR
Proc. IPAC 2024 3420 (2024).

B-142
H.Yasuda , et al.
DESIGN OF IH-DTL WITH PMQ FOCUSING FOR MEDICAL RI PRODUCTION
Proc. IPAC 2024 3536 (2024).

B-143
Yulian TAN , et al.
REAL-TIME DIGITAL CONTROLLER DESIGN BASED ON SOC FPGA FOR GENERAL USAGE IN J-PARC MR MAGNET POWER SUPPLIES
Proc. IPAC 2024 3735 (2024).

B-144
Y. MORITA , et al.
CORRECTING ASYMMETRY OF CLOSED-ORBIT DISTORTION IN J-PARC MAIN RING BY REDUCING CURRENT RIPPLES OF MAIN MAGNET POWER SUPPLIES
Proc. IPAC 2024 931 (2024).

B-145
P.K. Saha , et al.
BEAM LOSS AND BEAM EMITTANCE MINIMIZATION AT J-PARC RCS FOR SIMULTANEOUS OPERATION TO THE MLF AND MR
Proc. IPAC 2024 939 (2024).

B-146
S. Makimura, et al.
Muon production target at J-PARC
Proc. IPAC, 2024, 1941 (2024)

B-147
H. Iinuma, et al.
Beam alignment strategy at the beam transport line for J-PARC muon g-2/EDM experiment
Proc. IPAC, 2024, 2323 (2024)

B-148
S. Ogawa, et al.
Beam storage monitor to achieve 3-D spiral injection in muon g-2/EDM experiment at J-PARC
Proc. IPAC, 2024, 2922 (2024)

B-149
H. Yasuda, et al.
Design of IH-DTL with PMQ focusing for medical RI production
Proc. IPAC, 2024, 3536 (2024)

B-150
Ersin CICEK , et al.
DEVELOPMENT OF AN INTEGRATED MONITOR SYSTEM FOR REAL-TIME RELATIVE PHASE MEASUREMENT BETWEEN THE CAVITY-RF AND BEAM
Proc. LINAC 2024 411 (2024).

B-151
R. Iwai, et al.
Precision muonium spectroscopy
Proc. Muon4Future 2023, 007, (2024).

B-152
S. Kamioka
J-PARC g-2/EDM experiment, Muon cooling at J-PARC
Proc. Muon4Future 2023, 008, (2024).

B-153
T. Kutter
A Novel Highly Segmented Neutrino Detector: The Super Fine Grained Detector for the Upgraded T2K ND280 Near Detector
Proc. of Sci., ICHEP2024, 1107 (2024)

B-154
P. Dasgupta
Neutrino flux simulation for T2K using GEANT4
Proc. of Sci., ICHEP2024, 221 (2024)

B-155
X. Li
First Search for K0L→π0e+e-e+e- Decay Mode
Proc. of Sci., ICHEP2024, 285 (2024)

B-156
H. Nanjo
KOTO II at J-PARC to measure the branching ratio of KL→π0νν-bar
Proc. of Sci., ICHEP2024, 464 (2024)

B-157
J. Redeker
Latest Results from the KOTO Experiment: The Search for KL→π0νν-bar
Proc. of Sci., ICHEP2024, 467 (2024)

B-158
H. Nishiguchi
A search for muon-to-electron conversion at J-PARC: The COMET Experiment
Proc. of Sci., ICHEP2024, 469 (2024)

B-159
K. Ono
In-beam charged particle detector using 0.2-mm thick plastic scintillator for the J-PARC KOTO experiment
Proc. of Sci., ICHEP2024, 969 (2024)

B-160
F. Oura, et al.
Spectroscopic study of Kaonic nuclei using inclusive and exclusive 12C(K-,p) reaction at J-PARC
Proc. of Sci., QNP2024, 209 (2024)

B-161
F. Sakuma, et al.
Light Kaonic Nuclei at J-PARC
Proc. of Sci., QNP2024, 211 (2024)

B-162
Changdong Shin
Measurements from JSNS^2 and the status of JSNS^2-II
Proc. of. Sci., NOW2024, 41 (2024)

B-163
P. K. Saha, et al.
Beam loss and beam emittance at J-PARC RCS for simultaneous operation to the MLF and MR
Proceedings of 15th International Particicle Accelerator Conference, p.939 - 942, 2024/05

B-164
M. Chimura, et al.
Emittance growth calculations for bunched beam transport in self-induced electromagnetic fields dominated region
Proceedings of 21st Annual Meeting of Particle Accelerator Society of Japan, p.1064 - 1069, 2024/10

B-165
K. Kojima, et al.
Study on the mitigation of the beam loss for further beam power ramp-up in J-PARC RCS
Proceedings of 21st Annual Meeting of Particle Accelerator Society of Japan, p.118 - 122, 2024/10

B-166
P. K. Saha, et al.
5-year progress of H- laser stripping at J-PARC RCS
Proceedings of 21st Annual Meeting of Particle Accelerator Society of Japan, p.218 - 222, 2024/10

B-167
J. Kamiya, et al.
Dry Pumps in accelerator; Usage at the Japan Proton Accelerator Research Complex (J-PARC)
Vacuum and Surface Science, 67(4), p.186 - 191, 2024/04

B-168
J. Kamiya
Power source-free getter pump using advantage of the characteristics of titanium

Vacuum journal 189, p.6-11, 2024/07

KEK Reports

C-001
Safety Division, J-PARC Center
Annual Report on the Activities of Safety in J-PARC, FY2023
KEK Internal 2024-005

C-002
T. Ishida, et al.
Contrasting Irradiation Behavior of Dual Phases in Ti-6Al-4V Alloy at Low-Temperature Due to Omega-phase Precursors in Beta-phase Matrix
KEK Preprint 2024-11

JAEA Reports

D-001
Y. Yamaguchi , et al.
Preliminary experiment for measurement of radionuclide yield from nuclear capture reaction of negative muon
JAEA-Conf 2023-001 (2024), p.56

D-002
Y. Yamaguchi , et al.
Dataset of Nuclide Production from Nuclear Capture Reaction of Negative Muon Based on Monte Carlo Simulation
JAEA-Data/Code 2024-008, p.1

D-003
Safety Division, J-PARC Center
Annual Report on the Activities of Safety in J-PARC, FY2023
JAEA-Review 2024-060(2024)

Others

E-001
R. Kitamura, K. Hirano
BEAM PROFILE MONITOR
Japanese Patent, No.7564547

E-002
H. Harada, et al.
Commitment to sustainable Particle Accelerator Society of Japan; First roundtable meeting for communication with students and companies/research institutions
Kasokuki, 20(4), p.332 - 335, 2024/01

E-003
北村遼
日刊工業新聞の連載企画「原子力機構の価値」（第48回：高耐久のイオンビームモニター）
日刊工業新聞*28*面、*2024*年

J-PARC Annual Report 2024
Vol. 1: Highlight

December 2025

J-PARC

JAPAN PROTON ACCELERATOR RESEARCH COMPLEX

High Energy Accelerator Research Organization (KEK)
Japan Atomic Energy Agency (JAEA)

2-4 Shirakata, Tokai-mura, Naka-gun, Ibaraki 319-1195, Japan

https://j-parc.jp/